UNIVERSITY OF BIRMINGHAM

DEVELOPMENT OF AN ADVANCED MULTI-OBJECTIVES APPROACH TO OPTIMISE THE LONG-TERM PERFORMANCE OF ENHANCED GEOTHERMAL SYSTEM (EGS) RESERVOIRS

by

MALEAHA SAMIN

A thesis submitted to
the University of Birmingham
for the degree of
DOCTOR OF PHILOSOPHY

College of Engineering and Physical Science
School of Engineering
The University of Birmingham
June 2019

ABSTRACT

Enhanced geothermal system (EGS) reservoirs are artificial deep reservoirs designed to exploit geothermal power accumulated within hot dry rocks in order to generate electricity. EGS reservoirs have large potential to be exploited as a renewable source of energy. However, currently commercial exploitation is still not feasible and despite research that has attempted to achieve a cost-effective EGS reservoir design with high performance over long periods of exploitation. Previous studies have focused on investigating the impact of single or multi design parameters on EGS reservoir performance without considering their interdependency during heat extraction processes and impacts on reservoir total cost associated with creation and operation costs. This research has conducted an optimisation assessment taking into consideration many design parameters and their interdependency during optimisation process. The key contribution of the research is associated with the development of numerical analysis for both doublet and multi-wells reservoirs integrated with an artificial intelligence application, generated from genetic algorithm GA. During parametric study of doublet well reservoirs, results revealed that the maximum mass flow rate production was 30 kg/s, and this value was achieved during the parametric study of injection pressure and reservoir permeability. It was also observed that different designs of doublet well EGS reservoirs still could not maintain commercial mass flow rate (80 kg/s). However, commercial mass flow rate was achieved with multi wells reservoir through increasing injection pressure and number of wells. The results of two optimisation scenarios (with and without improving reservoir permeability) of doublet EGS reservoirs revealed that the permeability of the reservoir has a significant influence on selecting the other artificial design parameters. The proposed methodology established in this research can be used to transform the way EGS reservoirs are currently designed to be exploited leading to a cost-effective power source. In addition, the methodology has the flexibility and potential to be adapted during and post design of EGS reservoirs.

ACKNOWLEDGEMENT

I would like to express my deep gratitude to my supervisors Dr. Asaad Faramarzi and Professor Ian Jefferson for their very kind support, enthusiasm, patient guidance and encouragement. Without their support, the journey of this PhD would be very difficult. Also, my gratitude to Professor Ouahid Harireche for his kind support in developing the ideas and providing comments and feedback on my work.

I am particularly very grateful to the University of Birmingham (School of Engineering) for funding this research project and sponsoring all costs of my PhD study.

My special thanks to my husband Dr Jabar Rasul and my kids for their patience with me during the completion of this work.

In addition, I would like to express my gratitude to my Mum and Dad, and my brothers (Mr Taha, Mr tariq, Mr Mahmud and Mr Amin) and my sisters (Mrs Madiha, Mrs Rabia, Mrs Soela and Mrs Iman) and their partners for their kind support.

Furthermore, I would like to thank all of my friends for their moral support including Dr Aras Mirkhan, Mr Bestoon Asm, Dr Mosleh Tohidi, Mr Rebar Sherwani, Mr Ahmed Mahmood, Mr Chenar Qadir, Mr Farough Rahimzadeh, and Mr Mehdi Mahmud and last but not the least Dr Kawa Aziz.

LIST OF PUBLICATIONS

The following publications have been produced as a result of this PhD study.

1. **Samin, M. Y**., Faramarzi, A., Jefferson, I., Harireche, O, 2018. "A Hybrid Optimisation Approach to Improve Long-Term Performance of Enhanced Geothermal System (EGS) Reservoirs" *Renewable Energy*, 134, pp.379-389.
2. **Samin, M. Y**., Faramarzi, A., Jefferson, I., Harireche, O, 2019. "An integrated approach to analyse enhanced geothermal multi-wells reservoirs; impact for design" *Journal of Environmental Engineering and Science ICE* (under revision).
3. **Samin, M. Y**., Faramarzi, A., Jefferson, I., Harireche, O, 2019. "The novel coupled design and management models to optimise EGS multi-wells reservoirs" *Applied Energy* (under review).
4. **Samin, M. Y**., Faramarzi, A., Jefferson, I., Harireche, O, 2017. "The Optimisation of Production Well Numbers in Enhanced Geothermal System" *Proceedings of the Conference of 25th UK Association for Computational Mechanics (UKACM), 12-13/04/2017*. At: University of Birmingham, Birmingham, UK.

AWARDS

- Author has been awarded for **the best presentation by a postgraduate research student** in the 25th UK Association for Computational Mechanics (UKACM), 12-13/04/2017.

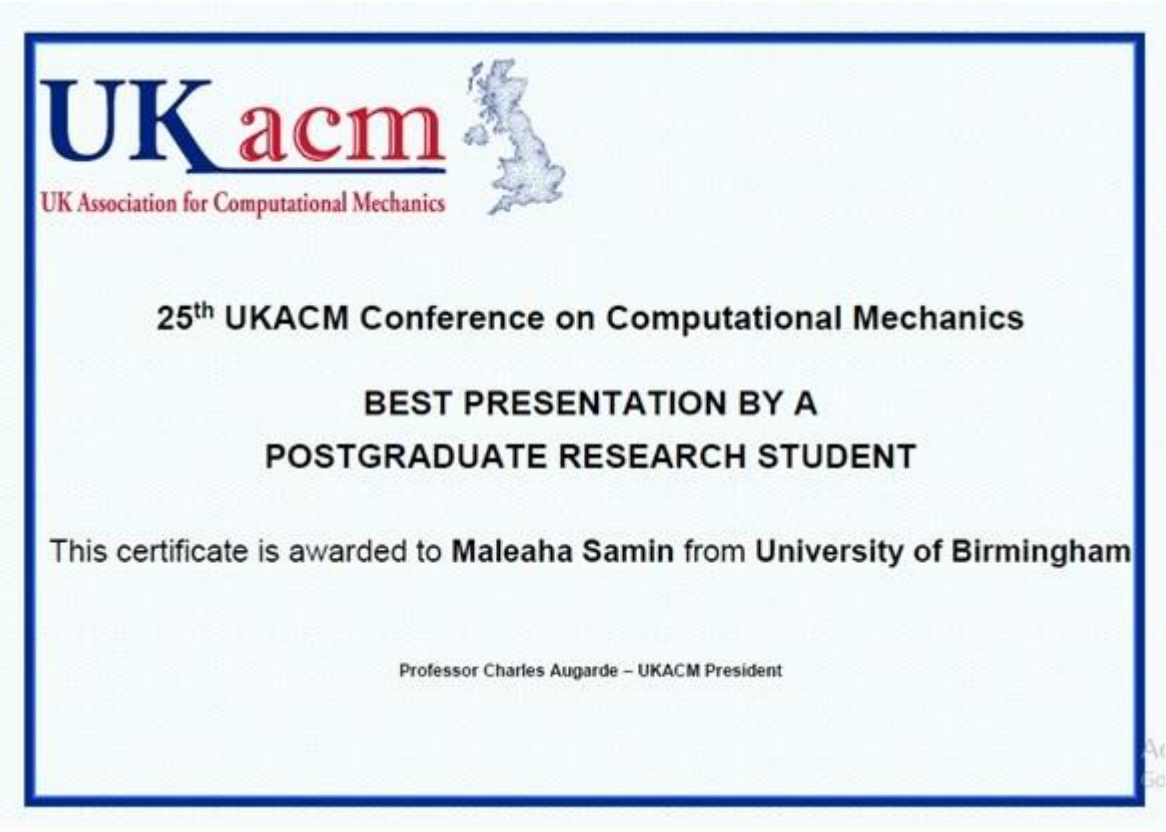

- Author has been shortlisted by the University of Birmingham for the **Michael K. O'Rourke Best PhD Publication Award** at the University of Birmingham 2019.

LIST OF CONTENT

LIST OF FIGURES

LIST OF TABLES

LIST OF SYMBOLS AND ABREVIATIONS

h_{inj}	Injection Enthalpy
h_p	Production Enthalpy
θ	Porosity
ρ_f	Fluid Density
ρ_r	Rock Density
ΔP	Pressure change at the production well
ΔT	Change in production temperature
BHI	Injection Well Head Pressure
BHP	Production Well Head Pressure
cp_f	Specific Heat Capacity of Fluid
cp_r	Specific Heat Capacity of Rock
d	Space Between Injection and Production Wells
EGS	Enhanced Geothermal System
GA	Genetic Algorithm
HDR	Hot Dry Rock
h_r	Reservoir Height
I_R	Hydraulic impedance
J	Number of years at the reservoir breakthrough time
k_r	Reservoir Permeability
kx	Permeability in x Direction
ky	Permeability in y Direction
kz	Permeability in z Direction
MIT	Massachusetts Institute of Technology

η	Efficiency of the power plant.
N	Number of Wells
Npw	Number of production Wells
$Pinit$	Reservoir Initial Pressure
$Pinj$	Fluid Injection Pressure
pp	Electrical power price
$Ppro$	Fluid Production Pressure
pr	Heat price
r	Discount rate with time
TE	Levelised Cost
$Tinit$	Initial Temperature
$Tinj$	Fluid Injection Temperature
TOUGH2	Transport of Unsaturated Groundwater and Heat Version 2
$Tpro$	Fluid Production Temperature
FD	Finite Deference
FE	Finite Element
FV	Finite Volume
λ_f	Thermal Conductivity of Fluid
λ_r	Thermal Conductivity of Rock
μ	Dynamic Viscosity

CHAPTER ONE

1 INTRODUCTION

1.1 Background

Geothermal power has been used for many centuries for different purposes, such as cooking, bathing and as space heating, mostly extracted from shallow sources and natural hot springs (Grant, 2013). Since the last century and particularly in 1904, electrical power generation started from geothermal sources, which the first instance was in Italy at Larderello site (Dickson and Fanelli, 2001). However, the majority of the generated power from geothermal sources are limited to conventional geothermal systems (hydrothermal), which is found within limited locations of the crust layer of the earth (Li, 2015). It is only recently that the technology to exploit hot dry rock (HDR) geothermal has advanced.

In 1974, the first HDR deep geothermal reservoir in Los Alamos was developed, where the heat of the subsurface at the depth of between 4 to 5 kilometres was extracted to generate electricity (Olasolo et al., 2016a). This was followed by trials of the technology in the UK at the Rosemanowes Quarry between 1977-1980 (Kolditz and Clauser, 1998).

The modern process of extracting heat from a geothermal reservoir has been used since 1990s. In this method, hot dry rock matrix is stimulated using hydraulic fracturing, at depths of over 2.5 kilometres, where temperature is at a range of 150-200 ^{o}C, producing energy in the form of hot fluid or steam, this process is known as Enhanced Geothermal System (EGS) (Duchane and Brown, 2000). There are 18 existing, under-development and operating of EGS sites around the world (Lu, 2018) and their locations are presented in Figure 1-1.

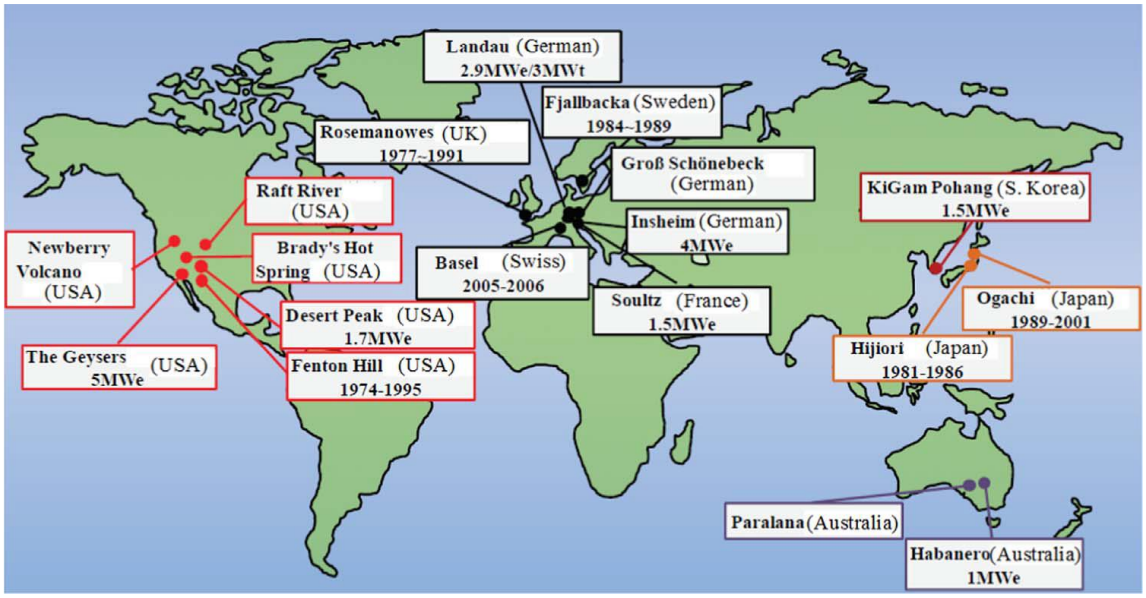

Figure 1-1. Global map of EGS (Lu, 2018)

In general, geothermal energy, due to its nature, is much more predictable than other renewable sources of energy such as wind or solar, hence it is a popular option in many countries (BP, 2015). For example, in China it is predicted that geothermal has the potential to produce enough energy for over 5000 years of China's annual total energy consumption of 95.2×10^{18}J at 2010 if just 2% of the country's EGS resources is recovered (Wang et al., 2013). However, due to technological and economical challenges, as well as uncertainties that exist at the high depths (DECC, 2013, GEA, 2013), EGS is still considered to be at the 'proof of concept' stage (Rybach, 2010a). For example, the Bad Urach project started 1977 in Germany and it was abandoned in 1981 because of the financial problems (DiPippo, 2012). The Basel project started 2006 in Switzerland and it is abandoned in 2009 due to inducing seismic events (Giardini, 2009).

Compared with other renewable energy sources, the growth rate of geothermal power is low, see Figure 1-2, yet if technology and understanding of EGS improves, it has the potential to grow exponentially (Li et al., 2015).

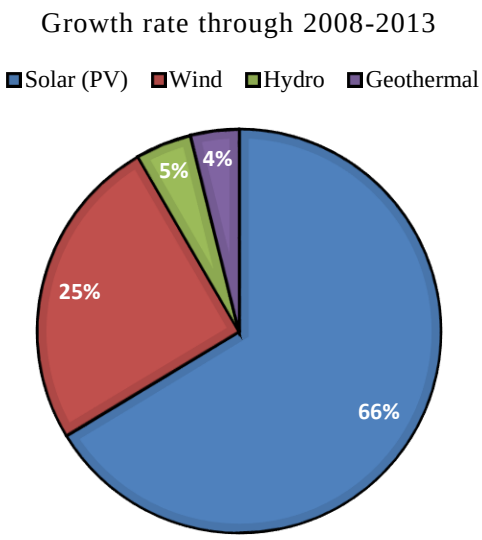

Figure 1-2. Average annual growth rates of energy capacity for different renewable sources, 2008–2013 (After Li et al. (2015)

Due to the high costs involved in field trials of HDR reservoirs, computational modelling of a reservoir is often used (Lu, 2018). This enables researchers to investigate different permutations of the use of EGS.

A comprehensive study conducted by Mudunuru et al. (2016) on numerical modelling of EGS reservoirs, using parallel reactive flow and transport model PFLOTRAN, indicated that, in general, numerical modelling can be divided into three different categories in terms of the performance of EGS reservoirs as follows:

- The first relates to improving the efficiency of heat extraction technologies for different rock deposits considering a wide range of useful temperatures;
- The second category aims to evaluate the commercial feasibility of the extracted thermal energy at various stages in the development of prospective resources;
- And the third aspect estimates the life span of existing and future potential EGS reservoirs based on the initial thermal energy extraction rate (Mudunuru et al., 2016).

In recent decades, different researchers have proposed a variety of numerical modelling strategies to obtain an understanding of EGS performance and to explore potential trade-offs relating to the above three key performance objectives (He et al., 2011, Kruger and Robinson, 1994, McClure and Horne, 2014, Robinson and Tester, 1984). Each of these studies offered useful understanding, interpretation and insights into the complex processes taking place in specific EGS reservoirs. However, these studies did not probe directly key site-specific factors that influence the long-term performance of the underlying field-scale problems (Mudunuru et al., 2016).

Recently, several studies used different optimisation approaches in order to achieve efficiency in one or more aspects of EGS performance (see the review paper of Olasolo et al. (2016a)). This showed that the designs proposed have limited focus on integrating both engineering and management models in terms of multi-variables multi-objectives, including heat production and efficiency performance in a single optimisation model taking into consideration the thermal production power and economic analysis altogether.

For a commercial EGS, it is important to develop a thermo-economic model to compile both engineering and management models together (Kong et al., 2014), in which the proposed model involves many contribution parameters such as distance between wells; depth of reservoirs; number of wells; permeability and porosity of reservoirs; and temperature and pressure of injection fluid. The contributed design parameters are shown in Figure 1-3.

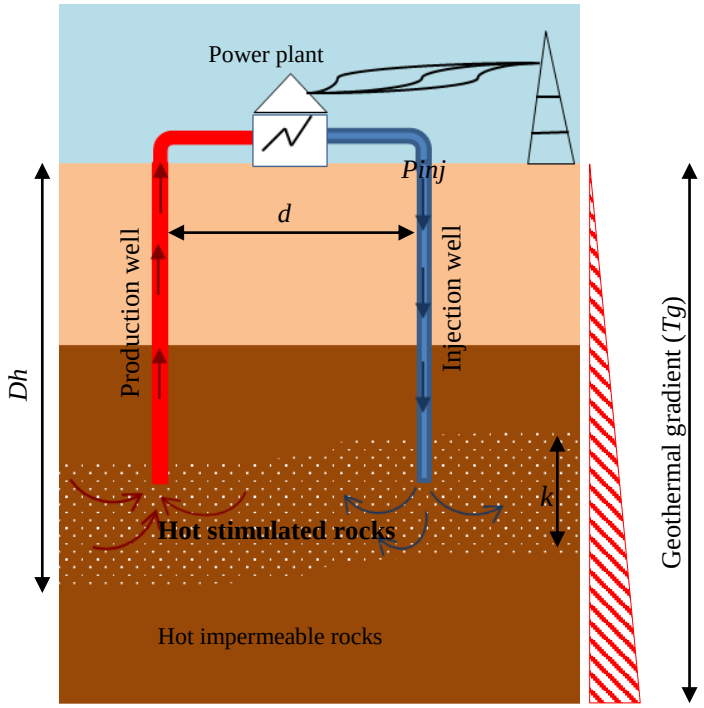

Figure 1-3. Presentation of contributed design parameters in an EGS reservoir; where, *d* is distance between injection and production wells, *Dh* is reservoir depth, *k* is reservoir permeability, *Pinj* is fluid injection pressure, and geothermal gradient *Tg*.

Thus, in this research a novel methodology has been developed to optimise the management and design of EGS reservoirs using a hybrid optimisation technique. This study integrates finite element (FE) analysis with artificial intelligence applications using genetic algorithm (GA) to evaluate the influence of contributed parameters and their interdependency in EGS reservoirs. Using this approach, an optimum EGS reservoir design has been facilitated, considering various key parameters as input variables, with respect to extraction efficiency, commercial feasibility and reservoir long life span for both EGS doublet and multi-wells reservoirs.

1.2 Problem Statement

Geothermal energy is a renewable energy source that has provided commercial baseload electricity around the world since the last century (Huenges et al., 2013, Pang et al., 2015). However, most of it is associated with hydrothermal systems and exists in the hot spot geologies meaning its distribution in the world is too limited to make a significant impact on energy supply (Tester et al., 2006).

EGS is assumed as another type of geothermal system, it has a widespread distribution, small footprint, and low emissions; it is a promising alternative power source. Nevertheless, it needs more investigations to achieve cost-effective production over long periods (Rybach, 2010a). EGS reservoirs involve drilling of one or more wells in high temperature rocks at depth more than 2500 m. In addition, it requires stimulation of the HDR matrix to provide flow path for the injection fluid to the production well (Doughty et al., 2018); and this experimental approach requires high capital costs (Jing et al., 2000). Therefore, the field experiments of the EGS reservoirs are not a favourable option to understand the enhancement of the long-term performance of EGS reservoirs. Subsequently, numerical modelling have been widely used for the last three decades (Lu, 2018). Thus, establishing a new procedure framework of optimisation techniques for numerical modelling is important to identify the most effective characteristics of such reservoirs during operation process.

Generally, a cost-effective production is a crucial target to achieve an economical energy power. Compared to the intensive numerical simulations and large number of research assessing the long-term performance of EGS reservoirs; the significant point seems rather to be why commercial feasibility of EGS is not yet achieved. Hence, investigating new optimisation techniques to find designs with optimum thermal-economic performance is of vital importance.

1.3 Aim and Objectives

Aim

In this research, the main aim is to develop an interconnection of design parameters of EGS reservoirs to define their impacts on both thermal power and financial consideration over long periods of heat exploitation. This was achieved through developing a combination of computational mechanics of EGS reservoir models (namely finite element) with artificial intelligence-based optimisation technique (namely genetic algorithm).

Objectives

The research objectives are as below:

1. To identify the criteria and targets for the long-term performance of EGS reservoirs to set the fitness function for the optimisation model, see Section 2.4 in Chapter Two.
2. To identify the critical design parameters that have influences on the thermal and hydraulic breakthrough of production wells of EGS reservoirs over long periods of heat exploitation (see Chapter Two).
3. To develop and validate a finite element (FE) model of fully thermal- hydro (TH) coupled process of EGS reservoirs to establish an accurate platform for the numerical simulations to explore the interconnectivity of several design parameters (see Chapter Four).
4. To investigate the sensitivity of EGS reservoirs performance to the design parameters and their impacts on the long-term performance of reservoirs (see Chapter Four).
5. To investigate the optimum design of a doublet EGS reservoir alongside with the optimum management of a better thermal power production (see Chapter Five).
6. To investigate the optimum well numbers of EGS multi-well reservoirs using multi-objectives optimisation (see Chapter Six).
7. To develop an integrated thermal-economy model for the long-term performance of EGS multi-wells reservoirs to achieve a full understanding of interconnections of reservoir design parameters including numbers of wells (see Chapter Seven).

1.4 Novelty and Contribution to Knowledge

The key contribution of the research is the consideration of the interconnectivity of several design parameters of EGS reservoirs and its impact on the long-term performance of the system. The novelty has been achieved through the development of a hybrid optimisation technique that integrates the power of artificial intelligence (AI) algorithms with a finite

element technique. The use of AI allows to capture the interdependency and complex relationship of contributing parameters to the long–term performance of reservoirs, which otherwise was not feasible using conventional modelling techniques. The contribution to the knowledge is presented in details as follows:

- Develop a full interaction of the design, management and economic models in one optimisation process for a doublet well reservoir design.
- Establish a method to define the interdependency of the design parameters and their resulting impacts on the long-term performance of EGS reservoirs at the end of reservoir service life, which considers the accumulative thermal power at the breakthrough time of the reservoir.
- The development of a hybrid optimisation technique via integration of FE models with a multi-variable and multi-objectives GA optimisation technique in doublet well reservoirs.
- The interrelating of the number of wells, design parameters, configuration of wells, boundary conditions and the economy analysis of EGS multi-wells in a single optimisation technique.

1.5 Thesis Outline

The structure of this thesis consists of eight chapters. Chapter One, presents the background, problem statement, aim and objectives. Chapter Two presents a comprehensive literature review of geothermal reservoirs, their development trend, challenges and the long-term performance characterisation of EGS reservoirs. The previous numerical modelling and optimisation techniques used to investigate optimum solutions of EGS reservoirs are also described in this chapter. Chapter Three describes the methodology have been used to develop the finite element model and the GA optimisation technique used in this research. Chapter Four presents the development of FE model for a doublet well reservoir. It also demonstrates the

parametric study of design parameters of EGS reservoirs. In this Chapter, the complex interrelation between design parameters and its impact on inducing challenges during optimisations are presented. Chapter Five demonstrates optimisation of doublet EGS reservoirs. Integration of FE models and GA correspondingly is presented and the understanding of the enhancement of long-term performance of EGS doublet reservoir is presented likewise. Chapter Six deals with the sensitivity analysis of the number of production wells in a multi-well EGS reservoir. Chapter Seven demonstrates the optimisation of EGS multi-well reservoirs in a novel method. This Chapter presents the number of production wells within the GA technique additionally to other design parameters as variables. Chapter Eight contains the conclusions and recommendations derived from the research project undertaken herein. Appendices are placed at the end of the thesis presenting the use of COMSOL Multiphysics code to develop the finite element models (both doublet and multi-wells designs) and the programing code that was used for the optimisation process.

CHAPTER TWO

2 LITERATURE REVIEW

2.1 Introduction

This chapter provides a critical review of the relevant literature related to the long-term performance of an enhanced geothermal system (EGS). This chapter reviews numerical methods for determining responses including: thermal energy, commercial feasibility, thermal and hydraulic breakthrough time and reservoir service life.

2.2 Background

The word "Geothermal" was originally derived from two Greek words (Geo and thermós), which means the earth and heat (Fytikas et al., 2005). The heat of the earth is stored in the subsurface, where the temperature rises with the depth towards the core of the earth, as can be seen in Figure 2-1. The core of the earth is located at a depth of over 6000 km and its temperature is estimated to be more than 5000 °C (Böttcher et al., 2015). The temperature of the earth's core is maintained by the slow decay of radioactive particles, which generates thermal energy continuously heating of the earth's core. The earth's core is surrounded by the Mantle layer (see Figure 2-2), which is a thick layer forming about 82% of the total size of the earth (Omer, 2008). According to the second law of thermodynamics, heat tends to move from high to low temperature regions (Schroeder, 1999). Therefore, the heat of the earth transfers from the core towards the surface at an average heat flux of 0.08 W/m^2 depending on the geology of the area and the tectonic characteristics of the region (Pollack et al., 1993).

The following subsections (Section 2.2.1 below) describes the methods of heat transfer mechanisms from the earth.

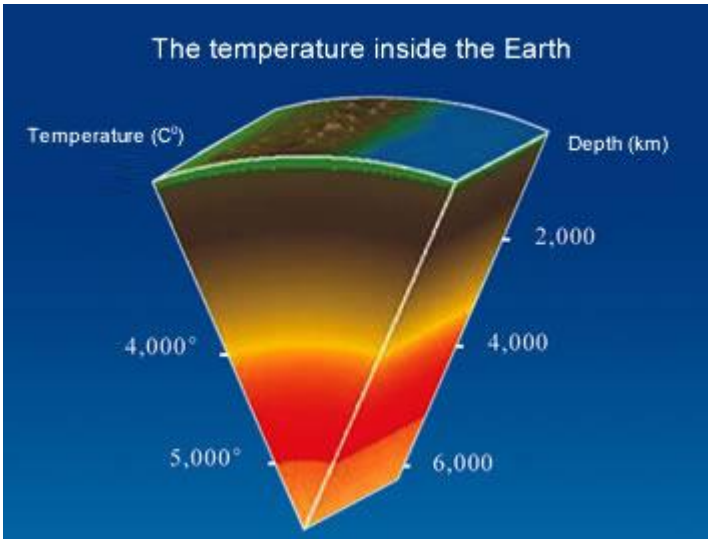

Figure 2-1. The heat of the earth (Omer, 2008)

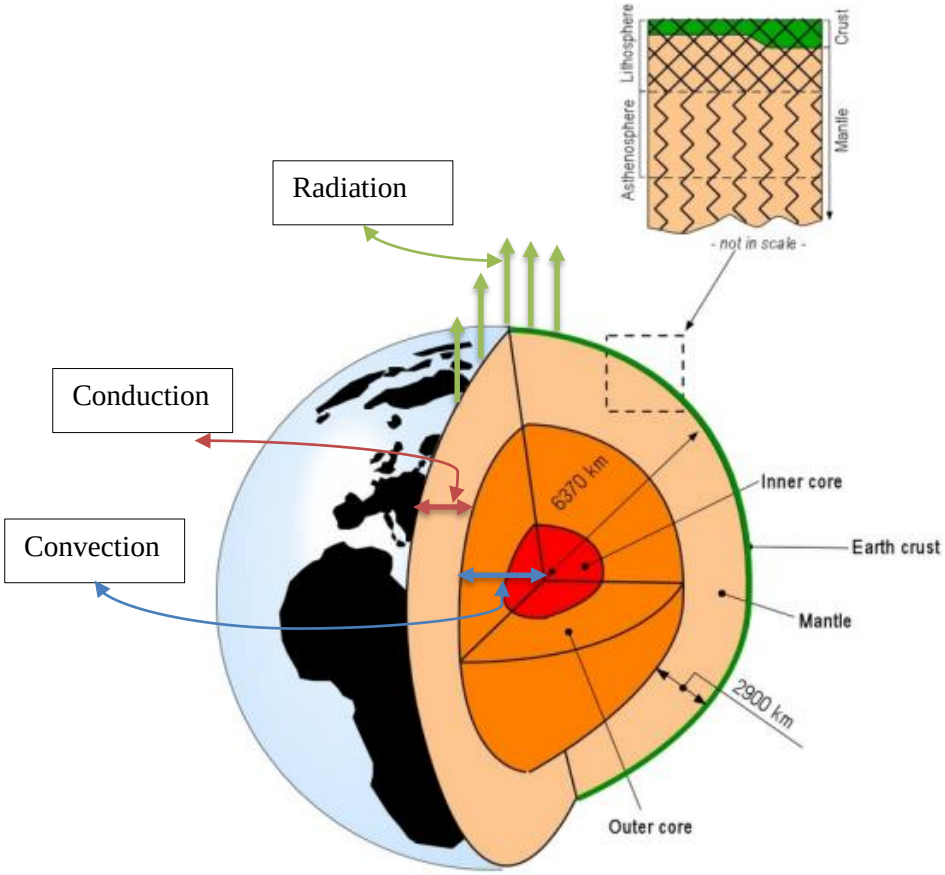

Figure 2-2. The layers of earth with showing the locations of heat transfer methods (after Dickson and Fanelli (2001))

2.2.1 Earth Heat transfer:

There are three main mechanisms of heat transfer from a heat source. These are conduction, convection and radiation (Böttcher et al., 2015).

2.2.1.1 Conduction

Conduction is the process by which heat is transferred in the form of molecular activity and is calculated using Fourier's law (Banks, 2012). In the case of the earth's heat transfer, the heat is conducted from the interior of the mantle layer of the earth to its exterior (i.e. heat transfers from the surface of the outer core to the mantle layer), see Figure 2-2. This process produces a geothermal gradient. According to Barbier (2002), the average geothermal gradient is 30 ^{0}C/km and this varies within the earth, depending on the geology of the area.

2.2.1.2 Convection

Convection is heat transfer between fluids and solids with different temperatures and it is calculated using Newton's law of cooling (Banks, 2012). In the case of the earth's heat transfer via convection, heat is transferred through subsurface fluid motion in the inner and outer core layer of the earth, see Figure 2-2. And convection could take place in porous medium and is calculated using Darcy's velocity multiplied by the volumetric heat capacity of the fluid as suggested by De Marsily (1986).

2.2.1.3 Radiation

Radiation is a heat transfer method, by which heat is transferred in the form of electromagnetic waves through the space between surfaces, or through a medium (Varzina, 2015). In the case of earth's heat transfer through radiation, heat transfers through the ground to the environment, see Figure 2-2. Heat transfer during extraction process of geothermal reservoirs usually ignored

radiation method due to its insignificant effects on the reservoir production compared to convection and conduction (Lam et al., 1988).

2.2.2 Mechanisms in Geothermal Reservoirs

In geothermal reservoirs, heat will be transferred in the reservoir through the rock matrix via conduction and to the injected cold fluid via convection and this lead to increase the temperature of the injected fluid during heat extraction process. However, compared to conduction and convection, heat transfer via radiation requires a longer time than the other two mechanisms. Accordingly, radiation has the lowest impact on EGS efficiency during extraction process. Thus, in this thesis, the effect of radiation heat flow in geothermal reservoirs is neglected.

2.3 Geothermal System

For over 2000 years, geothermal sources have been used for different purposes, such as the use of geothermal water for cooking, bathing and as space heating by many nations e.g. Romans, Icelanders, Japanese, Turks, the Maori of New Zealand and Central Europeans (Lund, 2007). However, it was at the beginning of the last century (in 1904) that the first instance of geothermally generated power, in Italy (at Larderello site using the steam of hot springs to turn small turbines), was demonstrated (Dickson and Fanelli, 2001). This technological breakthrough was further developed to build the first geothermal power station in 1911 and was followed by the first geothermal wells in Japan (1919) and the United States (1921). Subsequently, in 1942, the globally installed geothermal power capacity reached 127.65kW; while the first geothermal power plants were installed in 1958 and 1959 in New Zealand and Mexico respectively (Dickson and Fanelli, 2001).

The term geothermal system is a combination of all the previously mentioned development stages including the heat source (reservoir), drillied wells and power plants. The definition of

a geothermal system, by Grant (2013), is "*the total subsurface hydrologic system associated with a geothermal field. This includes all parts of the flow path, from the original cold source water, its path down to a heat source, and finally its path back up to the surface*".

Dispite the long history of the use of geothermal as a power source, still its installtion capacity and its installed capacity is very low compared to other sources of renewable energy such as solar, wind, bio and hydro power (Li et al., 2015). In general there are two types of deep geothermal reservoirs in terms of heat availability, in-situ permeability and existing fluid (Lu, 2018). These two types are presented in the following sections.

2.3.1 Different Types of Deep Geothermal Systems

There are mainly two types of deep geothermal systems, based on the heat exploitation process: conventional geothermal (hydrothermal) and unconventional geothermal (enhanced geothermal) (Lu, 2018), as shown in Figure 2-3. Both systems are briefly discussed in the proceeding sub-sections:

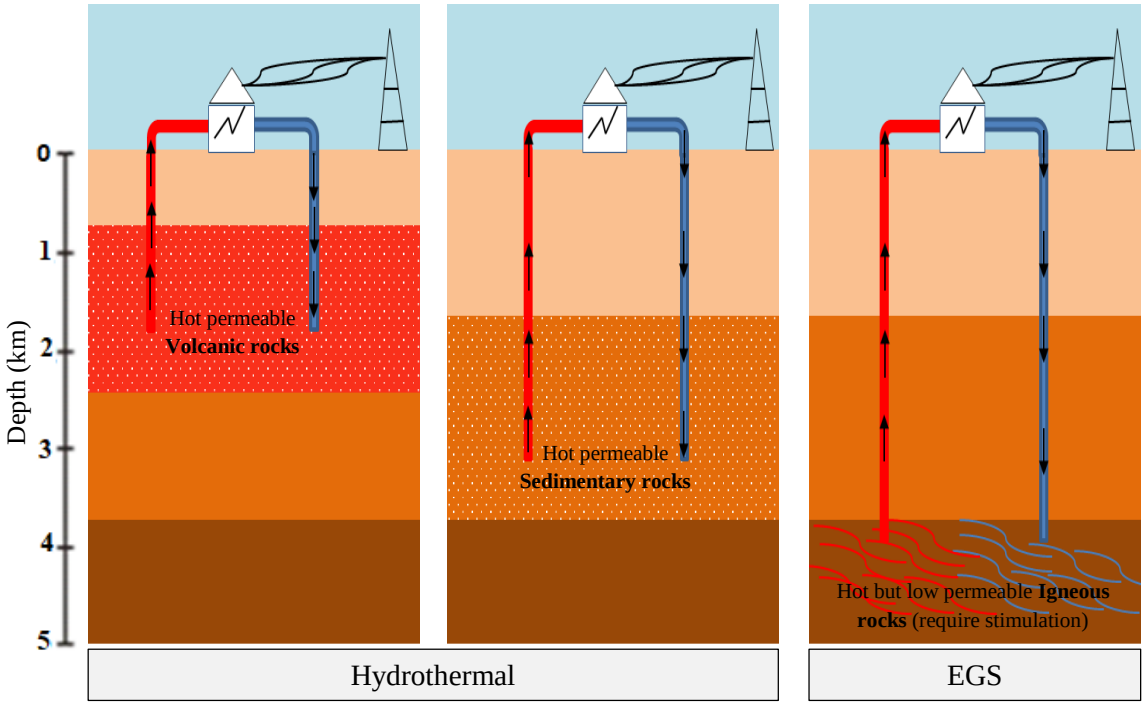

Figure 2-3. Deep geothermal system types (a) hydrothermal reservoirs and (b) EGS reservoirs

2.3.1.1 Hydrothermal System (Conventional)

Hydrothermal systems have been developed for approximately 100 years and thus have mature power generation techniques (Lu, 2018). This source of heat is located at depths between 1 and 4 km and contains fluid in the form of liquid water or steam at a temperature higher than 350 ^{o}C (Mock et al., 1997). Hydrothermal systems can be divided into two categories: Liquid dominated system (where the system lifts water to the surface) and vapour dominated system (where the collected steam is conducted by pipeline from various wells to a power generating plant). Compared to the liquid dominated systems, the vapour-dominated systems are the rarer type. However, the liquid dominated systems are still limited to recent active volcanic geologies or tectonic plate boundaries (Mock et al., 1997). According to Fridleifsson et al. (2008), Roney (2014) and Li et al. (2015) 11,700 MW of electricity was provided by geothermal sources across 23 countries in the world. Moreover, it is anticipated that geothermal sources (hydrothermal and EGS) have the potential to provide the global world target of 140 GWe by 2050, see Figure 2-4.

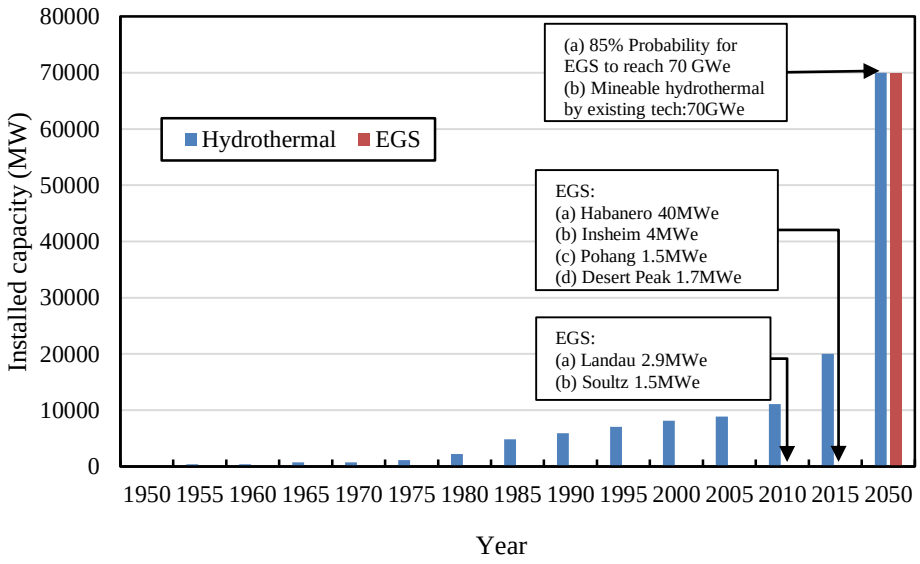

Figure 2-4. Global installed geothermal capacity (After Lu (2018))

However, the growth rate of geothermal power is low as compared to other renewable energy sources such as solar, wind and hydro power because it is limited to conventional geothermal systems (hydrothermal), which is found within the limit of the earth crust layer. To overcome these limitations, EGS can be used, which has the potential to grow energy geothermal sources exponentially (Li, 2015).

2.3.1.2 Enhanced Geothermal System (Unconventional)

The deep hot dry rock (HDR) has a vast storage of heat beneath the ground and is worldwide distributed such as Rosemanowes quarry in Cornwell in the UK, see Figure 2-5.

However, it has insufficient in-situ permeability to allow fluid flow during the heat extraction process and it requires enhancing the permeability to increase its potential for sufficient fluid flow (Tester et al., 2006). Therefore, the modern process of extracting heat from a deep geothermal reservoir stems from developments in the 1990s. Here, an HDR matrix is stimulated using hydraulic fracturing at depths over 2.5 kilometres where temperatures of 150-200 °C exist. This results in the development of the so called Enhanced Geothermal System (EGS), where energy in the form of hot fluid or steam can be produced (Duchane and Brown, 2000).

The experimental work of EGS initially began at Fenton Hill, New Mexico USA (in the late 1970s), using HDR to explore the potential of exploiting geothermal energy for EGS (Duffield and Sass, 2003). Later, many other sites worldwide were selected to carry out field experiments such as Rosemanowes quarry in the UK, Spa Urach in Germany, Soultz in France, Basel project in Swaziland and Ougashi in Japan (Olasolo et al., 2016a). However, it has insufficient in-situ permeability to allow fluid flow during the heat extraction process and it requires enhancing the permeability to increase its potential for sufficient fluid flow (Tester et al., 2006).

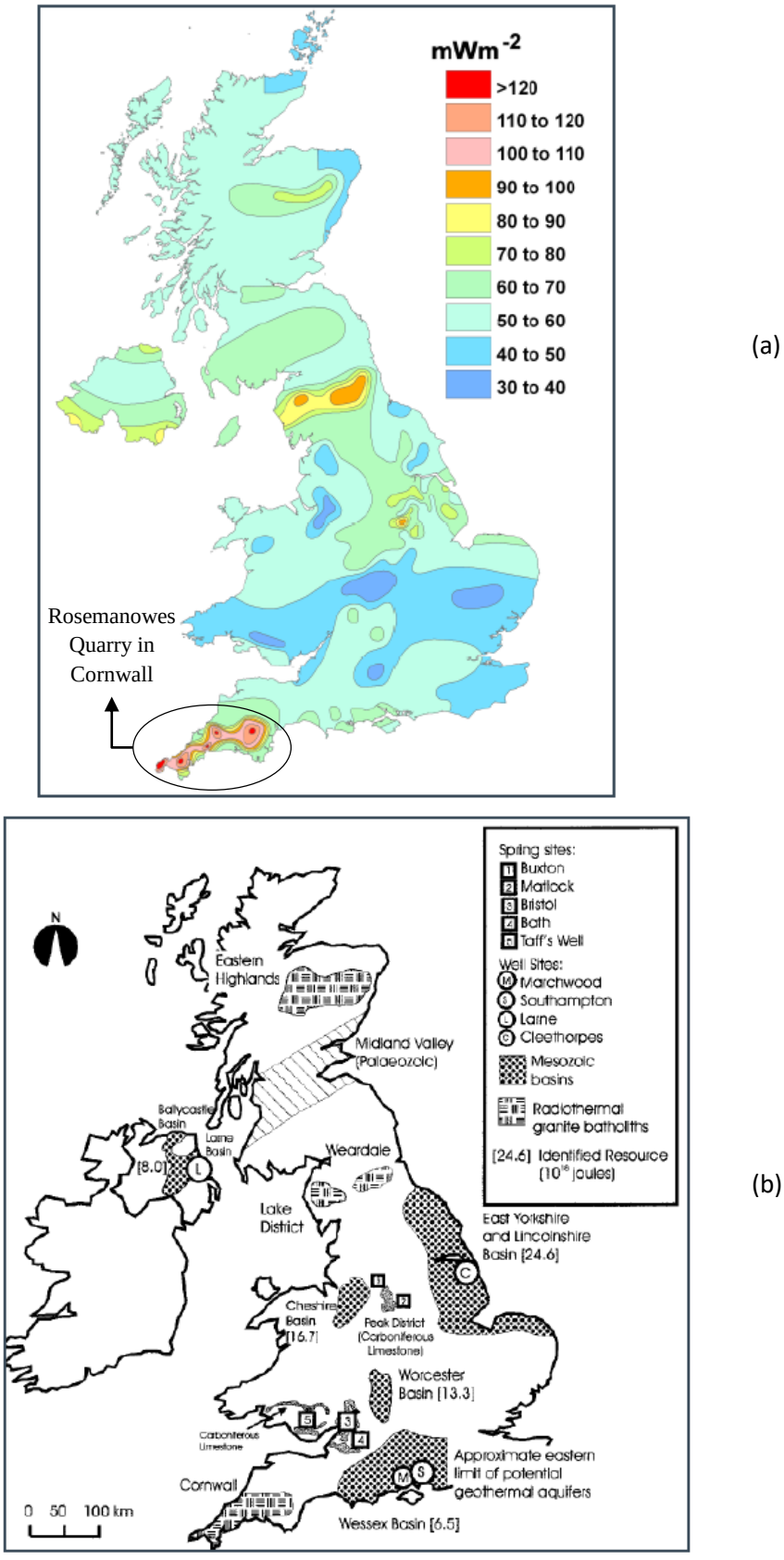

Figure 2-5. Geothermal resources of the UK; (a) Heat flow map and (b) Locations of sedimentary and granite geology (DECC, 2013).

Therefore, the modern process of extracting heat from a deep geothermal reservoir stems from developments in the 1990s. Here, an HDR matrix is subjected to hydraulic fracturing to stimulate the rock at depths over 2.5 kilometres, where temperatures of more than 150 °C exist. This results in the development of the so called Enhanced Geothermal System (EGS), where energy is extracted in the form of hot fluid or steam (Duchane and Brown, 2000).

The experimental work of EGS initially began at Fenton Hill, New Mexico USA (in the late 1970s), using HDR to explore the potential of exploiting geothermal energy for EGS (Duffield and Sass, 2003). Later, many other sites worldwide were selected to carry out field experiments such as Rosemanowes quarry in the UK, Spa Urach in Germany, Soultz in France, Basel project in Swaziland and Ougashi in Japan (Olasolo et al., 2016a).

EGS is a popular option in many countries due to its nature, which is weather dependent, and it is therefore more predictable than other renewable sources of energy (BP, 2015). For example, theoretically estimated that EGS have the potential to produce enough energy for over 5000 years of China's annual total energy consumption (i.e. 95.2×10^{18} Joules in 2010) if just 2% of its EGS resources are recovered (Wang et al., 2013). However, EGS requires advanced technology and high costs, which results in complex challenges for such power source (DECC, 2013, GEA, 2013), and it is therefore still considered to be at the 'proof of concept' stage (Rybach, 2010b).

These challenges have resulted in abandonment of many geothermal projects, e.g. the Spa Urach project, Germany, which started in 1977 but was abandoned in 1981 due to financial problems (DiPippo, 2012). Other examples include the Basel Project in Switzerland and Southeast Geysers in the USA, where the EGS were abandoned due to technical difficulties (see Giardini (2009) and Breede et al. (2013)).

Another key challenge that faces EGS reservoirs is the time taken for the cold fluid front to reach the production well; known as the thermal breakthrough (Gringarten and Sauty, 1975). This problem was first identified by Gringarten and Sauty (1975) during development of an analytical model for a sedimentary reservoir to optimise the distance between the injection and production wells in a doublet system with a constant heat for long-term production.

The thermal breakthrough of the reservoir has been observed in several projects such as the geothermal reservoir in the UK at Rosemanowes Quarry in Cornwell (MacDonald et al., 1992) and the Hijiori hot dry reservoir in Japan (Tenma et al., 2008), which led to the abandonment of both projects. Therefore, extensive research has been conducted to understand and develop methods to overcome the challenges facing the development of EGS reservoirs, by understanding the long-term performance of such systems.

The concept of EGS is based on stimulating a controlled fracture, to facilitate the circulation of fluid through rock in order to extract the heat in the form of hot water or steam. This process involves two stages. The first stage is the hydraulic stimulation of the rock matrix to enhance the permeability to be sufficient for fluid flow as well as to create a man-made reservoir. The second stage is the heat extraction through fluid circulation (i.e. injecting over-pressurised fluid into the injection well and circulating through the engineered reservoir into the production wells) to recover the heated production fluid. Then, after heat conduction in the heat exchanger, the cold fluid recirculates into the reservoir to extract more heat from the engineered reservoir. These experiments are, however, expensive and not viable to be repeated for the same wells due to the progression of irreversible changes in the engineered reservoir and its stimulated fracture system (Jing et al., 2000).

In addition, according to Jelacic et al. (2008), US$300 million to US$400 million is required to invest over 15 years, to test substantial reservoirs in different geothermal environments.

Therefore, for a foreseeable future, numerical analysis is the preferable choice to provide methods to assess and understand the long-term performance of EGS reservoirs under different conditions (Jing et al., 2000).

2.4 Reservoir Heat Production Performance

Even though HDR contains huge thermal storage, EGS is still economically not viable due to the high costs for creation and exploitation processes (Lu, 2018). In addition, the short life span of EGS reservoirs, when the cold front reaches production wells in early stages of the heat exploitation process (Gringarten and Sauty, 1975) and the pressure drop of the reservoir due to the injection of high over-pressurised fluid (Richards et al., 1994), represent further challenges which prevent EGS from being an economically viable alternative renewable energy source. Thus, long-term performance of EGS has been the key point of investigation for researchers over the last three decades (Lu, 2018).

The proceeding sections will present the characteristics and criteria of long-term performance of EGS reservoirs and the developed numerical models of previous research.

2.4.1 Long-Term Performance Characteristics

The long-term performance of EGS reservoirs has been set (based on the experimental data of the Rosemanowes quarry, Cornwall UK) as three characteristics including thermal performance, hydraulic impedance and the ratio of the water loss for long-term production (Richards et al., 1994). Therefore, the performance of an HDR geothermal reservoir has many criteria, based on the aforementioned characteristics (see Sections 2.4.1.1 to 2.4.1.3)

2.4.1.1 Thermal Performance (Thermal Drawdown)

During the heat extraction process, EGS reservoirs are subject to the circulation of injected cold fluid in a closed loop resulting in drop in reservoir temperature per unit time. This

temperature declination is calculated through the production fluid temperature using Equation 2.1 (Gringarten and Sauty, 1975):

$$TD = \frac{T_o - Tpro}{T_o - Tinj} \quad (2.1)$$

where, *TD* is thermal drawdown. T_o, *Tpro* and *Tinj* are initial, production and injection fluid temperatures respectively (K). The performance criterion of thermal drawdown is 0.1, which refers to the reach of fluid's cold front within the production well. This value has been set by Tester *et.al*. (2006) to be 0.1 *TD* is a thermal breakthrough point of an EGS reservoir.

2.4.1.2 Hydraulic Performance (Hydraulic Impedance)

Due to the injection of over-pressurised injection fluid, the reservoir is subsequently subject to a pressure drop as stated by Tester *et.al*. (2006). This results in development of hydraulic impedance within the reservoir, which is defined as, "the difference between inlet and outlet pressure divided by the flow rate at the outlet", and it is calculated using Equation 2.2 (Tenzer, 2001):

$$I_R = \frac{Pinj - Ppro}{q} \quad (2.2)$$

where, I_R is the reservoir impedance, *Pinj* and *Ppro* are the injection and production pressures respectively (MPa) and q is the fluid discharge (l/s). This issue has also been faced by both Rosemanowes (UK) and Fenton hill (USA) (Tester et al., 2006). For the hydraulic performance of an EGS reservoir, the criterion for I_R is set to be within the range of 0.1 to 0.3 (MPa/l/s) (Tenzer, 2001). To overcome the high hydraulic impedance, a high pumping capacity for fluid circulation is required (Tenzer, 2001).

2.4.1.3 Water Loss

This is a fraction of the injected fluid that is not recovered and it is a function of injection pressure and is calculated as an absolute flow rate using Equation 2.3 (Richards et al., 1994).

$$Q = \frac{4\pi r k P}{\mu} \quad (2.3)$$

where, Q is flow rate (l/s); r is radius of a spherical permeable reservoir (m); k is permeability (m^2); P is pressure (MPa) and μ is fluid dynamic viscosity (Pa. s). The performance criterion for water loss is to not exceed 10% of the injected fluid (Richards et al., 1994).

2.4.1.4 Summary

The above aforementioned performance characteristics of EGS reservoirs are dependent on many design parameters. Thus, it is important to investigate the design parameters that affect the long-term performance of EGS reservoirs in order to improve the efficiency of the system.

The following sub-sections review the design factors affecting the performance characteristics of EGS reservoirs.

2.4.2 Factors Affecting Performance Characteristics

Since long-term performance characteristics are function of many design parameters such as reservoir permeability, reservoir initial temperature, pressure and temperature of injected fluid and other parameters, see Equations 2.1, 2.2 and 2.3 in Section 2.4.1. Thus, many design parameters have influences on the long-term performance of EGS reservoirs, which are presented in the following subsections.

2.4.2.1 Reservoir Permeability

Insufficient in-situ permeability of reservoir rock is a key characterisation of any HDR system. Consequently, HDR reservoirs require stimulation of the rock matrix to enhance the permeability of the reservoir, using stimulation techniques to create sufficient volume reservoir for heat extraction. Thus, guaranteeing hydraulic connections between injection and production wells (Tester, 1990).

The low permeability of EGS reservoirs cause pressure drop through EGS reservoirs i.e. hydraulic impedance. Hydraulic impedance is a critical issue affecting the financial aspects of EGS because high pumping power is required for high-pressure drop in order to overcome the low connectivity of EGS reservoirs. Consequently, the process results in high capital cost for the operation process. In addition, in low permeability reservoirs, to maintain the criterion of commercial production mass flow rate of 80 kg/s, high downhole pressures are required, which result in water losses by exceeding the runaway fracture growth (Tester et al., 2006).

2.4.2.2 Reservoir Depth

The depths of injection and production wells are significant parameters, which affect the cost of EGS during creation process. However, and as it was reported by Breede et al. (2013), the depth of EGS reservoirs cannot have a universal value due to the different geology and temperature gradients of EGS reservoirs. The common accepted design parameters assume depths more than 3km and temperature more than 150°C (Jung, 2013). Nevertheless, the complications of the drilling process in such deep and high temperatures impose high costs. However, prescribed fractures are important for creating a flow path between injection and production wells with lower impedance less than 0.29MPa/l/s and a separation of wells of around 600m (Baria et al., 2006).

2.4.2.3 Injection Pressure

Fluid injection pressure is an important factor to be considered as long as the higher pressure increases the production mass flow rate and resulting in high generation of the power plant at initial stages of exploitation process. However, high injection pressures need high capital cost, in addition to its impact on accelerating temperature drawdown during heat extraction over long periods (Tester et al., 1994).

It has been found that the fluid injection pressure increases the fracture aperture near the injected zone due to the high pore-water pressure (which exceeds the effective stress of the fracture), if it is idealised to be without any flow leak-off within the reservoir. However, the aperture of the fractures might reduce due to the flow leak off which produces pore water pressure around the aperture. The thermal stress around the injection well and the production well has significant effects on the aperture size and direction. In other words, the reduction in the temperature of the rock matrix induces the compression of the rock surface due to the cooling process. Thus, it increases the aperture of the fractures within the reservoir (Cheng et al., 2001, Hicks et al., 1996, Lee and Ghassemi, 2010). Furthermore, in low permeability EGS reservoirs, to maintain commercial mass flow rate with low hydraulic impedance, there is a need for high injection pressure. However, high operation pressure requires high costs. In addition, a high injection pressure results in accelerating thermal breakthrough of EGS reservoirs (Polsky et al., 2008).

2.4.2.4 Injection Temperature

Temperature of the injected fluid has a significant influence on the reservoir performance during the geochemical process. According to Seol and Lee (2007), cold water can affect the porosity and the permeability of the reservoir because of geochemical interactions. This interaction results in a cut off for the fluid flow due to the produced calcite in the fractures, as a chemical deposition when the injected fluid has a small temperature value (Tester et al., 2006). It has been reported by McDermott et al. (2006), that to reduce the geochemical influence of the injected fluid, a minimum injection temperature of 50^{o}C should be considered for their research.

2.4.2.5 Wells Number and Configuration

There are two main designs of EGS reservoirs based on the number of wells; 1) doublet well reservoirs and 2) multi-wells reservoirs (Chen and Jiang, 2015).

Doublet wells design has been widely used to explore the energy in EGS reservoirs (Mottaghy et al., 2011, Pang et al., 2015). According to a report by Massachusetts Institute of Technology (MIT), the production target for a commercial EGS reservoir needs to meet a mass flow rate of 80 (kg/s) at a 200 ^{o}C temperature (Polsky et al., 2008). In order to meet this flow rate, high permeability of the fractured zone of the reservoir, high injection pressures (Polsky et al., 2008) and short distances between the injection and production wells are required in a doublet EGS reservoirs (Zimmermann et al., 2010). However, all the three design parameters can have negative impacts on the thermal breakthrough and the hydraulic impedance of the reservoir (Tester et al., 2006, Zimmermann et al., 2010).

It has been reported by Tester et al. (2006) that stimulation of EGS reservoirs is limited to control permeability given its negative impact on accelerating the breakthrough time of the thermal production. Similarly, high injection pressures result in increasing the production mass flow rate, which also accelerates the thermal breakthrough and increases the hydraulic impedance of the reservoir. Same argument as the above can be made for shortening well spaces (Polsky et al., 2008). A significant amount of research has attempted to propose techniques to overcome the problems that lead to premature breakthrough time and hydraulic impedance such as Smit et al. (2014), Biagi et al. (2015), Sun et al. (2018) and others are presented in Section 2.6 of this chapter.

Suggestions have focused on increasing the number of production wells to meet the commercial target of production mass flow rate of EGS reservoirs (Chen and Jiang, 2015, Polsky et al., 2008, Tester et al., 2006). The number of wells and their configurations can significantly

influence the long-term performance of EGS reservoirs given their impacts during both creation and operation processes (Tester et al., 2006). Recently, more research focus on the understanding of the optimisation and investigation of the long-term performance of EGS multi-well reservoirs. A number of numerical studies have been carried out to investigate the design of EGS multi-well reservoirs (Chen and Jiang, 2015, Chen et al., 2015, Fu and Carrigan, 2014, Vörös et al., 2007, Yang and Yeh, 2009).

According to Tester et al. (2006), the rate of heat extraction from a geothermal reservoir depends on the difference between the temperature of the rock and the circulating fluid at any point within the reservoir. The larger this difference, the more quickly heat will move from the rock into the injected fluid and consequently more heat is extracted. However, if the cold injected fluid reaches the production well without being sufficiently heated, the total amount of heat extracted from the rock will be less efficient, and the project will not achieve its performance criteria. Nevertheless, when the extracted fluid has no temperature decline over time, there is insufficient flow rate to extract the heat contained in the rock efficiently. In this case, a project will not be economically optimised because less total thermal energy will be recovered.

Ideally, it is desired to maximise the total amount of useful energy extracted from the reservoir. According to Tester et al. (2006) for an EGS reservoir, the differences of the mass flow rate and the specific enthalpy between injection and production fluid produce a heat extraction rate. High mass flow rate produces a drop in fluid temperature and its specific enthalpy, thus offsetting a potential increase in heat extraction rate. An optimal balance is accordingly achieved between heat extraction rate and thermal drawdown rate at some mass flow rate values. Short distances between the injection and production wells are thus required in doublet EGS reservoirs to maintain high mass flow rate (Zimmermann et al., 2010). However, this has

a negative impact on the thermal breakthrough of EGS reservoirs by accelerating 10% of thermal drawdown in the early stages of the operation process.

According to Jelacic et al. (2008) and Polsky et al. (2008), a production fluid of 80 kg/s with a temperature of 200 ^{o}C is a target for a commercial EGS to be equivalent to a commercial conventional geothermal reservoir. Based on the experimental data, this target cannot be achieved from a doublet well reservoir; therefore, there is a strong need to increase the number of wells and design a multi-well reservoir to maintain the commercial mass flow rate with a minimum temperature of 200 ^{0}C (Chen and Jiang, 2015). This research also could not achieve a target of 80 kg/s for the production mass flow rate for a doublet well design reservoir using numerical modelling, see Section 3-6 for further discussions. However, the main challenge that still remains is to mitigate the thermal breakthrough and the hydraulic impedance for an optimal design of EGS multi-wells reservoir to achieve a cost-effective generation of electricity to meet an economic target, which is expected to reach 0.06 US$/kW by 2030 (Lu, 2018).

2.4.2.6 Spatial Distribution of Temperature (Geothermal Gradient)

According to Tester et al. (1994), the geothermal gradient of HDR reservoirs has a significant effect on the overall cost of the heat extraction project. As can be seen in Figure 2-6, the overall cost of the reservoir is simulated in different temperature gradient ranges 20 to 80 °C/km. With an increase in the gradient, the cost of the drilling is decreased from 95% to 42% of the capital cost. However, the ratio of the stimulation cost to the overall cost increased from 1 %< to 6%. This shows that the drilling cost is most important for consideration, according to the reservoir gradient for modelling an HDR geothermal reservoir. Because of these outputs, developing models with less drilling costs (higher temperature gradients to a point) is significant.

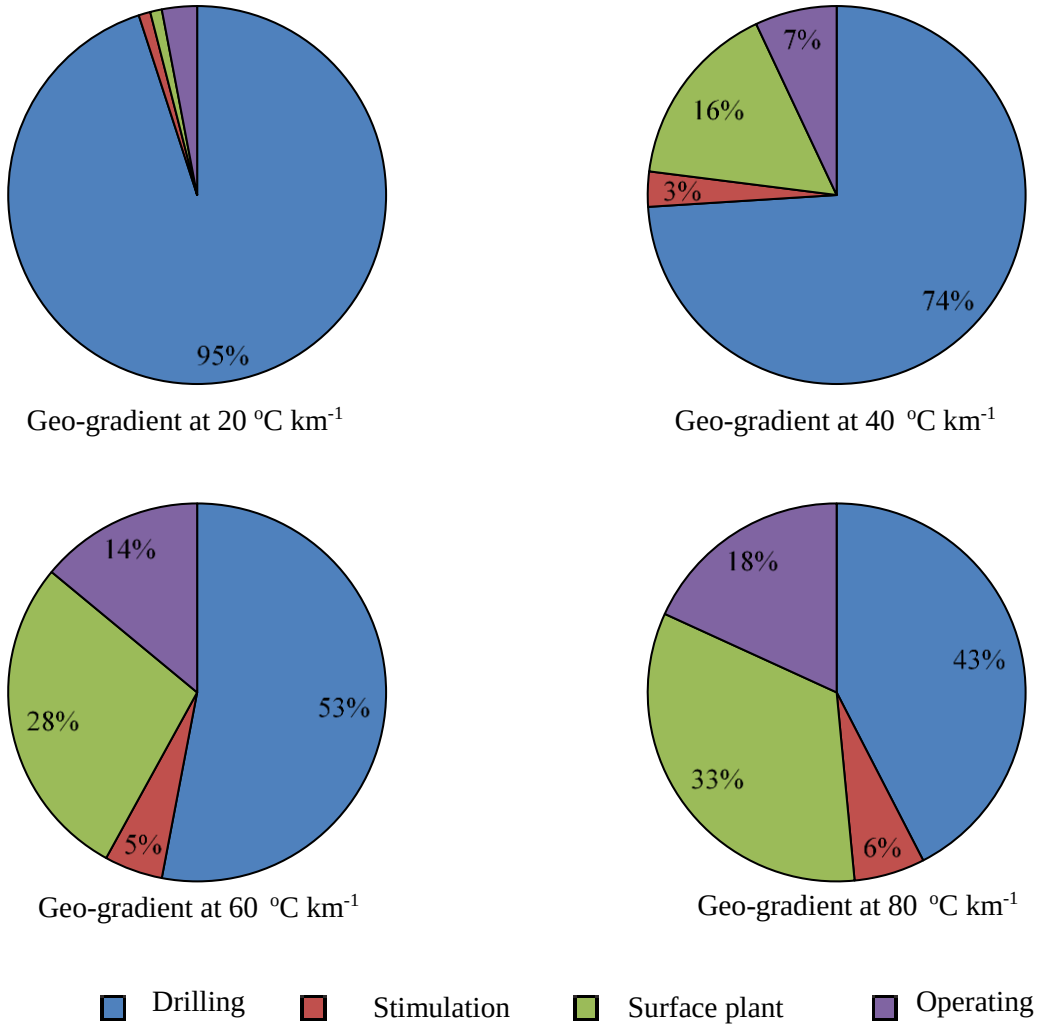

Figure 2-6. The temperature gradient effects on the optimization cost model (Tester et al., 1994)

However, in the case of EGS reservoirs, high temperature gradient exists in very deep reservoirs and the depth of the wells would subsequently affect the drilling cost. It has been stated by Tester et al. (1994) that the drilling cost ranged from 42%-95% of the power plant total cost of EGS reservoirs and was a function of the reservoir depth. Therefore, the determination of the economic feasibility for the overall creation costs of EGS reservoirs is mainly contributed to the cost of drilling wells.

2.4.2.7 Summary

The long-term performance of EGS reservoirs has several characteristics including reservoir lifetime (thermal drawdown), pressure drop in the reservoir (hydraulic impedance), thermal

energy, commercial mass flow rate and the total cost of the system. These features are affected by many factors. However, the impact of the factors on these targets are nonlinear. Therefore, a complex challenge arises during the decision-making process for the design parameters of EGS reservoirs and thus many studies have attempted to find optimum designs for EGS reservoirs.

2.5 Financial Consideration of EGS Reservoirs

The technology of EGS helps to increase the availability of geothermal power worldwide from its rather limited existence in areas with volcanic or tectonic activities to greater depths, which is almost available anywhere in the world (Frei et al., 2013). However, EGS technology has not yet become commercially feasible and the existing EGS pilot plants are solely funded by governments for trails, research and future developments (see Bertani (2012) and Horne and Tester (2014)). Olasolo et al. (2016b) suggested essential tools to estimate and simulate costs of EGS for a better understanding of financial consideration of such renewable source of power. The following subsections outlines the required costs for both creation and operation processes of an EGS system.

2.5.1 Drilling Cost

For drilling process, the total cost of well drilling comprises of steel prices and energy costs including drilling machinery that uses diesel-fuelled and electric generators (Olasolo et al., 2016b). According to Heidinger (2010), drilling costs exponentially increase with the reservoir depth. As it can be seen in Figure 2-7, the cost of well drilling at a depth of 4000m is less than half of drilling cost for a 6000m reservoir depth.

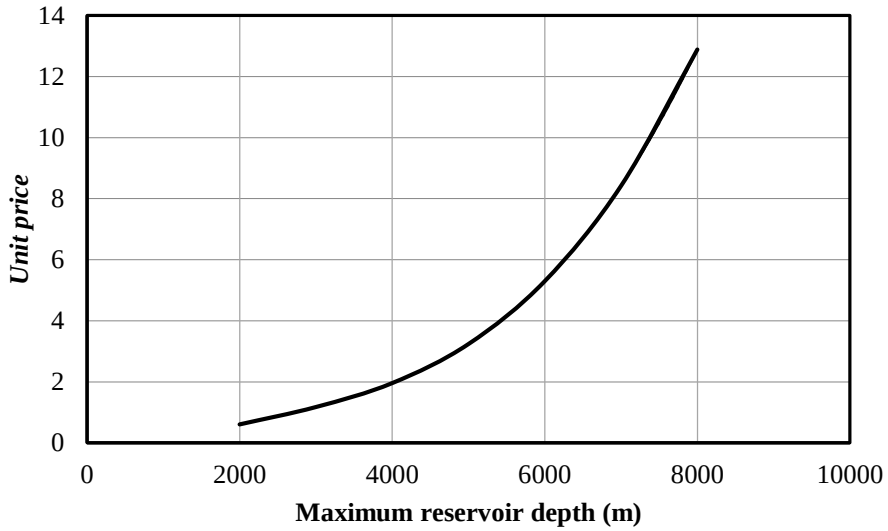

Figure 2-7. The total drilling cost of doublet wells reservoir versus depth (adopted from Heidinger (2010))

Other studies indicate similar trends for example according to Olasolo et al. (2016b), the depth of wells has high impacts on the drilling cost as it is estimated that the drilling cost of two wells to a depth of 3 km would cost €6 M, while it would cost €17 M to a depth of 5 km. Furthermore, additional costs are involved before drilling of wells including the cost of purchase and exploration of the land, which is estimated to be €1 M, and costs of transportation and erection of works machinery and the drilling platform, which is estimated to be €0.5 M.

2.5.2 Re-injection and Production Pumps' Cost

In order to maintain the circulation of injected fluids, pumps are used for both injection well (to re-inject cold fluids) and production wells to upward the heated fluids. This requires significant amount of electricity, which is dependent on many factors, such as productivity rate, mass flow ratios and the losses due to friction and floatability effects (Augustine et al., 2010). The difference in densities between water columns is the main reason to make those factors that affect the required electricity for the re-injection pressure.

In a geothermal reservoir the density of fluids are dependent on three main factors, which are pressure, temperature and chemical composition (Champel, 2006). During thermal drawdown

of the reservoir, the required electricity for the re-injection pressure increases due to the drop of the reservoir temperature (Olasolo et al., 2016b). In a similar way, changes in the other two factors can also have impact on electricity consumption during operation.

According to Olasolo et al. (2016b), the cost of the production pumps is estimated to be €0.8 M, while reinjection pumps can cost 0.1 M. The difference of pump costs is because production pumps are usually installed at a depth of 400 m, which is hard to be maintained. However, re-injection pumps are located at the surface and hence easier to be maintained.

2.5.3 Stimulation Cost

Hydraulic stimulation process of the rock matrix of EGS reservoirs is important in order to enhance their in-situ permeability in order to determine the injection and the productivity rates of each well (Izadi and Elsworth, 2015). According to Heidinger (2010), the process of stimulating an EGS reservoir needs fixed costs of €1 M independently of its depth.

2.5.4 Costs from Incentivized Prices

The applied incentives prices for the type of electricity generation of EGS power plant are vary depending on the country, where the plant is located (Shokri et al., 2014). For example, in Germany, all the generated energy can be sold. While in France, only the energy output, which refers to the difference between the total generated and the parasitic energy consumed by the plant itself, can benefit from incentives set up. Thus, the effective-cost of EGS plant differs obviously from a country to another based on governing regulations (Olasolo et al., 2016b).

2.5.5 Summary

Financial consideration of an EGS reservoir requires a full understanding of the involved total cost including the required costs for drilling, re-injection and production pumps, stimulation of the rock matrix and costs arising from incentivised price for the energy output. In order to

optimise the long-term performance of the system, total cost of EGS reservoirs, including both creation and operation processes, has to be considered. However, the calculation of the total cost requires taking into account the interdependency of design parameters of EGS reservoirs over long periods of exploitation process.

2.6 Computational Modelling

2.6.1 Overview

As mentioned before (see Section 2.3.1.2), numerical simulation is the most favourable method to understand, and assess behaviour and performance of EGS reservoirs. Therefore, several different studies have utilised numerical modelling techniques to model more than 100 geothermal fields worldwide. This was done to study various aspects of HDR geothermal reservoirs, including the influence of coupled physical processes and key design parameters on the behaviour of a reservoir (Stephansson et al., 2004).

In general, simulation of heat extraction in an EGS reservoir involves thermal-hydraulic-mechanical and chemical (THMC) coupled processes (Laughlin et al., 1983, Taron and Elsworth, 2009). The analysis of a coupled THMC process is important for an EGS system (Bower and Zyvoloski, 1997, McDermott and Kolditz, 2006, Tsang, 1991). However, fully coupled THMC processes result in complex mathematical solutions due to the non-linear values of initial and boundary value problems, which require numerical solutions using finite element (FE) methods, finite difference (FD) methods or finite volume (FV) methods (Borja and Aydin, 2004, Borsetto, 1980, De Boer, 2006, Kohl, 1992, Lewis and Schrefler, 1998, Noorishad et al., 1984, Rutqvist et al., 2008).

Nevertheless, Faust and Mercer (1976) conducted an analysis to compare FD and FE techniques for geothermal reservoir simulation; and based on the research results, it is suggested by Faust and Mercer (1976) that the FE method is more suitable for hot-water

reservoirs than the FD model because of the less numerical diffusion and better approximations of boundary and internal geometries with using FE method. Nevertheless, Faust and Mercer (1976) stated that the FD model appears superior for vapour dominated systems, because it reduces mass and energy balance errors and exhibits less numerical oscillation.

For the long-term performance the mechanical and chemical (MC) processes have insignificant influence compared to the thermal hydraulic (TH) processes in the reservoir performance (Neuville et al., 2010). Accordingly, reserchers have studied a full coupling TH processes to optimise the long-term performance of EGS reservoires such as Bedre and Anderson (2012); Bujakowski et al. (2015); Li et al. (2016); Aliyu and Chen (2017a); Benim et al. (2018) and others can be seen later in Section 2.6.

Therefore, for a time-dependent heat transfer with a fully coupled TH processes model, the solution of two sets of differential equations representing the heat transfer in porous media (heat energy conservation) and the mass conservation (fluid flow equation) are required.

2.6.2 Methods to Model Fractured Reservoir Geometry

There are mainly two methods to model the fractured reservoir geometry. The first is discrete fracture network (DFN) and the second is equivalent permeability of the porous media, in which it represents the permeability of both fracture and rock matrix. DFN model is able to simulate the transport of fluid and heat, for ideal and realistic geological structure of reservoirs such as the simulation of Soultz reservoir by Bruel (1995), Kolditz (1995) and Kolditz and De Jonge (2004). However, the applicability of DFN as a general application is limited due to the lack of knowledge of the geometry of the fracture structures (Jing, 2003), and in terms of fully coupled THM analysis, it is still restricted to simplified problems (Walsh et al., 2008). Therefore, equivalent permeability of the porous media is subsequently used to analyse the fully coupled THM and TH processes (Birkholzer et al., 2008).

2.7 Current Studies on Numerical Optimisation of Reservoir Performance

In the late 1960s, the numerical solution of complex non-linear partial differential equations became possible. However, modelling geothermal reservoirs using these techniques lagged behind their applications in groundwater, and oil and gas reservoir modelling because of the additional considerable complexity of the coupling between mass and energy transport in a geothermal reservoir (O'Sullivan et al., 2001). However, since the 1980s, computer modelling has become a standard practice used in the planning and management of the development of geothermal fields (O'Sullivan et al., 2001). Many simulators have been used for EGS reservoir modelling such as TOUGH2, TETRAD, STAR, GEOCRACK, FEHM, FRACTure, GEOTH3D, FRACSIM-3D and others listed in Tables 2-1, 2-2 and 2-3. Each simulator has many capabilities to model EGS reservoirs with its strengths and weaknesses. Therefore, for all EGS projects or at every stage of a given project, a single type of model may not be suitable to be used alone (Sanyal et al., 2000).

Different designs have been numerically simulated to investigate the performance of EGS reservoirs, though the standard design is doublet well reservoirs (Chen and Jiang, 2015) and this is widely used in exploit the energy in EGS reservoirs (Mottaghy et al., 2011, Pang et al., 2015). However, lots of research such as (Bedre and Anderson, 2012, Biagi et al., 2015, Chen and Jiang, 2015, Jiang et al., 2014, Pan et al., 2018, Tenma et al., 2008) attempt to investigate multi wells reservoirs due to its promising to provide commercial targets of EGS designs in terms of mass flow rate and long service life as stated by the MIT report (Tester et al., 2006).

Tables 2-1, 2-2 and 2-3 list various numerical designs carried out to optimise the performance of EGS reservoirs. The objective of these tables is to present key information, such as variables and objectives of optimisation of EGS reservoirs, as well as past and present research on optimisation of reservoir long-term performance. The review was carried out for different categories of simulation of the rock matrix and fracture of the reservoir, which have been

grouped in terms of the simulation of fractures and rock matrix of reservoirs. The first group assumes the reservoir has an equivalent permeability representing both rock matrix and fractures with a single porosity. The second category assumes a discrete fracture network (DFN) with a single porosity. In the third category, the reservoirs are modelled as dual porosity, which considered fractures to have high permeability and low porosity compared to the rock matrix, which contrary has low permeability and high porosity, from which key lessons can be learnt for the current research from the previous studies.

The EGS studies identified in the review tables are classified by numerical methods (2 and 3 dimensional designs), reservoir designs (doublet and multi-well reservoirs), case studies, optimisation techniques, coupled processes and software packages while presenting the variable and optimisation objectives of each research. In addition, Tables 2-1, 2-2 and 2-3 also explain the outcomes of each study by presenting the influence of selected design parameters in the long-term performance of EGS reservoirs. This classification criterion allows an immediate overview of previous research, better appreciation of the challenges faced by EGS (design parameters affecting the long-term performance of EGS reservoirs), and develops an understanding of the level of research and development efforts put into EGS study, and the desire to move such energy source into a commercially viable stage.

Table 2-1. Equivalent permeability

References	Numerical model	Optimisation tool	Optimisation variables	Performance objectives	Outcomes
(Bedre and Anderson, 2012)	**3D** FD, TH, Multi-well reservoir, five spot reservoir in West Virginia, USA	Parametric study using a two-level (L=2) Plackett-Burman design based on numerical results of TOUGH2	Reservoir temperature, Injection flow rate and temperature, Porosity, Rock thermal conductivity, Water loss and well spacing	Net discounted amount of heat extracted	• Reservoir temperature is the most effective parameter in heat production. • Both porosity and rock thermal conductivity have insignificant influence in reservoir performance. • The amount of heat extracted from a reservoir decreases with high injection fluid temperature. • Large distances between wells increase thermal productivity of the system due to increase reservoir volume of heat extraction.
(Zeng et al., 2013)	**3D** FD, TH, two horizontal wells, Desert Peak, USA	Parametric study using TOUGH2-EOS1 code	Reservoir permeability, mass flow rate and injection temperature	Electricity production power and energy efficiency.	• Electricity production power mainly depends on the water production rate and the injection temperature. • Fluid flow impedance mainly depends on the reservoir permeability, fluid production rate and injection temperature. • Energy efficiency mainly depends on the reservoir permeability and the water production rate. • Low depth of production wells requires lower investment and operation costs.
(Jiang et al., 2014)	**3D** FV, TH, Multi-well reservoir, An imaginary EGS	Parametric study using CFD flow solver (Fluent)	Number of production well	Production temperature and reservoir service life.	Triplet reservoir is more efficient than doublet reservoirs

(Smit et al., 2014)	**2D** FE, TH, Doublet well, West Netherlands Basin.	Automated gradient-based optimization method using COMSOL Multiphysics	Optimize well-doublet placement and layouts in a homogeneous reservoir and heterogeneous reservoir.	Net Present Value (NPV) of EGS projects.	• Well spacing has significant impact on the long-term performance of reservoir; and there is an optimum well spacing for doublets that can improve the lifetime of reservoirs. • Different doublet layouts can optimise heat production of the reservoir. It is concluded that a checkers-board well arrangement is more effective than a tram-rail well arrangement.
(Biagi et al., 2015)	**2D** FD, TH, Multi-well reservoir, West Virginia, USA.	GA-TOUGH2	The CO2 injection rate is optimised for both constant mass and constant injection pressure.	CO2 injection rate and heat extraction rate.	• Mass flow rate has high influence in maintain the temperature profile of production well. • Investigating optimum injection pressure is important for the reservoir long-term performance through sustaining both temperature profile and heat extraction of the system.
(Chen and Jiang, 2015)	**3D** FE, TH, Multi-well reservoir	Parametric study using CFD flow solver, Fluent®	Number of wells	Heat extraction performance.	The HDR heat recovery factors significantly depend on the well layout, whereas relatively slight dependence on the parameters like the reservoir permeability, the geothermal gradient, the fluid flow rate, and the fluid injection temperature.
(Cheng et al., 2016)	TH, doublet reservoir, Fenton Hill, USA	Parametric study using the SIMPLE (Semi-Implicit Method for Pressure Linked Equations) algorithm made in FORTRAN program	Average reservoir and surrounding formation permeability, geothermal gradient, the distance between the injections well and reservoir centre, well spacing, reservoir volume, open-hole length, injection and production pressure.	Production temperature and flow rate, water loss rate and heat extraction rate.	• Breakthrough time depends on water loss and production flow rate. • High reservoir permeability increases water loss through surrounding boundaries, resulting in decreasing heat extraction rate. • Wells on the edge of the reservoir result in restrained of heat extraction rate. • Maximise reservoir volume with a fixed well layout has insignificant impact on heat extraction value. • Lower production pressure efficiently enhances heat extraction due to reduce water loss rate and increase production mass flow rate.

(Kong et al., 2017)	**2D** FE, TH, Doublet reservoir,(Tanggu district of China)	Parametric study using OpenGeoSys (OGS)	Optimize well-doublet placement	The ratio of heat price to electricity price	It is concluded that the optimal distance is related more to the ratio of heat price to electricity price than the single parameter of heat or electricity price
(Sun et al., 2018)	A single horizontal wellbore reservoir (idealized reservoir)	Parametric study using numerical method on space.	Optimise fluid (CO2) injection parameters pressure, mass flow rate and temperature	Geothermal energy extraction rate	• Injection rate is significantly affecting geothermal production efficiency, because high injection rate requires a high injection pressure, which can exert too much requirement on the equipment. • Large mass flow rate and low injection temperature are required to achieve a higher geothermal energy extraction rate.
(Pan et al., 2018)	**3D** FD, TH, multi-well reservoir, geothermal systems in Mexico	Parametric study using TOUGH2 (T2Well/ECO2N) code	Injection flowrate and temperature, well spaces and the penetrating depth of the production wellbore into the reservoir, reservoir permeability	Pressure difference between injection and production well, production temperature, net heat flow and CO2 mass fraction.	• Reservoir pressure management and heat extraction are influenced by well layout, the penetrating depth of the production wellbore into the reservoir, mass flow rate and temperature of injected CO2, and reservoir permeability. • The thermosiphon characteristics of the system affects by CO2 injection temperature.

Table 2-2. DFN models

References	**Numerical model**	**Optimisation tool**	**Optimisation variables**	**Performance objectives**	**Outcomes**
(Tenma et al., 2008)	**3D** FE, TH, multi-well Two layered reservoir, Hijiori HDR, Japan	Parametric study using Finite Element Heat and Mass (FEHM) solver and applied to simulations of the LTCT.	Injection rates in both reservoirs.	Heat production rate.	Manipulation of injection flow rates and well depths are important to control and optimize the net thermal output of a complex HDR geothermal reservoir.
(Held et al., 2014)	**3D** FE, multi-well reservoir, TH, Soultz-sous-Forˆets, France	Parametric study using FRACTure	Number of wells for operation process	Levelised cost of energy.	The lowest levelised cost of energy (LCOE) could be with high, but not maximum production.
(Kalinina et al., 2014)	Fracture continuum model (FCM), TH, Multi-well reservoir,	Parametric study using Fracture continuum model (FCM)	Well directions (i.e. horizontal, inclined and vertical wells), fracture properties, well separation and stimulation volume.	Optimise production efficiency	The length of the injection interval, well separation distance, and fracture properties are significant design parameters that affect thermal performance of EGS reservoirs.
(Chen et al., 2015)	TH, Multi-well reservoir, Superstition Mountain Geothermal	A multivariate adaptive regression spline (MARS) technique prospect (SMG)	Optimal well placement and control re-injection well location and production rate.	Net profit value	Reservoir service life and thermal production are very likely to be over-estimated by optimizations without appropriate constraints on natural conditions.

(Bujakowski et al., 2015)	**3D** FD, TH, doublet well reservoirs, Polish Lowland area (central Poland))	Parametric study using TOUGH2	Volume and permeability of the artificially fractured zone and pump flow rate	Energy performance and net plant power	• The power consumed by the circulating pumps that stimulate the flow governs the net power of EGS system. • Volume and permeability of the artificially fractured zone control energy performance of EGS plants.
(Li et al., 2016)	**3D** Finite fracture spacing analytical solution, TH, doublet horizontal wells, Soultz-sous-Forˆets, France	Built-in Matlab optimization function "fmincon."	(1) flow rate, (2) the number of fracture stages, (3) the spacing between the wells, (4) total well length, and (5) reservoir transmissivity	Present value (PV) of revenue of an EGS doublet and thermal drawdown.	• Stimulating with multiple stages greatly improves economic performance, delays thermal breakthrough, and allows a higher flow rate to be circulated through the system. • At low well spacing and low number of stages, it is optimal to circulate fluid more slowly than the maximum possible rate in order to delay thermal breakthrough.
(Pandey and Vishal, 2017)	**3D** FE, THM, doublet wells, Soultz-sous-Forˆets, France	Parametric study using Finite Element Heat and Mass (FEHM) solver	Wells distance, reservoir permeability and geothermal gradient.	Thermal drawdown and the net energy output.	• High permeability of the reservoir increases water loss inside the reservoir. • Increasing the distance between wells, improve heat extraction performance. • More heat extraction occurred in higher geothermal gradients, but steep decrease of production temperature, Energy and pressure drop inside the reservoir.
(Li et al., 2018)	**2D** FD, TH, Doublet-well reservoir, Northern Songliao Basin, northeast China	Parametric study using TOUGH2-EOS1 code	Correlation distance and coefficient of variation for the random field model.	Heat production performance.	• Spatial variability of the hydrological parameters has significant influence on the heat production performance. • Correlation distance and coefficient of variation are two key parameters that influence the distributions of reservoir parameters and cause the variation of heat production performance in random field models.

(Song et al., 2018)	**3D** FE, TH, Multilateral-well, Soultz-sous-Forˆets, France	Parametric study using COMSOL Multiphysics	Four well arrangements comprise three types of multilateral-well EGS.	Thermal power, production temperature, heat extraction ratio and accumulative thermal energy of the multilateral-well EGS.	The heat extraction performance of the multilateral-well EGS is more efficient than conventional double vertical wells EGS.
(Benim et al., 2018)	**3D** FV, TH, Multi-well (triplet wells reservoir)	Parametric study using CFD code ANSYS Fluent	Injection fluid flow rate, different depths of the production well.	Production temperature, investment costs and operation costs.	• Low depth of production wells requires lower investment costs and lower operation costs because smaller pressure drops through the system. • It is important to investigate a favourable flow rate to maintain sufficiently high production temperature over 20 years.

Table 2-3. Dual porosity models

References	**Numerical model**	**Optimisation tool**	**Optimisation variables**	**Performance objectives**	**Outcomes**
(Shook et al., 2004)	**3D** double-porosity FD, TH, Geysers, U.S	Parametric study using TETRAD	Formation properties and operational variables (working injection fluid, injection temperature)of wellbore heat exchangers (WBHX)	Production temperature and thermal energy rate	• Formation thermal properties have significant impact on production temperature (i.e. large thermal conductivities and thermal diffusivities improve energy extraction. • Interchanges exist between the heat capacity of injection fluid and production temperature, which concluded that water have optimal properties as a working fluid.
(Sanyal and Butler, 2005)	**3D** double-porosity FD, TH, Desert Peak, U.S	Parametric study using TETRAD	Number of production wells, injector-producer spacing, stimulated thickness, enhancement level (fracture spacing and permeability) and production rate.	recoverable heat fraction to rock temperature	Well configuration, fracture spacing and permeability has insignificant impact on recovery factor as long as the stimulated volume exceeds 1e8 meter cubic.
(Sanyal, 2010)	**3D** FD, TH, Desert Peak, U.S	Parametric study using TETRAD	Production well number, injector-producer spacing, stimulated thickness, enhancement level (fracture spacing and permeability) and production rate.	(a) Net generation profile (net generation versus time over project life), (b) net power produced per unit injection rate, and (c) heat energy recovery factor.	• Small injection and projection rates, reduces thermal drawdown and consequently, more commercially attractive net generation profile can be achieved. • Heat recovery is low with low injection and projection rates. • Improving permeability without reducing fracture spaces has small impact on heaty recovery. • Increasing stimulation volume increases the generation power of the system. • For a constant fracture spacing and permeability, average net generation is linearly proportion with stimulation volume and it is independent of well configurations.

(Aliyu and Chen, 2017b)	**3D** FE, TH, Multi-well reservoir, Soultz-sous-Forˆets, France	Parametric study using COMSOL Multiphysics and factorial experimental	Artificial design parameters (Injection fluid parameters, such as temperature and pressure, and Lateral well spacing; naturally-occurring parameter such as geothermal gradient, permeability, thermal conductivity and porosity	Production temperature.	The results showed that artificial design parameters have more influence in the reservoir performance, while the naturally occurring parameters has less impact.
(Aliyu and Chen, 2017a)	**3D** FE, TH, Multi-well reservoir, Soultz-sous-Forˆets, France	Parametric study using COMSOL Multiphysics	Injection fluid parameters, such as temperature and pressure, and Lateral well spacing	Production temperature.	Injection flow rate is more efficient, in terms of reservoir productivity, than injection temperature and lateral well spacing.

Overall, Tables 2-1, 2-2 and 2-3 capture a detailed analysis of 25 studies. Based on each simulation category (i.e. equivalent permeability, DFN and dual porosity):

1) From the information provided in Tables 2-1, 2-2 and 2-3 shown earlier, it appears that EGS research is currently under development as the reservoir long-term performance compiled reservoir service life; effective thermal production power and commercial feasibility have not been yet numerically achieved. Overcoming problems, gaining experience and trying to introduce advanced methodologies to optimise the long-term performance of EGS reservoirs are therefore active research areas.
2) The presented research already concluded that relevant understanding is needed for the optimisation of EGS, its commercial feasibility and analogy for upcoming developments in this aspect.

Essential issues that need addressing for the optimisation of EGS long-term performance were discussed and the corresponding lessons learnt were highlighted as follows:

1) For the reservoir geometry, well placement in doublet well reservoir designs and well numbers and configurations in multi-well reservoir designs, have the main impact on a reservoir's thermal production rather than the size of stimulated reservoir when wells configuration is constant (Kong et al., 2017).
2) Defining an optimum value of mass flow rate that satisfies both thermal power, reservoir lifetime and operation cost is significantly important for the optimisation of EGS long-term performance.
3) The natural design parameters such as porosity, rock thermal properties (thermal conductivity and diffusion) have insignificant impacts on thermal production power. However, reservoir temperature has significant impacts on the thermal production

power. Nevertheless, high temperatures exist in deep reservoirs, which requires high drilling cost and results in negative impacts on the total cost of EGS reservoirs.

4) Artificial design parameters (injection and production flow rate, reservoir permeability, wells layout and configuration) have the main impact on the long-term performance of EGS reservoirs.
5) The heat extraction process involves a coupled thermal-hydraulic-mechanical and chemical (THMC) process in the subsurface reservoir (Karrech, 2013, Taron and Elsworth, 2009). However, most of the presented studies ignored the impact of the MC processes because they have insignificant impact on a reservoir's long-term performance compared to TH processes.

All the studies reviewed in Tables (2-1, 2-2 and 2-3) considered the optimisation of the reservoir long-term performance using each single design variable rather than a combination of many design variables. The main optimisation techniques that were used in the presented 25 cases were parametric study, GA integrated with FD, fmincon and multi variate adaptive regression spline (MARS). All the employed optimisation techniques in the literature were able to find optimum solutions for reservoir designs through testing single variables. However, in order to optimise the long-term performance of EGS reservoirs, it is important to build a robust methodology taking into consideration multiple variables and multiple objectives during the optimisation technique. Such methodology will be crucial to tackle complex interdependency of contributing factors and their non-linear behaviour.

2.8 Factors Induce Complexities in Optimisation of EGS Reservoirs

This section presents the factors that affecting the numerical analysis of the long-term performance of EGS reservoirs in terms of increasing challenges during optimisation process.

2.8.1 Inter-Relationship between Design Parameters

The complex inter-relationship between design parameters and non-linear and nontrivial behaviour in terms of contract impact on reservoir output (thermal production power and service life), inducing many challenges for both research development and industry's ability to develop methods to find optimum solutions of long-term performance of EGS reservoirs (Grippi, 2018). In addition, the operation cost consists of electricity cost for the hydraulic head down of production wells and additional cost due to the reservoir thermal breakthrough (Kong et al., 2017). Thus, the complex interaction of reservoir design parameters also affects the capital cost of the system in terms of operation cost since it has a non-linear impact on the reservoir service life (thermal breakthrough time). Consequently, a single variable (design parameters) and a single objective (power or economy) would not be appropriate enough to find optimum solutions (Kong et al., 2014). To overcome these complex interactions between EGS design parameters, a robust methodology for an optimisation method is required.

2.8.2 The Characterisation of Fracture

The exact geometry of the existing and stimulated fractures is quite difficult to apply to the numerical models, particularly when the model is used to investigate the long-term performance of EGS reservoirs. This is a consequence of the difficulty of estimating the fracture orientation, location, density and spaces between fractures (Long et al., 1982). In addition, during the heat production process, fracture design (i.e. aperture, permeability and geometrical shape) may change (Zeng et al., 2013). Consequently, challenges during the modelling of fractures in EGS reservoirs are in terms of explicitly representing fracture distribution, particularly the variations of fracture aperture versus local effective stress. Furthermore, fracture design would change in terms of rock deformations due to shear failure and the effect of self-propping and the relationship between fracture aperture and fracture conductivity in addition to the impact of

thermo-elastic and mineral deposition and dissolution on rock deformation (Sanyal et al., 2000). The poro-elastic deformation can reduce the aperture of the fracture if leak-off happened, which induces pressure around the fracture. In contrast, the thermo-elastic deformation can increase the fracture aperture with time due to the induced thermal stress (Sanyal and Butler, 2005). Therefore, many researchers have attempted to apply the assumption of constant equivalent permeability for the reservoir, see Table 2-1.

2.8.3 Computational Efficiency

The performance of an HDR geothermal reservoir has been measured using experimental tests such as the Rosemanowes quarry in Cornwall in the UK. The test data showed that the performance of the reservoir was significantly affected by the boundary conditions. With the increase of the injection pressure, the hydraulic impedance can be improved. However, the higher mass flow rate yields cool down of the reservoir and thus early thermal breakthrough of the reservoir (Richards et al., 1994). The selected boundary conditions of the fracture domain within the model can be considered as critical inputs, as it has a significant consequence on the degree of freedom within a finite element simulation because of the different permeability values of the fracture and the impermeable rock matrix. Therefore, assumptions are applied to the fracture as being an internal part within the matrix and the Numen boundary condition is applied to the fracture boundary (Romano-Perez and Diaz-Viera, 2015). The coupled THMC processes are another factor, which induce a complexity to the computational stage and it is computationally expensive (Kalbacher et al., 2008, Wang and Kolditz, 2007, Watanabe et al., 2009).

2.8.4 Summary

Reservoir design parameters (such as well configurations, numbers and depth), reservoir materials (such as permeability), fracture properties, and management parameters (such as injection flow rate, pressure, temperature and fluid type) have complex interconnectivity. Thus, have significant impact on EGS long-term performance of EGS reservoirs. In addition, both closing of fractures or degradation due to scaling may equally occur over time during heat exploitation. The change in fracture, in this case, may have the least impact on the long-term performance.

Furthermore, the potential area of heat extract around the injection well decreases significantly in the early stages of the circulation process. The significance of the effect of this area depends on the performance criteria set in the modelling.

2.9 Conclusions and Identification of Key Gaps in Knowledge

This chapter reviewed the development and types of geothermal systems particularly for deep geothermal reservoirs. The review also included the long-term performance characterisations of EGS reservoirs and their criteria. In addition, the numerical techniques used to simulate heat production of EGS reservoirs were considered in this chapter. The focus of this chapter was to review the existing reservoir optimisation techniques used to understand the long-term performance of EGS reservoirs in order to render the system that is commercially feasible for development or continued exploitation. The review concluded the following points:

- The review showed that HDR reservoirs have insufficient in-situ permeability to achieve commercial exploitation. However, a reservoir can be assumed as a huge heat energy resource if the system is artificially enhanced to recover the stored heat, through application of EGS approaches.

- EGS has been shown to be a promising source of power as it can be an appropriate energy source for electricity through the optimisation of design parameters of reservoirs. However, considering the non-linear interrelation of the reservoir design parameters making a decision on the long-term performance of a reservoir through a single variable is a complex issue.
- In addition, the objectives of the long-term performance of EGS reservoirs show contradictory behaviour with the optimisation variables. It is worth noting that to achieve the commercial feasibility of EGS, the cost of the system, both during and post design, are important. However, it is significantly influenced by the interconnectivity of design parameters over long periods of exploitation. Thus, the economic objective leads to increase in the complexity of the optimisation process.
- Different optimisation techniques have been used in previous research to investigate optimum solutions for EGS reservoir designs. However, they have overlooked to take into consideration the interdependency of reservoir design parameters and its impact on the efficiency of the system.

Consequently, to overcome all of these challenges, a robust optimisation framework is necessary. Such framework requires consideration of the non-linear interrelation of reservoir design parameters and the total capital cost that include all costs up to the end of the reservoir service life. These goals can be achieved by identifying the optimum values of the critical design parameters yielding an efficient long-term performance of EGS reservoirs.

CHAPTER THREE

3 RESEARCH METHODOLOGY

3.1 Introduction

This chapter describes the proposed methodology to optimise the long-term performance of EGS reservoirs. In this chapter, the assumptions applied for EGS reservoirs during the numerical analysis are presented by providing justifications drawn from previous research studies available in the literature. Next, the governing equations involved in the research are presented in detail. In addition, details about economic analysis, the genetic algorithm and the proposed optimisation technique are also presented in this chapter. Parts of this chapter have been published in Samin et al. (2018).

The objectives of this research mainly consist of investigating applicability of a new optimisation approach for the long-term performance of EGS reservoirs. This was achieved through identifying the economically accepted thermal drawdown and thermal power production for EGS reservoirs over long periods. The methodology applied in this research is based on a hybrid optimisation approach to understand the enhancement of the long-term performance of EGS reservoirs. The hybrid technique is an integration of FE and Multi-Objectives GA to achieve the optimisation objectives, which are maximising reservoir life span, minimising the reservoir impedance and cost, and the maximisation of the thermal power production, see Section 2.4.1, Chapter Two.

Figure 3-1 presents a flow chart of the methodology that demonstrates both challenges and the proposed solutions in the current research study.

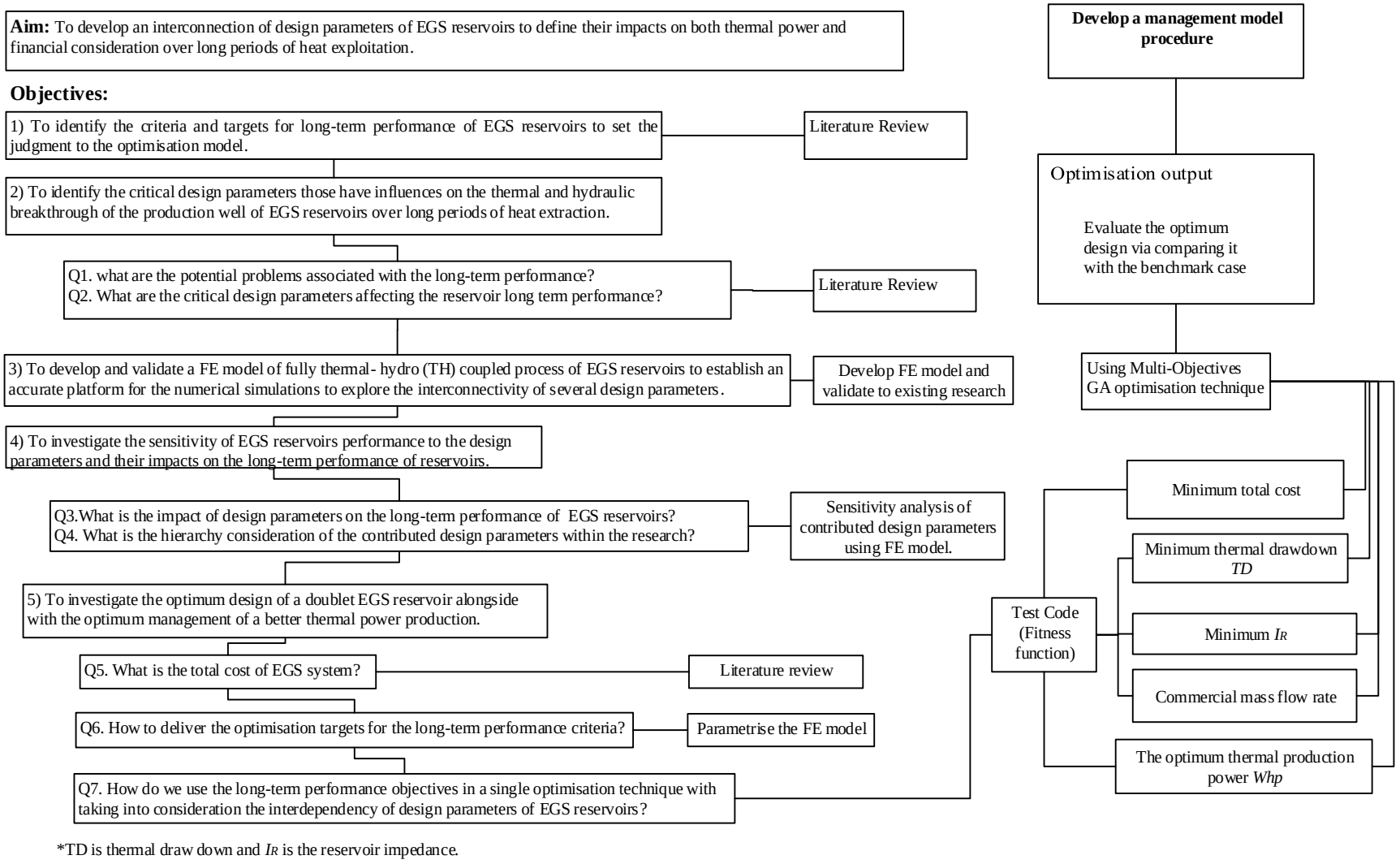

Figure 3-1. Flow chart of the research methodology

Based on previous research studies presented in the literature review (Chapter Two), artificial design parameters tend to have a dominating impact on the reservoir's long-term performance. Thus, in this research, the focus is laid onto finding optimum solutions for designing EGS reservoirs through testing the artificial design parameters of EGS reservoirs. Therefore, the variables of the optimisation technique were the artificial design parameters, such as well numbers and configurations, reservoir depth, fluid injection pressure and temperature, and the equivalent permeability of the reservoir.

The proposed variables involved in different parts of the numerical modelling. These parts include reservoir materials, initial and boundary conditions, reservoir geometry, and design. However, many challenges face the optimisation process due to the complex inter-relationship between design parameters and their behaviour. This is in terms of contradicted impacts on reservoir outputs. Nevertheless, considering all of these variables in a single optimisation process would result in a better understanding of EGS long-term performance through taking into consideration the interdependence of the contributed parameters.

GA has the potential to optimise problem objectives with large and complex search spaces without requiring any function derivative and it is based on function evaluation only (Javadi et al., 2012b). The decision to use such techniques is therefore in line with the aim of this research.

The development of FE models for doublet and multi-wells reservoirs are presented in Chapters Four and Six respectively. Two case studies are considered as benchmarks for both designs. The Spa Urach in Germany is used for the doublet well reservoir and the Soultz-Sous-Forêts in France is used for the multi-well reservoir design, (see the location of both case studies in Figure 3-2). More details about both case studies are presented in Chapters Four and Six.

The following sections present the FE modelling and GA processes used in this research.

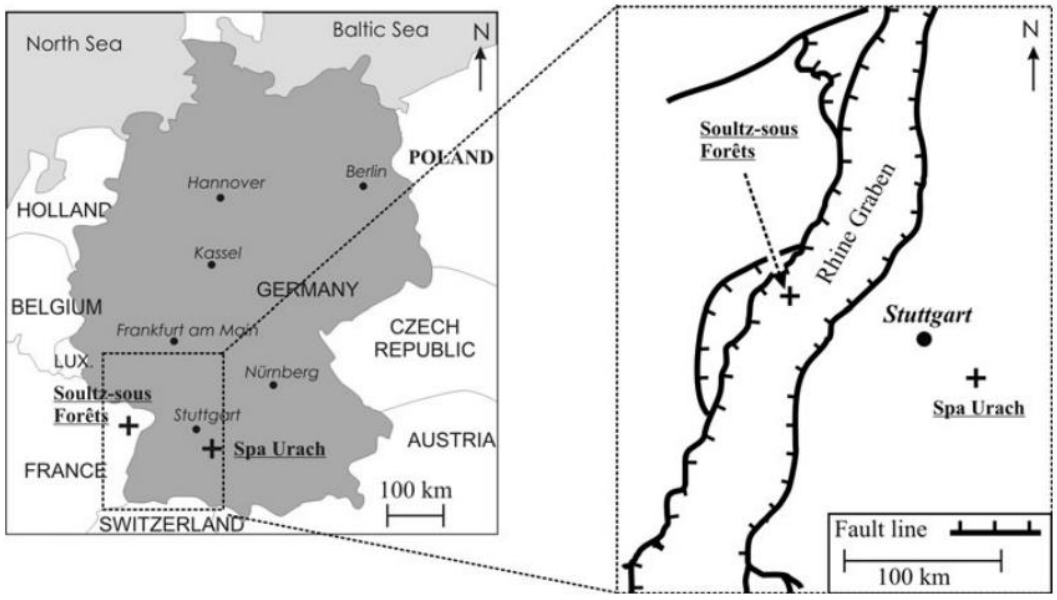

Figure 3-2. Locations of Spa Urach and Soultz-Sous-Forêts sites (Tenzer et al., 2010)

3.2 Development of Methodology

Engineering problems can be mathematically defined in a model of physical conditions, which consist of a set of differential equations representing the physical situation in terms of variables (Moaveni, 1999, Reddy, 2006). To achieve the solution for some mathematical models using exact methods is difficult, if not impossible. Thus, numerical methods are routinely used as an alternative or sometimes the only way to achieve approximate solutions (Reddy, 2006).

Faust and Mercer (1976), conducted an analysis to compare FD and FE techniques for geothermal reservoir simulation; and based on the research results, it was suggested that the FE method is more suitable for hot-water reservoirs than the FD model due to the lack of numerical diffusion and better approximations of boundary and internal geometries with using FE method. Nevertheless, they stated that the FD model appears superior for vapour dominated systems; because it reduces mass and energy balance errors and exhibits less numerical oscillation.

However, reservoir design parameters have complex influences on the long-term performance of reservoirs and have nonlinear interdependency with other parameters. Consequently,

decision-makers face a great challenge when optimising reservoir designs. Furthermore, reservoir design parameters influence different parts of numerical analysis including reservoir geometry (number and configurations of wells), materials (reservoir permeability) and boundary and initial conditions (pressure and temperature of injection well and reservoir depth), hence contributing to complexity of the problem.

Compared to FD, FE is more efficient for the integration with GA as a result of more accurate approximations of boundary and internal geometries, thus less numerical diffusion than FD (Faust and Mercer, 1976). Therefore, in this research, the FE model was selected to integrate with multi-objective GA to consider the interdependency of reservoir design parameters and its impact on the long-term performance of EGS reservoirs.

Recently, COMSOL Multiphysics software package has been widely used for FE method simulation of geothermal modelling. This is used as a method of computing the power generation of renewable sources due to its high efficiency in solving complex coupled processes (Aliyu and Chen, 2017b, Aliyu and Chen, 2017a, Aliyu and Chen, 2018, Daanen et al., 2012, Ekneligoda and Min, 2014, Maier et al., 2012, Saeid et al., 2013, Smit et al., 2014, Sun et al., 2018). In this research, COMSOL Multiphysics has been used to solve differential equations for heat transfer in porous media for both doublet and multi-wells reservoirs (see Chapters 4, 5, 6, and 7).

To calculate thermal power, a variety of objectives was considered. These objectives include the reservoir service life (thermal drawdown), reservoir impedance, production mass flow rate and the total cost of the system.

3.2.1 Assumptions Applied for the Numerical Modelling

In this research, the COMSOL Multiphysics package is employed to carry out a three-dimensional (3D) transient model for both EGS reservoir designs i.e. doublet well and multi-well designs. To do so, the following assumptions are applied for the FE model to reduce the degree of freedom and thus avoid a computationally expensive modelling:

1. The reservoir is assumed to be a fully saturated porous medium because of the water loss phenomena (Evans, 2010, Hayashi et al., 1999, Tester et al., 2006). This may continue forever and cause the water to distribute into the micro-fractures of the reservoir during the creation process of the reservoir. Hence, the reservoir rock remains fully saturated for long periods of the heat exploitation (Brown et al., 1999, Brown, 1991, Duchane, 1993, Murphy et al., 1999).
2. In addition, water loss is ignored and thus the injection flow rate equals to the production flow rate. This assumption is viable as long as the reservoir is considered a fully saturated porous media (Pashkevich and Taskin, 2009, Sanyal and Butler, 2005, Vörös et al., 2007).
3. The reservoir is considered to have an equivalent permeability representing both rock matrix and fractures. This assumption is applied because the simulation of exact fracture distributions, the hydraulic and thermal coupled process and its impact on the fracture increase the complexity of the numerical modelling of EGS reservoirs (Sanyal et al., 2000). This complexity will not add any benefits to the optimisation process and can even cause problems for the computational efficiency.
4. The fracture and therefore equivalent permeability is assumed to be unchanged during exploitation, because of both the degradation due to fracture scaling and enhancement of fractures due to the thermal contraction of the rock with time are occurring during

the heat exploitation (Sanyal and Butler, 2005). Other studies (Pruess, 1990, Sanyal et al., 2000, Sanyal et al., 2005, Watanabe et al., 2010, Willis-Richards and Wallroth, 1995, Zeng et al., 2013) have also applied this assumption.

5. A fully coupled TH process is assumed for the physics involved during the optimisation development. Because, while simulation of heat extraction in an EGS reservoir involves thermal-hydraulic-mechanical and chemical (THMC) coupled processes (Laughlin et al., 1983, Taron and Elsworth, 2009). For the long-term performance, the mechanical and chemical (MC) processes have insignificant influences compared to the thermal hydraulic (TH) processes in the reservoir performance (Neuville et al., 2010). Accordingly, researchers have studied a full coupling TH processes to optimise the long-term performance of EGS reservoirs such as Bedre and Anderson (2012); Bujakowski et al. (2015); Li et al. (2016); Aliyu and Chen (2017a); Benim et al. (2018) and others can be seen in Section 2.6. Thus, the conservation equation of energy and mass balance were used for the 3D transient model to predict the generated thermal power of EGS multi-well reservoirs.
6. The temperature of the injected fluid assumed to be constant at the surface of the reservoir by ignoring temperature gradient of the subsurface. This assumption is applied in order to reduce the complexity of the modelling because the temperature gradient of the subsurface is not constant and has different values (Genter et al., 2010).

The primary focus of this project is to find optimum solutions for thermal production of EGS reservoirs. While alternative methodologies have been used in the past to optimise one or more objectives of EGS performance (as described in Chapter Two). However, they have considered contributed parameters in isolation and therefore failed to present a holistic approach that take into account all elements of the problem.

3.2.2 Governing Equations

For a time-dependent heat transfer with a fully coupled TH processes model, the solution of two sets of differential equations representing the heat transfer in porous media (heat energy conservation) and the mass conservation (fluid flow equation) are considered in this research.

3.2.2.1 Governing Equations of Heat Transfer

Heat energy conservation and mass balance are the governing equations for the coupled TH processes. The conservation of energy is applied for the heat transfer in porous media because the energy movement in such an environment is due to a difference in temperature. Hence, the mathematical model of heat transfer in porous media is represented by Equation 3.1 (Kolditz and Clauser, 1998):

$$\left(\rho c_p\right)_{eff} \frac{\partial T}{\partial t} + \rho_w c_{p_w} \mathbf{u}.\nabla T + \nabla.\mathbf{q} = \mathrm{Q} \tag{3.1}$$

$$\mathbf{q} = -\lambda_{eff} \nabla T \tag{3.2}$$

$$\left(\rho c_p\right)_{eff} = \theta \rho_w c_{p_w} + (1-\theta)\rho_r \, c_{p_r} \tag{3.3}$$

$$\lambda_{eff} = \theta \lambda_w + (1-\theta)\lambda_r \tag{3.4}$$

where ρ, ρ_w, ρ_r are the equivalent, fluid and rock matrix density, respectively (kg/m^3). c_p, c_{p_w}, c_{p_r} are the equivalent, fluid and rock matrix heat capacity at constant pressure (J/(kg.oC)), $\left(\rho c_p\right)_{eff}$ is the equivalent volumetric heat capacity at constant pressure, $\lambda_{eff}, \lambda_w, \lambda_r$ are the equivalent, fluid and rock matrix thermal conductivity (W/(m.^{o}C)), **u** is the Darcy velocity (vector), T is the temperature (^{o}C), θ (dimensionless) is the porosity of the rock matrix and *Q* is the heat source/sink term, and **q** is the conductivity heat flux of the rock matrix (vector).

In this research, since the reservoir is assumed fully saturated; there is no fluid flow in the surrounded boundary of the rock matrix. Consequently, no heat flux at the boundary is assumed. Thus, Q was zero during the optimisation process.

In addition, the porosity θ is assumed as constant and the fluid parameters are considered to be both pressure and temperature dependent in order to guarantee fully coupled TH processes. Thus, fluid properties were the governing parameters for the transient study because they changed over time during the heat extraction process.

3.2.2.2 Governing Equations of Fluid Flow

In the hydraulic process, the mass conservation is applied for the FE model. For instance, in the fluid porous media flow, Darcy's Law is used to balance the mass. Thus, the mathematical model of the subsurface fluid flow in porous media is represented by Equation 3.5 (Kolditz and Clauser, 1998):

$$\frac{\partial}{\partial t}(\theta \rho_w) + \nabla.(\rho_w \mathbf{u}) = Q_f \tag{3.5}$$

$$\mathbf{u} = -\frac{k}{\mu}\nabla p \tag{3.6}$$

where, θ is the porosity of the rock matrix and ρ_w is the fluid density (kg/m^3); $\mathbf{u}$ is the Darcy velocity (vector); k is the permeability of the porous media (m^2); μ is the fluid dynamic viscosity (Pa.s); Q_f is the fluid sink/source term, and p is the fluid pressure (Pa). Darcy's Law is used because the fluid flow is assumed laminar.

Q_f is assumed zero in this research as long as the reservoir boundaries are considered no flow allowed.

3.2.3 Thermal Model

Taking into account the long-term performance of EGS reservoirs and based on the previous studies in Chapter Two, two optimisation objectives are considered for the thermal model; i) thermal drawdown and (ii) accumulative thermal power. These objectives have been selected as fitness functions for the optimisation process in this research based on the literature (e.g. see (Bödvarsson and Tsang, 1982, Pruess, 2006, Tester et al., 1994). Each of these performance objectives is briefly described below:

3.2.3.1 Thermal Drawdown (TD)

Thermal drawdown is described in detail in Chapter Two, Section 2.4.1. According to the MIT report 2006 (Renner, 2006), when EGS reservoirs reach thermal breakthrough time, the reservoir is considered depleted. Therefore, further power that is produced during the numerical analysis is disregarded.

3.2.3.2 Accumulative Thermal Power (∑Whp)

Thermal power of a reservoir is the heat production power of EGS and it is calculated based on the first law of Thermodynamics (Pruess, 2006), see Equation 3.7:

$$Whp = q(h_{pro} - h_{inj}) \tag{3.7}$$

where, h_{pro} and h_{inj} (J/kg) are the production and injection specific enthalpy; q (kg/s) is the mass flow rate of the fluid. The accumulative thermal power is calculated up to the end of the reservoir service life, which occurs at the breakthrough time. Thus, the accumulative thermal power is calculated using Equation 3.8 (Samin et al., 2018):

$$\sum W_{hp} = \sum_{t=0}^{J} W_{hp} \tag{3.8}$$

J (years) is the number of years at the reservoir breakthrough time; t (years) is the time of exploitation at the thermal breakthrough of the reservoir.

In the case of multi-well reservoirs, the accumulative thermal power is considered as a total power production of EGS reservoir design.

3.2.4 The Economic Model

The total cost of EGS reservoirs can be defined into two main parts: namely, the creation cost and the operation cost over time, see Section 2.5. This is explained in detail in the following subsections.

3.2.4.1 Creation Cost

According to Tester et al. (1994), the total drilling cost of boreholes is a high fraction (about 70% as a conservative value) of the total capital creation cost of EGS. In this thesis, the drilling cost (C_D) of wells was considered as a key parameter for the evaluation of the economic analysis using an empirical model proposed by Lukawski et al. (2014). Their model was used as it provides a reasonable estimate of cost due to similarities in the conditions under consideration, and the fact that any economic analysis can only be at best, an estimate. The model provides an estimated drilling cost per each well as a function of depth using Equation 3.9.

$$C_D = 1.72 \times 10^{-7} \times (Dh)^2 + 2.23 \times 10^{-3} Dh - 0.62 \quad (3.9)$$

where, *Dh* (m) is the depth of the reservoir base. Equation 3.9 shows that the drilling cost increases non-linearly with the increase in the reservoir depth.

In the case of multi-well reservoirs, the drilling cost is considered for all the wells within the multi-well reservoir. Thus, the total drilling cost ΣC_D (millions USA$) is calculated using Equation 3.10.

$$\Sigma C_D=(Npw+1)\times C_D \quad (3.10)$$

where, *Npw* is the number of production wells in a multi-well reservoir design.

3.2.4.2 Operation Cost

The operation cost of heat extraction (C_e) of EGS reservoirs is calculated based on Equation 3.11 by Kong et al. (2017).

$$Ce = q.\sum_{t=0}^{J}\frac{(\Delta P.pp + \rho_l.c_l.\Delta T.pr.\eta)_t}{(1+r)^t} \quad (3.11)$$

While, for multi-well reservoirs, exploitation cost can be calculated using Equation 3.12.

$$Ce = N.q.\sum_{t=0}^{J}\frac{(\Delta P.pp + \rho_l.c_l.\Delta T.pr.\eta)_t}{(1+r)^t} \quad (3.12)$$

where, *N* is the number of production wells; q (m^3/s) is the exploited fluid volume; *J* (years) is the number of years at the reservoir breakthrough time; t (years) is the time of exploitation; ΔP (Pa) is the pressure change at the production well; *pp* (US$/kwh) is the electrical power price; *pr* (US$/GJ) is the heat price; *r* (%) is the discount rate with time, a very important parameter during the economic analysis to take into consideration the time value of money (see International Energy Agency in 2012 (IEA, 2012)); ΔT(K) is the change in production temperature and η is the efficiency of the power plant.

Thus, the total cost (C_t) of the reservoir, can be calculated using Equation 3.13:

$$C_t = C_w + C_e \quad (3.13)$$

In the present study, the long-term performance of EGS is achieved via maximising thermal power *Whp* and minimising both the thermal drawdown *TD* and the total cost C_t using a multi-objective optimisation strategy.

3.2.5 The Genetic Algorithm Optimisation Technique

This section presents an overview of the principles of genetic algorithm (GA) including selection, crossover and mutation operations. The required formulations to develop a multi-objective GA is also presented by introducing the implementation of multi-objective optimisation algorithm to optimise EGS reservoir designs.

3.2.5.1 Genetic Algorithm Stages

Genetic algorithm (GA) is an optimisation technique in which its basic operations represent biological processes. It has the potential to optimise objectives with large and complex search spaces without requiring function derivative and it is based on function evaluation only (Javadi et al., 2012b). GA solves problems through a random generation of numbers of populations with specific upper and lower limits for involved variables. GA involves three main operators including selection, crossover and mutation operators (Boschetti et al., 1996).

Since the GAs search a population of points rather than a single point, it is therefore an efficient optimisation technique in locating the global optimum. The operation of selecting the fittest individuals and creating a new population of solutions using the genetic information mating and the mutation operation enable the genetic algorithm seeking to maximise the fitness of the population.

The following subsections presents the three main operators of GA.

3.2.5.1.1 Selection Operators

In GA, the selection operator has a significant role during the optimisation process. This operator controls the selection of individuals with high fitness more often than lower fitness ones in order to improve populations throughout the generations (Francisco, 2013). According

to Holland (1975), the fitness of an individual (f_i) to the total fitness of (N) population refers to the probability (P_i) of selecting an individual for the next generation using Equation 3.14:

$$P_i = \frac{f_i}{\sum_{i=1}^{N} f_i} \tag{3.14}$$

where, P_i is the probability of individual selection; f_i is individual fitness and N is the number of population.

Selection operator is the principle of pushing the population of GA towards a final solution based on the measurement of objectives.

The first step of selection is assigning a fitness measure to each individual based on the optimisation objectives. Then, a rule for selecting individuals based on the fitness measures is used to create the next generation (Boschetti et al., 1996). For this process, there are different methods to select individuals, including linear normalisation selection (Davis, 1987), and parent selection (Cavicchio, 1970); each method has its influence in premature convergence, which has the risk of trap the optimisation in a local minimum.

Compared to the parent selection, the normalised selection ranks the individuals based on their fitness and thus, selects the number of offspring for the next generation that will be proportional to its rank position. Therefore, this process has a high selection pressure, which allows for a fast convergence. However, that which appears disadvantageous is the fact that it concentrates on most of the population in a small space. Contrastingly, the parent selection method, regardless of the individual fitness, is allowed to generate only one offspring. The individuals are randomly coupled using crossover operation to create two offspring. The selection is then based on the better fitness of the created offspring and their parents. The better fitness between offspring and parents is substituted in the population of the next generation. Although this

method has low selection pressure, it has a low risk of premature convergence (Boschetti et al., 1996).

3.2.5.1.2 Crossover Operators

Crossover is the coupling operator of two individuals to create an offspring, and it is a key stage in GA. The responsibility of crossover is to create offspring more fit than their parents through exchanging information between solutions (Francisco, 2013).

Equation 3.15 shows the random selection of one or more crossover points and the genes exchanging between parents (Francisco, 2013):

$$paranet1 = [P_{f_1}, P_{f_2}, P_{f_3}, P_{f_4} \uparrow, P_{f_5}, P_{f_6}, P_{f_7}, \ldots . P_{f_{Nvar}}]$$

$$paranet2 = [P_{m_1}, P_{m_2}, P_{m_3}, P_{m_4} \uparrow, P_{m_5}, P_{m_6}, P_m, \ldots . P_{m_{Nvar}}] \quad (3.15)$$

$$offspring1 = [P_{f_1}, P_{f_2}, P_{f_3}, P_{f_4}, P_{m_5}, P_{m_6}, P_{m_7}, \ldots . P_{m_{Nvar}}]$$

$$offspring2 = [P_{m_1}, P_{m_2}, P_m, P_m, P_{f_5}, P_{f_6}, P_{f_7}, \ldots . P_{f_{Nvar}}]$$

In this research, an intermediate crossover is used with an optimum ratio of 0.7 based on trial and error method for the proportion of a population that is mated after each generation.

3.2.5.1.3 Mutation Operators

A mutation operator has the responsibility to change some parameter values randomly in selected individuals, in which it helps to maintain genetic diversity in the population through recovering lost genetic materials and the random distribution of genetic information (Francisco, 2013). Low probability of mutation increases the chance of keeping good individuals present in the population (Boschetti et al., 1996). In this research, the mutation was kept low at a value of 0.25 to generate the decision variables within the upper and lower limits.

3.3 The Proposed Optimisation Approach

Understanding the enhancement of the long-term performance of deep geothermal reservoirs is important for decision-makers and geothermal engineers in order to design optimum commercial geothermal reservoirs. This research presents an optimization approach based on multi-objective genetic algorithm (GA) integrated with numerical simulation models of fully coupled thermal-hydraulic process, which is utilised as a way to find optimum designs of EGS reservoirs.

3.3.1 FE Integration with GA

To implement the hybrid optimisation technique used in this research, FE models are integrated with Matlab using the COMSOL Matlab LiveLink tool in order to be benefit from robust GA toolbox and available library in Matlab. This step allows the use of Matlab and its toolbox to pre-process, model manipulate and post-process of the EGS models, which is necessary while building new designs using the GA technique.

Through the COMSOL and Matlab LiveLink, the outputs of the FE simulation are used as inputs in the Matlab to build the fitness function of the GA, see Appendix B. The fitness function of the optimisation process is divided into four main steps:

1. Define the variables and their constraints. The optimisation variables in this optimisation process are related to geometry, material and boundary and initial conditions. The variables were normalised for a range of 0 to 1, with which 0 refers to the minimum value and 1 refers to the maximum value of variables' constraints. Normalisation of the values allow to draw conclusions independence of particular geometry and conditions.

2. Then, the fitness function calls the COMSOL model with the selected variables to run the new design. At this stage, the normalisation is reversed to perform FE analysis.
3. The outputs from the COMSOL model including temperature, mass flow rate, enthalpy, density and viscosity of both injection and production wells, are used as inputs in the fitness function to calculate the objectives (thermal draw down, impedance, thermal power and EGS total cost) and make a decision of the viability of the selected model.
4. In the fitness function, both thermal power and reservoir total cost are considered and presented in the Pareto front. Other performing indicators such as thermal drawdown, reservoir impedance and the commercial mass flow rate are considered implicitly during the optimisation process. This had been considered through applying the long-term performance criteria as conditions within the fitness function as follow:
    - Thermal drawdown after 10 years≥10%.
    - Reservoir Impendence > 0.1 (MPa.s/l).
    - Mass flow rate ≥ 80 (kg/s).

Since the reservoir is assumed as fully coupled TH, and since the fluid properties are considered as temperature and pressure dependent, matrices are calculated for the reservoir thermal draw down, mass flow rate and impedance to define the long-term performance criteria. Once any of these criteria are met, the reservoir is considered to be at the breakthrough time.

In the hybrid optimisation technique (i.e. combined FE and GA), the objectives of the reservoir long-term performance are repeatedly computed using the simulation model and their values subject to the control variables.

The actual *Whp* and *Ct* are calculated in the GA code based on the outputs of the FE, by changing the design parameters, selected by genetic operators. The efficiency value (cost value)

is finally evaluated taking into account overall population for several generations to select the best design of the proposed EGS reservoir. Different scenarios can therefore be taken randomly to search the optimum EGS systems based on GA (Abd-Elhamid and Javadi, 2011, Javadi et al., 2012a, Javadi et al., 2012b).

This approach was adopted to model the optimization approach to control seawater intrusion (Abd-Elhamid and Javadi, 2011), the optimisation of auxetic materials (Javadi et al., 2012b) and the optimisation of the mass flow rate of CO_2 in EGS reservoirs (Biagi et al., 2015). In addition, GA has proven quite successful in optimisation and understanding other subsurface systems such as petroleum reservoirs and hydrogeological systems (Artus et al., 2006).

There are two sets of design parameters in EGS affecting the long-term performance of geothermal reservoirs, which are natural and artificial parameters (Bedre and Anderson, 2012). Since the natural parameters are related to the geology of the area and are ungovernable, in this study, the controlled (artificial) design parameters are considered for the optimisation process. These parameters are 1) the maximum reservoir depth *Dh*; 2) the distance between the injection and production wells *d*; 3) the fluid injection pressure *Pinj* and Temperature *Tinj*; 4) the equivalent permeability of the reservoir *k* and 5) number of wells *N*.

In this research, first the model is a transient three-dimensional (3D) reservoir, which considers constant values of *Pinj*, *d*, *Dh*, *k* and *N*. However, through the Multi-Objectives GA evolution, the 3D model is transformed in variables *Pinj*, *d*, *Dh*, *k*, and *N*. The fully coupled thermal-hydraulic TH process is solved with the finite element model. Then, the results are evaluated in the fitness function to find the cost of the proposed objectives in each generation of the optimisation process. Figure 3-3 represents the flow chart of the FE analysis and Multi-Objectives GA integration.

The finite element model is developed using the approach implemented in COMSOL Multiphysics solver for the fully coupled thermal-hydraulic processes. In addition, the multi-objectives GA in the Matlab toolbox is employed. This provides an influent manipulation of optimisation parameters such as rate of mutation, number of individuals in each generation and the rate of natural selection. Therefore, it is easy for GA to diverse the optimisation of complex problems. At the end of the proposed generations, the best costs of the objectives are dependent on seeking the optimal design of EGS reservoir.

It is worth mentioning that at earlier stages of this PhD, Open Geosys (OGS) software was used for the FE modelling of this research; see some preliminary results in Appendix C. However, due to technical difficulties in integrating OGS and GA, OGS was replaced with COMSOL Multiphysics, which produces more flexibility in this regard.

The proposed methodology in this research provides a medium to compile both management and design stages to model a cost effective design of EGS reservoirs at the preliminary decision making stage. Figure 2-3 shows the proposed optimisation flow chart.

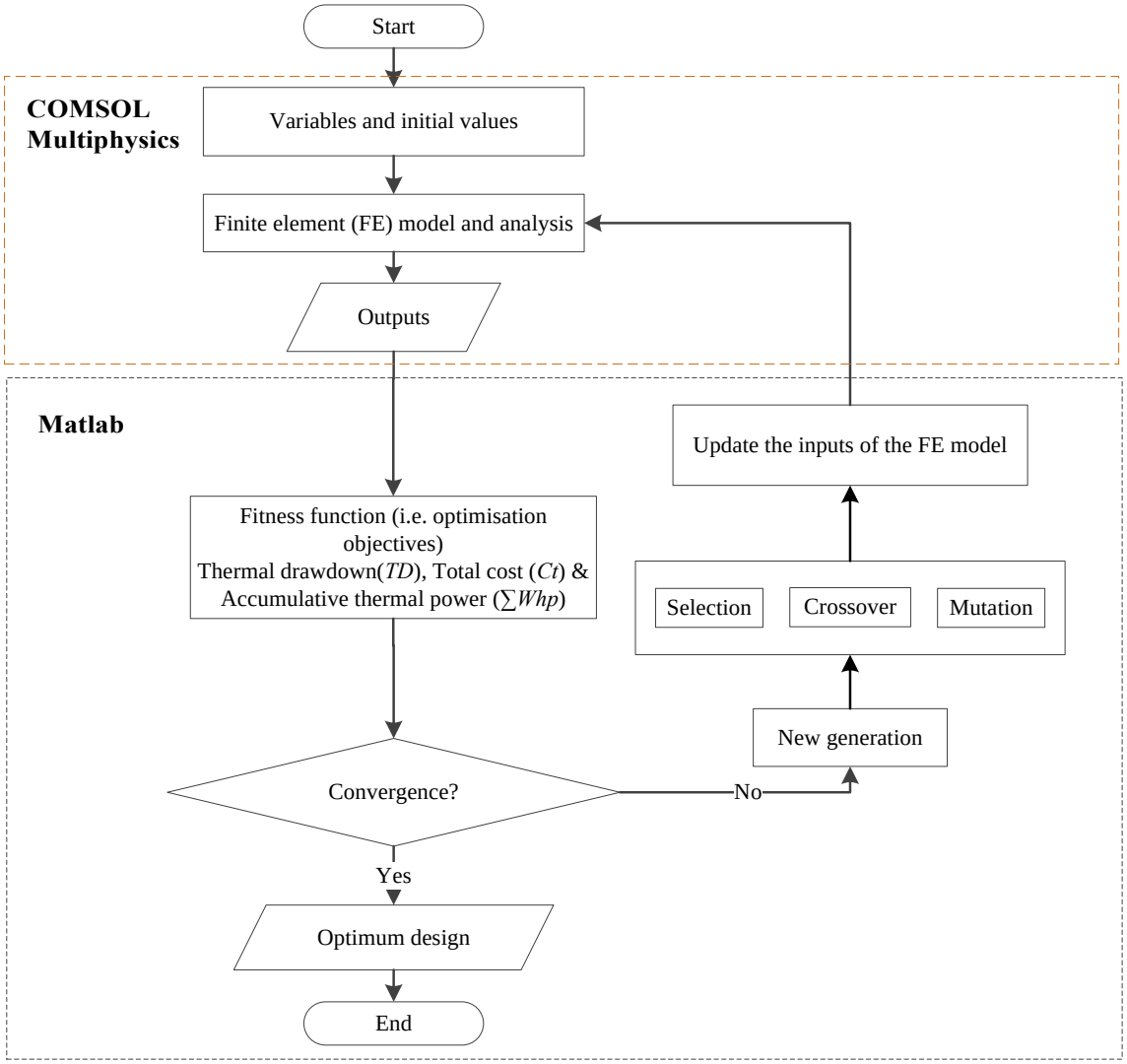

Figure 3-3. Integration of FE analysis with the Multi-Objectives GA flow chart (Samin et al., 2018)

CHAPTER FOUR

4 FINITE ELEMENT DEVELOPMENT FOR DOUBLET WELLS RESERVOIR

4.1 Introduction

This chapter describes the FE model of a doublet wells reservoir, which was built using COMSOL Multiphysics code. In addition, it also presents a parametric study conducted to investigate the sensitivity of the reservoir performance to the artificial design parameters. This chapter is a part of published results in Samin et al. (2018).

4.2 The Finite Element Model (FEM)

This research employs the single porosity model in which it assumes the hot reservoir as a medium with single porosity. In addition, the work presented here considers the equivalent permeability of the fractured zone to be anisotropic. The local thermal non-equilibrium is also adopted and a fully coupled TH processes are assumed. Thus, in this research, the governing equations of heat transfer and fluid flow are employed; see Chapter Three, Sections 3.2.2. Appendix A presents a brief explanation the software package used in finite element analysis.

The following subsections describe the development of the FEM in details.

4.2.1 Geometry and Material Properties

The Spa Urach geothermal reservoir in Germany is considered as a benchmark scenario for the doublet well reservoir design. A three dimensional finite element model is developed to simulate the reservoir between 3,850 m and 4,150 m depth as shown in Figure 4-1. The temperature gradient is 0.03 ^{o}C/m and the reservoir is a doublet well system of an injection and production well at a separated distance of 400 m, see Figure 4-1. The equivalent fracture zone

permeability is assumed to be 1.53e-15 m^2 in x direction and it is 3/8 of *kx* in y and z directions (Rutqvist et al., 2008). Material properties of both solid and fluid are presented in Table 4-1.

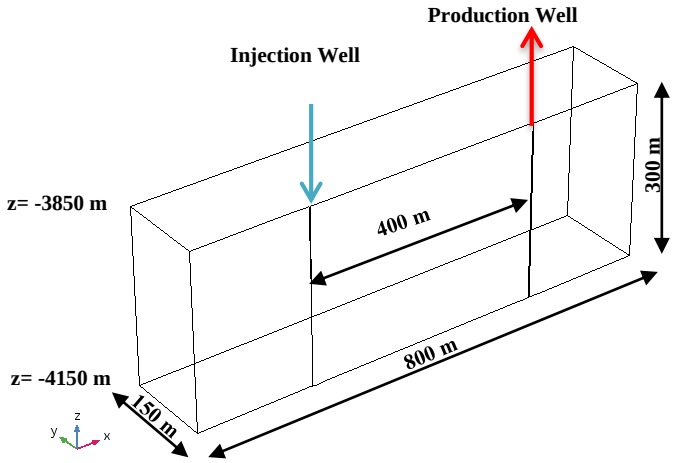

Figure 4-1. The 3D geometry of the doublet well reservoir for EGS simulation for the present FE model, based on the benchmark site

Table 4-1. Geometrical parameters and material properties of the FE model (adopted from Watanabe et al. (2010)).

Parameters		*Symbols*	Value	Unit
Rock matrix	Domain length	L_r	800	m
	Domain width	W_r	300	m
	Domain height	H_r	300	m
	Reservoir surface depth	D_s	3850	m
	Reservoir base depth	*Dh*	4150	m
	Density	ρ_r	2750	kg/m^3
	Permeability	k	*kx*=1.53e-15, *ky*=*kz*=3/8**kx*	m^2
	Porosity	$\emptyset$	0.005	
	Specific heat capacity	c_{p_r}	850	$J/(kg.^oC)$
	Thermal conductivity	λ_r	3	$W/(m.^0C)$

Injection fluid	Density	ρ_f	1000	kg/m^3
	Specific heat capacity	c_{p_f}	4210	J/(kg.^{o}C)
	Thermal conductivity	λ_f	0.6	W/(m.^{o}C)
	Dynamic viscosity	μ	2e-4	Pa.s
Others	Well length	L_w	300	m
	Well diameter	d_w	1	m
	Well separation	d	400	m
	Reference temperature at 4445.0 m	T_{ref}	162	^{o}C
	Temperature gradient	T_g	0.03	^{o}C/m

4.2.2 Initial and Boundary Conditions

There are two sets of initial and boundary conditions in the present work. The first set is the thermal condition of the reservoir and the injection well. The second set is the hydraulic condition of the reservoir and the pressure in both injection and production wells.

4.2.2.1 Initial Conditions

The initial condition of the model for both sets is represented in Figure 4-2. The initial condition of the temperature is assumed to be a linear depth-dependent distribution and the temperature gradient (T_g) of the Spa Urach site is 0.03 ^{o}C/m (Watanabe et al., 2010). The reference temperature (T_{ref}) at a depth of 4445.0 m is 162 ^{o}C and the initial distribution of the temperature in the reservoir is calculated by Equation 3.1 (Watanabe et al., 2010):

$$T_\circ = T_{ref} + T_g(-4445 + z) \quad (4.1)$$

where, z is depth (m).

4.2.2.2 Boundary Conditions

For the boundary temperature conditions of the model, it is assumed that the fluid injection temperature is 50 ^{o}C at the injection well (McDermott et al., 2006). For a constant injection temperature, the Dirichlet boundary condition is applied for the injection well. For the hydraulic and thermal boundary conditions of the reservoir, the reservoir is assumed fully saturated; thus, there is no fluid flow in the surrounded boundary of the rock matrix (Pashkevich and Taskin, 2009, Sanyal and Butler, 2005, Vörös et al., 2007). Consequently, no heat flux at the boundary is assumed. To guarantee these assumptions, the Neumann boundary condition using Equation 4.2 and Equation 4.3 is applied for the surrounded rock matrix surfaces. The injected fluid is assumed to have a pressure of 10 MPa at the surface of the site and it increases linearly as an over-pressurised fluid with depth as stated by McDermott *et al.* (McDermott et al., 2006) by using Equation 4.4; while the production well is assumed to be under-pressurised by -10 MPa on the top surface linearly varies according to Equation 4.5.

$$\mathbf{n} \,.\, \rho_f \mathbf{u} = 0 \tag{4.2}$$

$$\mathbf{n} \,.\, \mathbf{q} = 0 \tag{4.3}$$

$$Pinj = \rho_f g z + 10 \text{ (MPa)} \tag{4.4}$$

$$Ppro = \rho_f g z - 10 \text{ (MPa)} \tag{4.5}$$

where, *Pinj* and *Ppro* are the injection and production fluid pressure (MPa), **n** is the normal vector to the boundary.

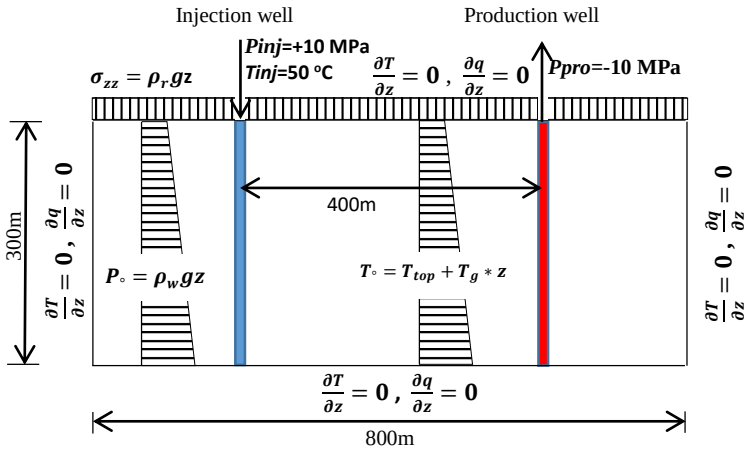

Figure 4-2. Initial and boundary conditions for the numerical model (adopted from (Watanabe et al., 2010))

4.2.3 Meshing

The mesh used for the presented model consists of predefined fine mesh applied to the injection and production wells and grows outwards to the area surrounding the wells. This predefined mesh is important to control the fluid mass flow rate and heat transfer, see Figure 4-3.

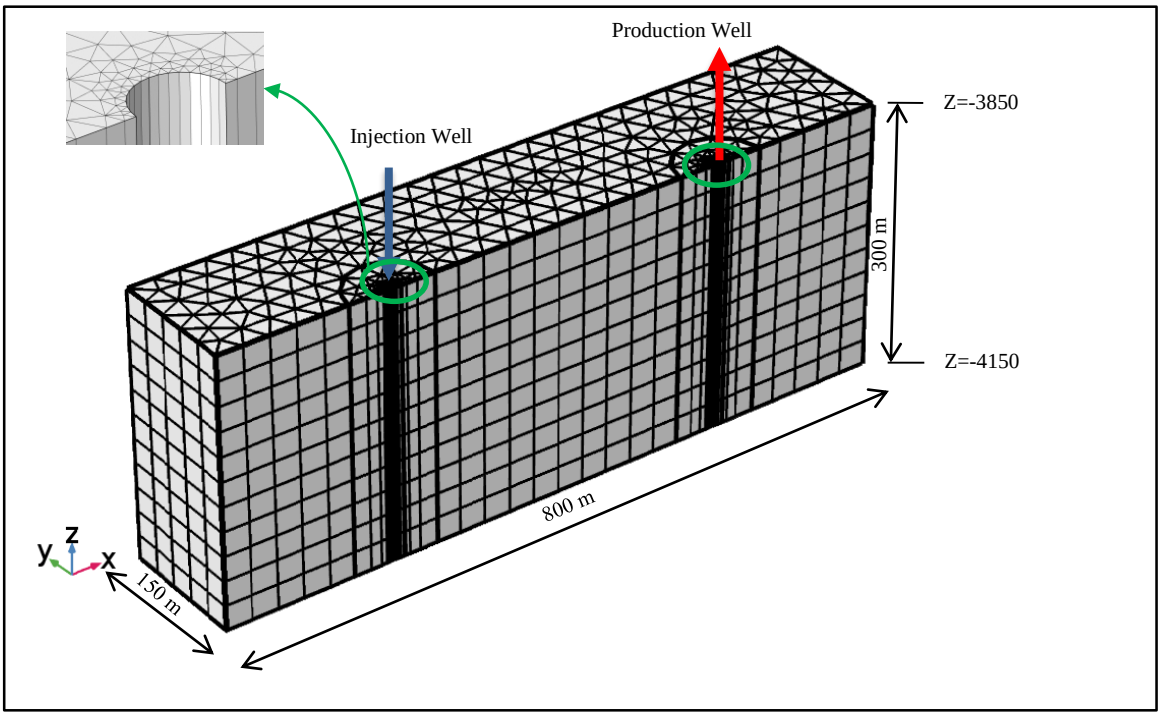

Figure 4-3. FE mesh of the proposed model

Since the hybrid approach can involve millions of runs of FE models, particular attention is paid to the meshing to maintain the accuracy of the response results while reducing the execution time of the FE model, three different mesh sizes were examined. Mesh 1: coarse mesh is selected where the complete mesh consists of 9709 elements; Mesh 2: is 16672 elements; Mesh 3: is 23881 elements; Mesh 4: very fine mesh 39920 elements. These cases were compared with respect to the production mass flow within 50 years of heat extraction.

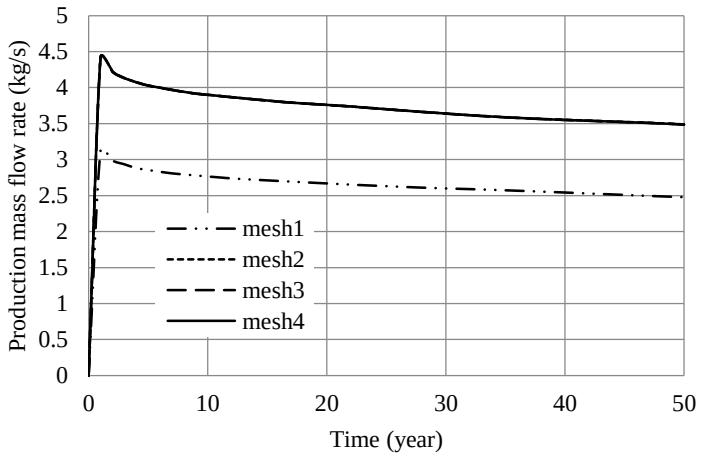

Figure 4-4. Mesh convergence with response to the production mass flow rate

From Figure 4-4, it is clear that mesh size has significant impact on the flow accuracy. Therefore, the normal mesh size (mesh 2) has been selected for the present research.

4.3 Validation of the FE model

To demonstrate the of the FE modelling process, COMSOL Multiphysics was used to replicate the numerical simulation of the Spa Urach geothermal reservoir as a validation problem. Results are compared with those of Watanabe et al. (2010) who used GeoSys/RockFlow code (Kolditz and Shao, 2009). The three-dimensional transient FE of the model for this benchmark problem follows the fully THM coupled process. The results contribute the thermal evolution between the injection and production well at a distance of 60 m from the injection well. The injection

pressure is assumed 10MPa and the injection temperature is 50 ºC with a reservoir temperature gradient 0.03 K/m. In general, the present results and those of Watanabe et al. (2010) are in close agreement, see Figure 4-5. Some difference in the two sets of the results can be attributed to the modelling of the injection and production wells in which it is assumed as one-dimensional 1D in Watanabe et al. (2010) and it is 2D in the present study.

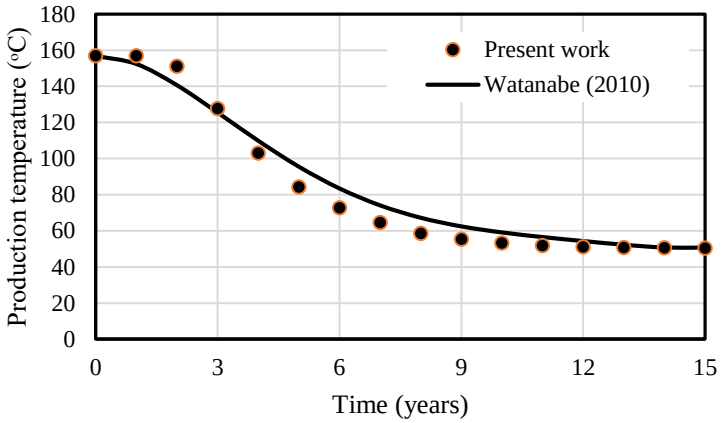

Figure 4-5. Comparison of the present FE model and Watanabe et al. (2010) (Samin et al., 2018)

In addition to the first validation, the present FE model is also validated against the FE simulation conducted by Chen and Jiang (2015) for an artificial reservoir to verify the TH coupled processes. The reservoir is designed with a temperature gradient of 0.04 ºC/m; injection flow rate of 50kg/s; injection temperature of 70 ºC; ground surface temperature of 27 ºC and the permeability of 1e-14 m^2. The TH coupled process is developed in the present FE model utilising the heat transfer in porous media and Darcy's Law modules. Figure 4-6 indicates that the values of the production temperature of the present study agree very closely with FE study conducted by Chen and Jiang (2015) for heat extraction over a period of 24 years.

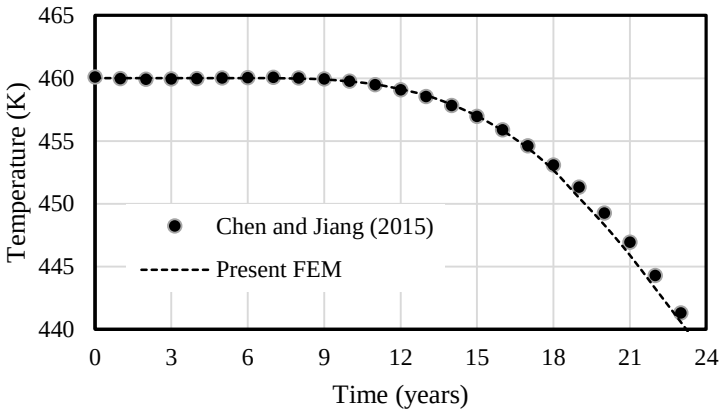

Figure 4-6. Comparison of the present FE model and Chen and Jiang (2015) (Samin et al., 2018)

4.4 Sensitivity Analysis of Design Parameters on the Reservoir Long-Term Performance

In order to complete this research, it was necessary to undertake a parametric study on the artificial design parameters of the reservoir. Then, later in Chapter Four, the sensitivity analysis results would be the constraints of the optimisation process. Two of the significant variables in EGS, which have been widely considered to be optimised, are the well placement within the reservoir and the fluid injection pressure; see Section 2.6 of Chapter Two. This study examined the effect of their change on the production temperature, thermal power and mass flow rate over exploitation time. In addition, the permeability of the fractured zone, the temperature of the injected fluid and the depth of the reservoir are also examined for their impacts on the reservoir long-term performance.

4.4.1 Effect of Distance between Injection and Production Wells (d)

The configuration of the injection and production wells within EGS reservoirs is a significant artificial design parameter; this has been considerably investigated in detail by others such as Asai et al. (2018), Bedre and Anderson (2012), Chen et al. (2015) and others, see Section 2.6 in Chapter Two.

In this section, the distance between the injection and production wells (*d*) was varied from 200 m to 600 m. The effect of well spacing is investigated for production temperature, mass flow rate and the produced thermal power over 50 years of heat extraction. During the sensitivity analysis, all the other artificial design parameters were kept at their medium values.

Figure 4-7 (a) presents the results for the temperature of the production well at three values of *d*, which are 200 m, 400 m and 600 m. The results show that when *d* is at 200 m, production temperature declines drastically after 5 years, and it continues decreasing to the temperature of the injected fluid (50 ^{o}C) within the first 15 years. While, when *d* is 600 m, the production temperature declines gradually and does not drop below 140 ^{o}C during the 50 years. This shows that the reservoir design with *d* of 600 m did not exceed the 10% of its thermal drawdown at the end of heat extraction process.

Figure 4-7 (b) is a surface plot for production temperature at a range of distances between injection and production wells, with a least value at 200 m and maximum value at 600 m.

The surface plot shows that when *d* is at the least value (i.e. 200 m), the reservoir cannot provide high temperature fluid and its temperature drops to 50 ^{o}C during short-term of exploitation. However, the production temperature improves with increasing *d* during long periods of exploitation.

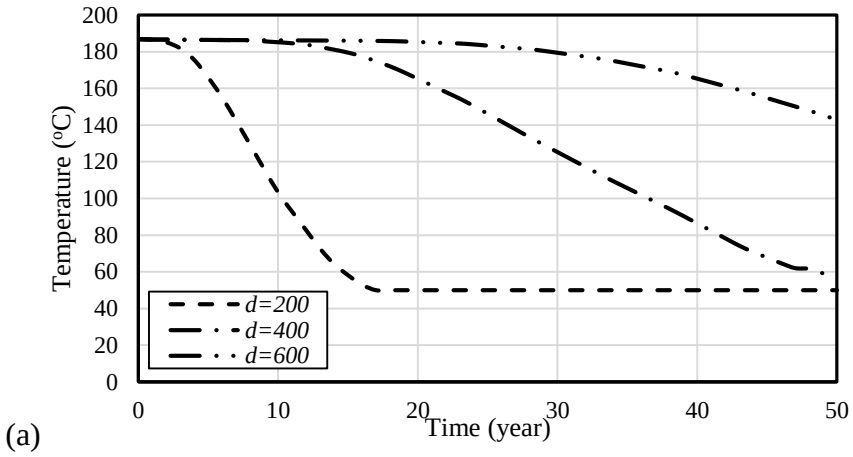

(a)

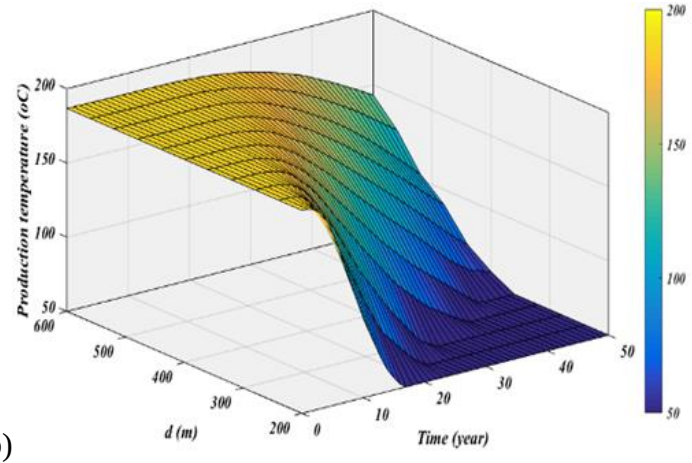

(b)

Figure 4-7. Sensitivity of production temperature to the distance between injection and production wells; (a) 2D diagram and (b) is a 3D surface plot.

On the other hand, Figure 4-8 (a) shows that a short distance of 200 m produces a mass flow rate of about 15.5 kg/s at early stages of heat extraction, which is higher than the produced at 600 m, which is about 12.5 kg/s.

Figure 4-8 (b) is a surface plot represents the mass flow rate of the production well over 50 years. The highest mass flow rate is produced by the reservoir with the least value of *d*. However, after 20 years of heat extraction, different values of *d* are nearly having the same mass flow rate ranged between (10-11) kg/s.

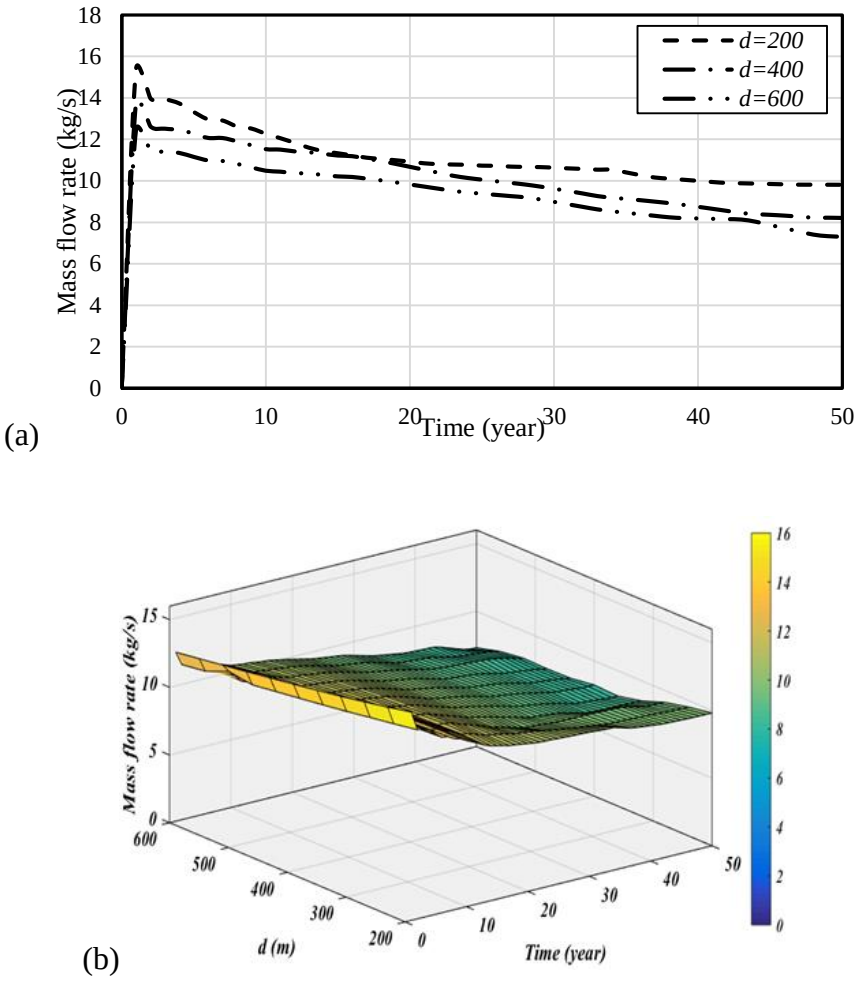

Figure 4-8. Sensitivity of mass flow rate to the distance between injection and production wells; (a) 2D diagram and (b) is a surface plot.

Furthermore, the produced thermal power has a considerable declination at short distances of 200 m at early stages of heat extraction. However, with longer distances (at 400 and 600) m, the power declination become gradually low, see Figure 4-9 (a).

Figure 4-9 (b) represents the trend of the produced power over 50 years for a range of distances between injection and production wells. The results show that the highest production at the least *d* (200 m) in the first 5 years. Then, the produced power drops significantly and it becomes stable around 25 years to the end of the heat extraction process with a very low production of

about 2.5 MW. While, the produced thermal power at maximum well spacing (i.e. 600 m) has a steady decline with time and does not drop below 5 MW.

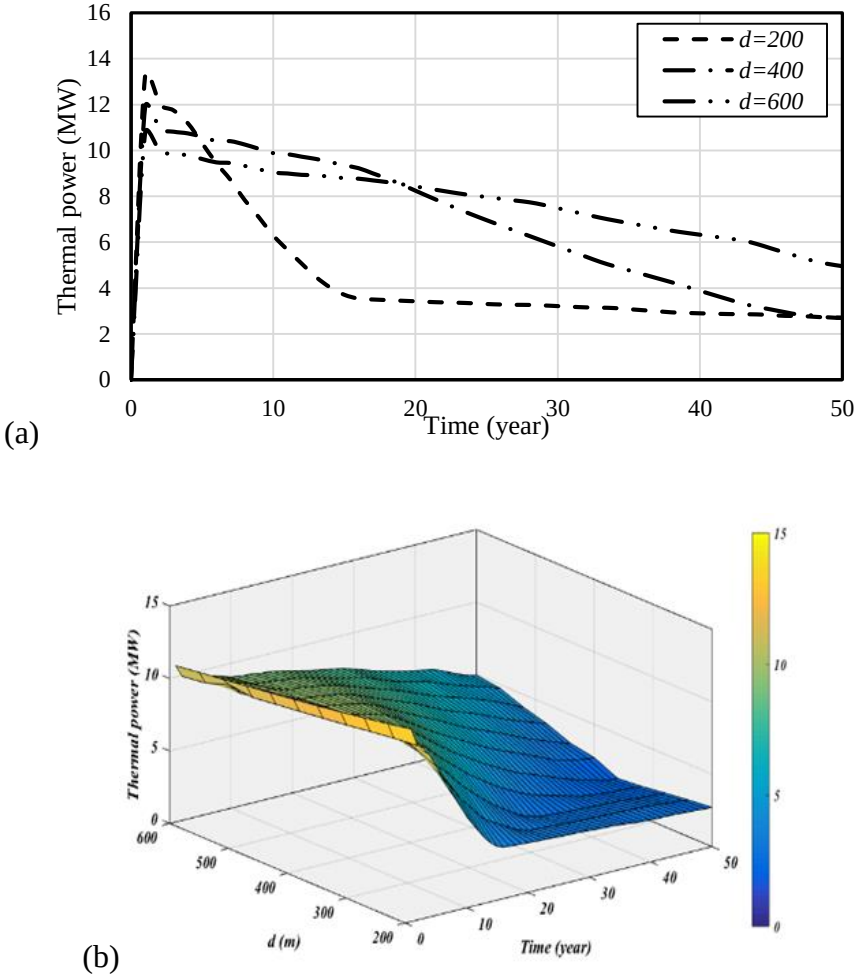

Figure 4-9. Sensitivity of thermal power production to the distance between injection and production wells; (a) 2D diagram and (b) is a surface plot.

When the well spacing reduced, the mass flow rate for a constant injection pressure is increased. Consequently, the temperature of the reservoir dropped dramatically. In addition, decline in thermal production power is observed because of the determination of the primary coverage volume of the reservoir by the distance between the injection and production wells. When the distance between the wells is increased, injection and production wells cover a larger volume than they do when the distance between them is smaller. Meanwhile, the available heat content

is directly proportional to the volume of rock (Asai et al., 2018). The larger volume of heated rock covered for *d* at 600 m is depleted slower than the smaller volume associated with 200 m of well spacing.

4.4.2 Effect of Injection Pressure (Pinj)

The injection fluid pressure was varied from 1 MPa to 30 MPa with keeping the other artificial design parameters at their medium values.

For an EGS design, with increasing fluid injection pressure in a given time period, the production temperature decline faster, see Figure 4-10 (a). However, with low injection pressure of 1 MPa, the production temperature does not drop below 180 ^{o}C. On the other hand, for a reservoir design with the highest injection value (30 MPa), there is a drastically drop in the production temperature during the initial 10 years.

The behaviour of the impact of *Pinj* on the production temperature is presented in Figure 4-10 (b). The surface plot in Figure 4-10 (b) shows a rapid drop of production temperature with increasing *Pinj*.

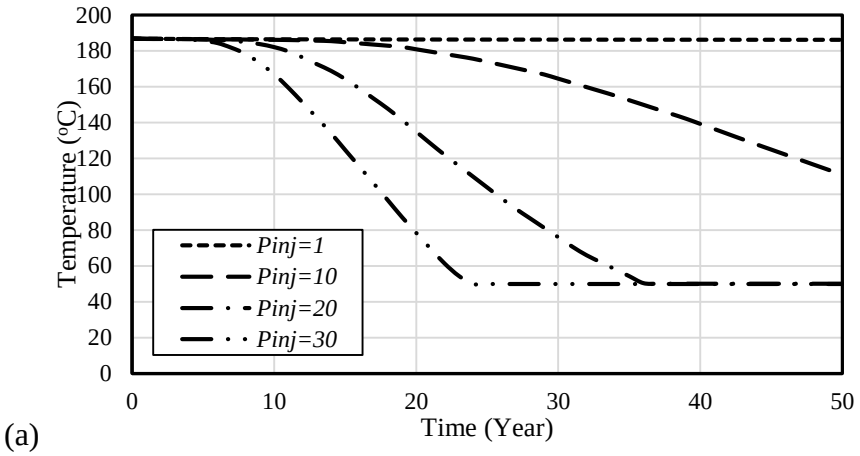

(a)

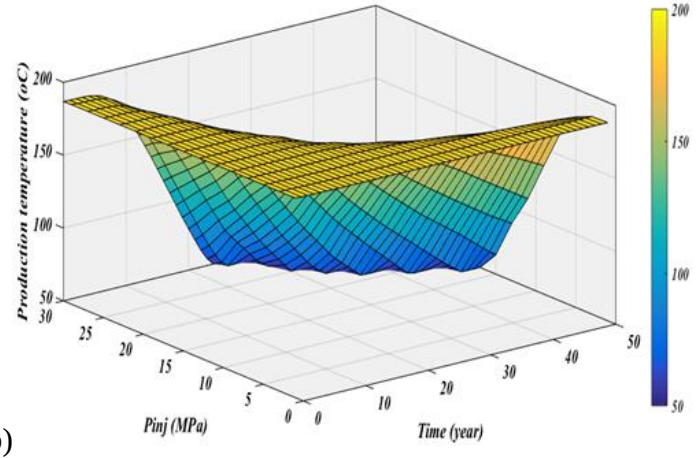

(b)

Figure 4-10. Sensitivity of production temperature to the fluid injection pressure; (a) 2D diagram and (b) 3D surface plot.

Figure 3-11 (a) shows that high injection fluid pressure produces high values of mass flow rate. However, over long periods of exploitation, the drop in mass flow rate of designs with high injection pressure is more noticeable than others with lower *Pinj*. Thus, the mass flow rate production is directly proportional to the fluid injection pressure.

Figure 3-11 (b) shows that the difference between mass flow rates of various *Pinj* values is lower after 25 years than the values of the first 5 years. This is because high injection pressures accelerate the declination of the production temperature, resulting in reducing the mass flow rate of the production well because the fluid properties are pressure and temperature dependent.

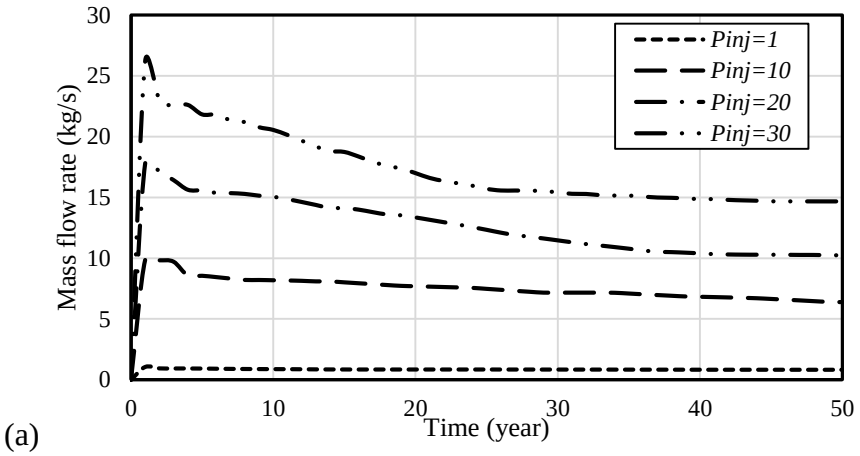

(a)

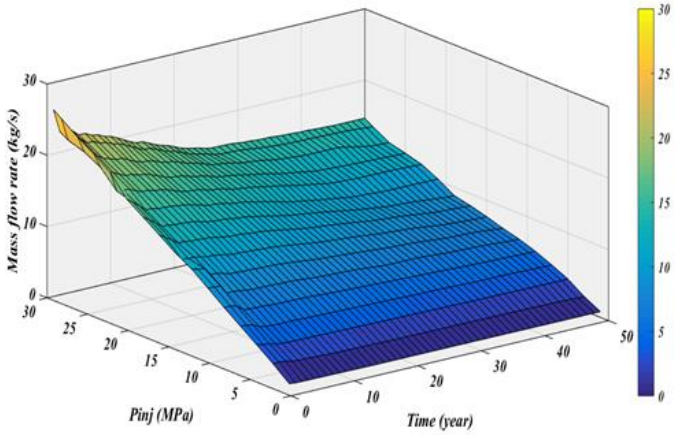

(b)

Figure 4-11. Sensitivity of mass flow rate to the fluid injection pressure; (a) 2D diagram and (b) 3D surface plot.

Furthermore, the produced thermal power, see Figure 4-12 (a), has the highest value at the highest injection pressure (30 MPa) in the first 8 years, which produces an average of 19 MW. Then, the produced thermal power drops drastically to 15 MW, and later it becomes gradually stable around 25 years to the end of the heat extraction process with a very low thermal production power of about 4.5MW. While, the produced thermal power at minimum *Pinj* (1 MPa) is almost stable around 0.75 MW over 50 years.

Figure 4-12 (b) presents the behaviour of the thermal power of EGS reservoirs to the fluid injection pressure. It shows the high impact of injection fluid pressure on the thermal power over long periods.

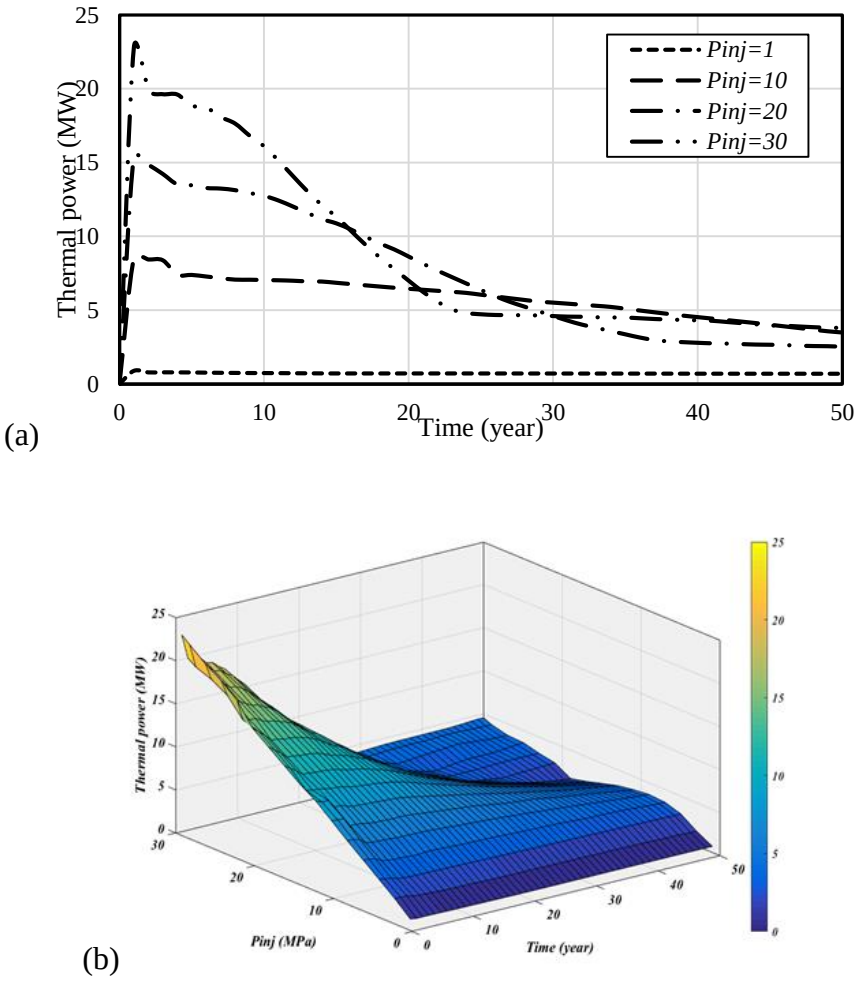

Figure 4-12. Sensitivity of thermal production power to the injection fluid pressure; (a) 2D diagram and (b) is a surface plot.

Since the thermodynamic properties of the fluid is not constant and it is temperature and pressure dependent, the decline in the mass flow rate is observed through different trends at different injection pressures. This shows that the fully coupled of the thermal and hydraulic process induces complexity to EGS engineers.

4.4.3 Effect of Fractured Zone Permeability (k)

The equivalent permeability of x direction was varied over the range of (5e-16 m^2 to 5e-15 m^2) and the permeability of the other directions y and z are changed accordingly as explained in Section 4.2.1.

Figures 4-13 (a & b), 4-14 (a & b) and 4-15 (a & b) shows that the sensitivity of the reservoir to different equivalent permeability values, in terms of production temperature, mass flow rate and produced thermal power, are similar to its behaviour to fluid injection pressure in Section 4.4.2. This is because both design parameters (i.e. *Pinj* and *k*) have the similar impacts on the production mass flow rate and consequently accelerate the thermal drawdown of reservoirs with increasing their values.

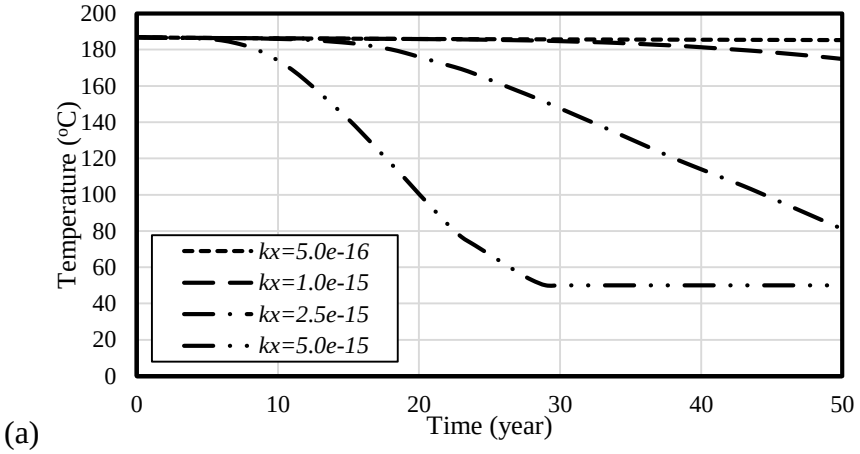

(a)

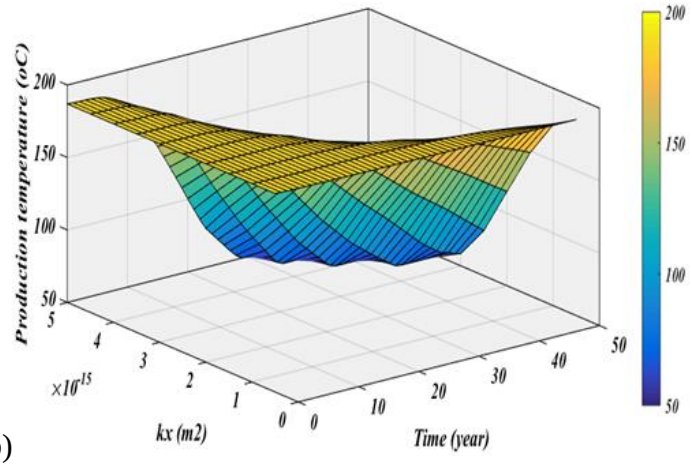

(b)

Figure 4-13. Sensitivity of production temperature to the reservoir permeability; (a) 2D diagram and (b) is a surface plot.

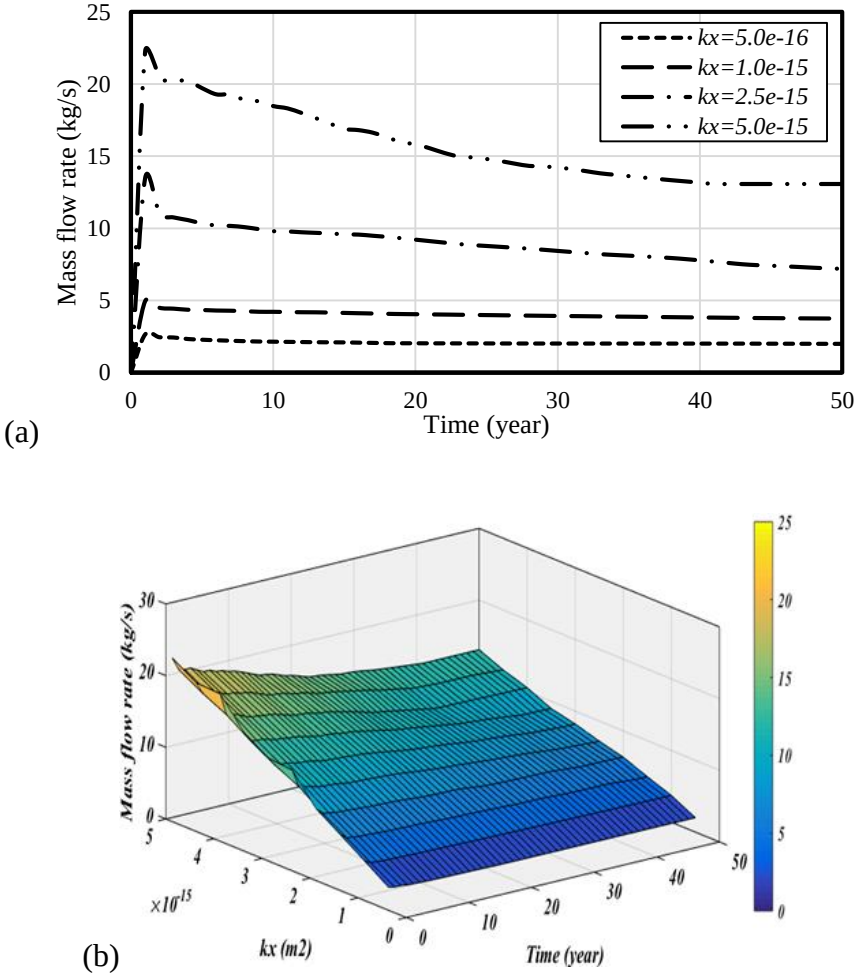

Figure 4-14. Sensitivity of mass flow rate to the reservoir permeability; (a) 2D diagram and (b) is a 3D surface plot.

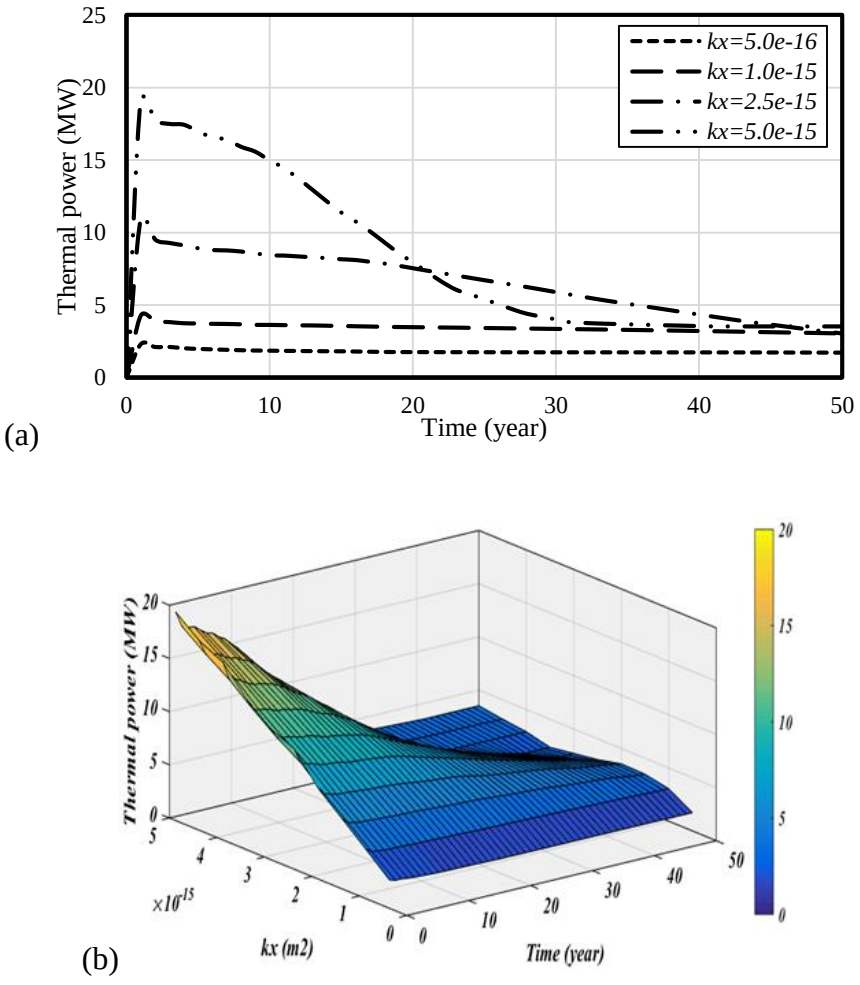

Figure 4-15. Sensitivity of thermal power to the reservoir permeability; (a) 2D diagram and (b) is a 3D surface plot.

4.4.4 Effect of Maximum Reservoir Depth (Dh)

As discussed in section 2.5.1 in Chapter Two, the total drilling cost is a significant fraction of EGS capital cost (Tester et al., 1994). It is therefore important to investigate the impact of the maximum reservoir depth on the long-term production of thermal power of EGS reservoirs. The maximum depth of the reservoir was changed over the range of 4000 m to 6000 m.

Figure 4-16 (a) presents the production temperature for three different designs (4000, 5000 and 6000) m over 50 years of exploitation. The results show that the design with 4000 m depth

produces lower temperature than the others. However, it can be seen that after about 40 years of exploitation, different designs can produce the same production temperature.

The declination of production temperatures over the 50 years of heat extraction for different values of *Dh* have the same trend, see Figure 4-16 (b).

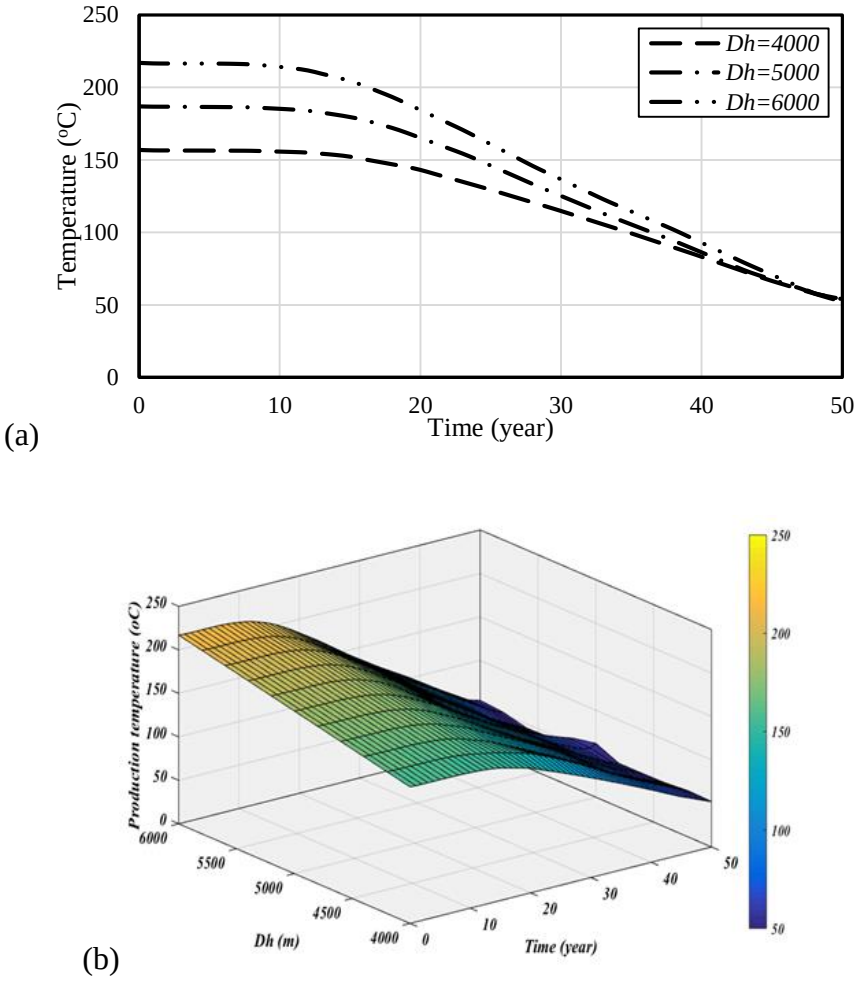

Figure 4-16. Sensitivity of production temperature to the maximum reservoir depth; (a) 2D diagram and (b) is a 3D surface plot.

In addition, since fluid properties are temperature and pressure dependent, the production mass flow rate is increasing with deeper reservoirs at early stages, see Figure 4-17 (a). However, it has the same trend of declination with different values of *Dh*, see Figure 4-17 (b).

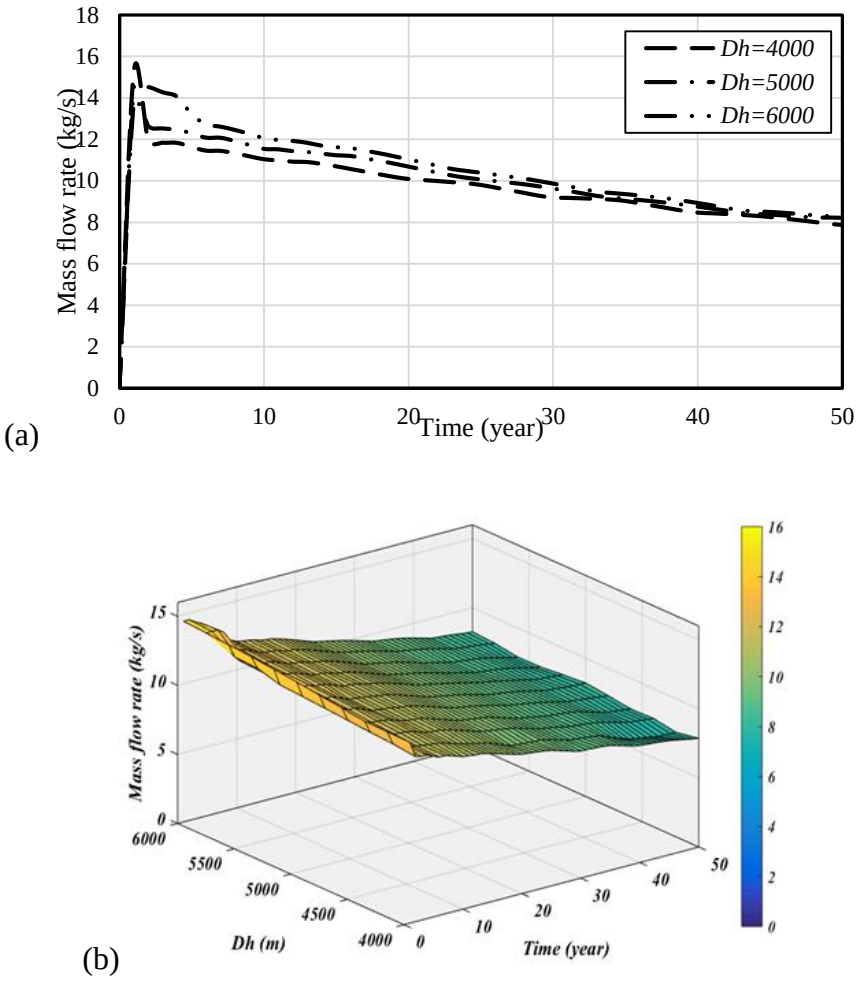

Figure 4-17. Sensitivity of mass flow rate to the maximum reservoir depth; (a) 2D diagram and (b) is a 3D surface plot.

Figure 4-18 (a) shows that deeper EGS reservoirs produce higher thermal power up to 30 years of exploitation. However, the produced thermal power after that tend to be equal with time up to 50 years of heat extraction. In addition, as the thermal power is directly proportional to the temperature and the mass flow rate, its declination trend is the combination of them and this can clearly be seen in Figure 4-17 (b).

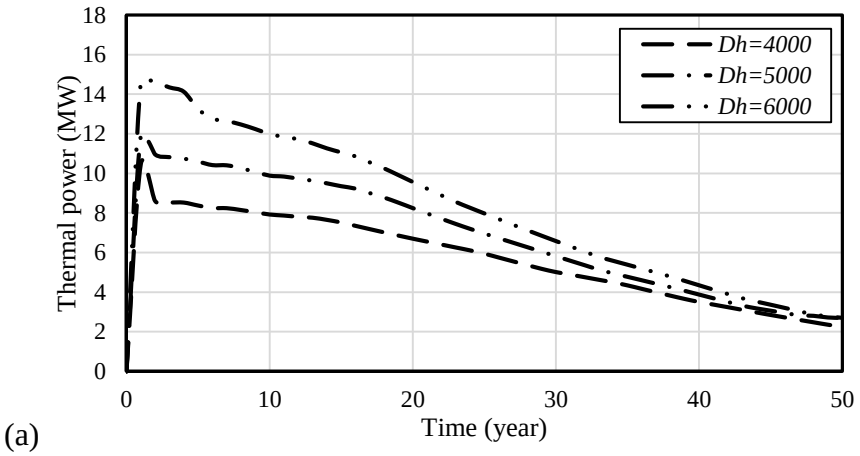

(a)

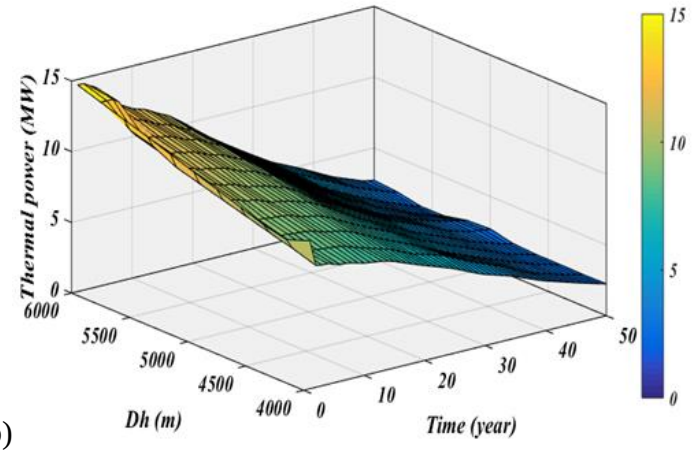

(b)

Figure 4-18. Sensitivity of thermal power to the maximum reservoir depth; (a) 2D diagram and (b) is a 3D surface plot.

4.4.5 Effect of Injection Fluid Temperature (Tinj)

The temperature of the injected fluid was changed over the range of 40 °C to 75 °C for the sensitivity analysis.

Figure 4-19 (a) shows that the impact of injection temperature on production temperature is insignificant at the early stages of heat extraction process up to 10 years. Then, the drop of the production temperature is mostly noticed at high injection temperatures rather than lower values.

Figure 4-19 (b) represents the surface plot for the production temperature at different injection temperatures. It shows that when the injected temperature is the least (40 °C), the production temperature declines slower than that when the injection temperature increased and it is more noticeable at the highest injection temperature (75 °C).

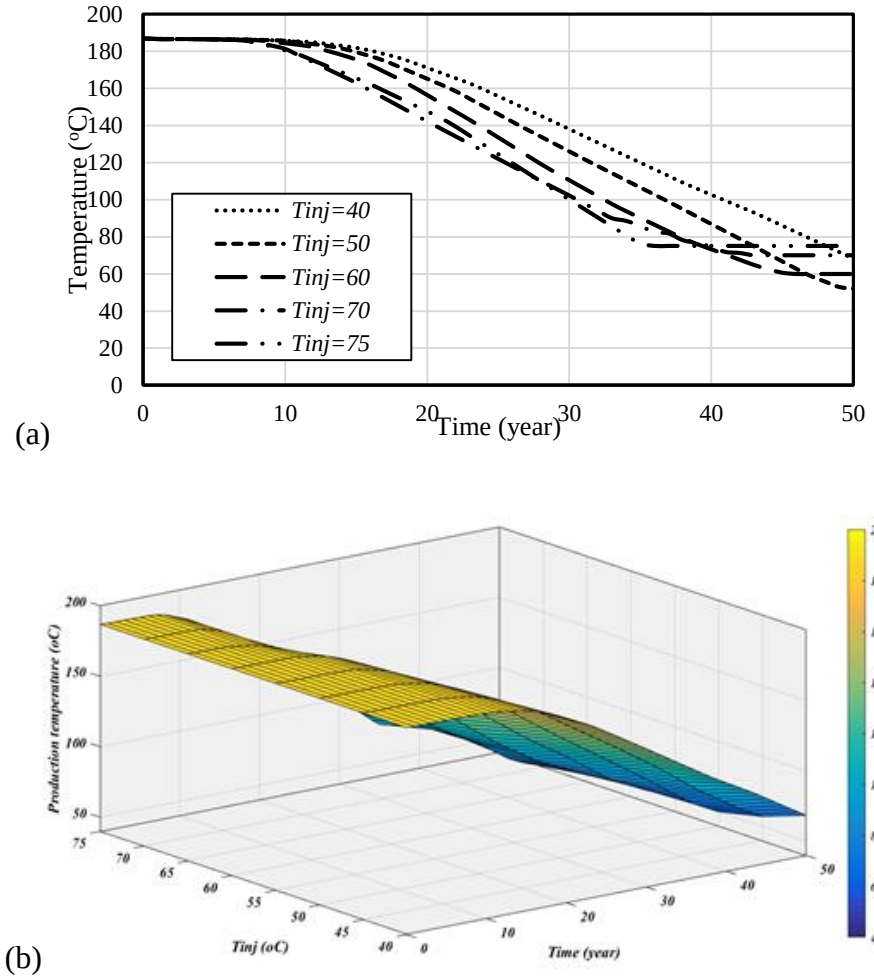

Figure 4-19. Sensitivity of production temperature to the fluid injection temperature; (a) 2D diagram and (b) is a 3D surface plot

On the other hand, the mass flow rate for designs with high injection temperature is higher than they do with lower temperature values; see Figure 4-20 (a). The change in the mass flow rate for designs with different injection temperatures is presented clearly in Figure 4-20 (b).

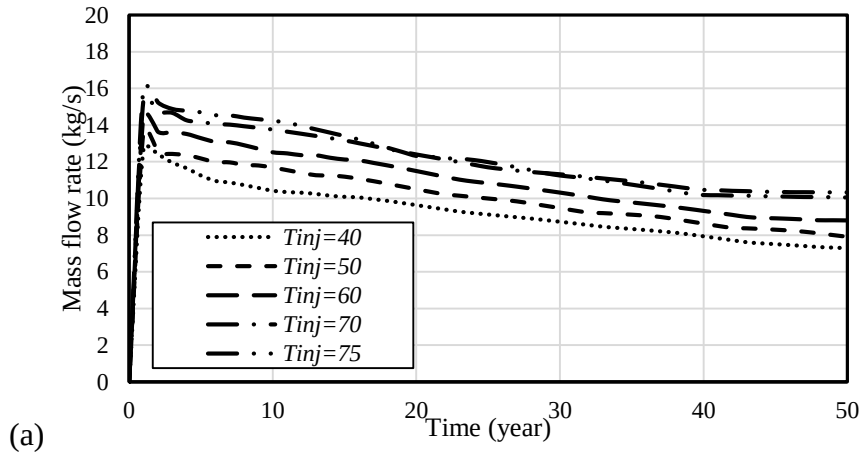

(a)

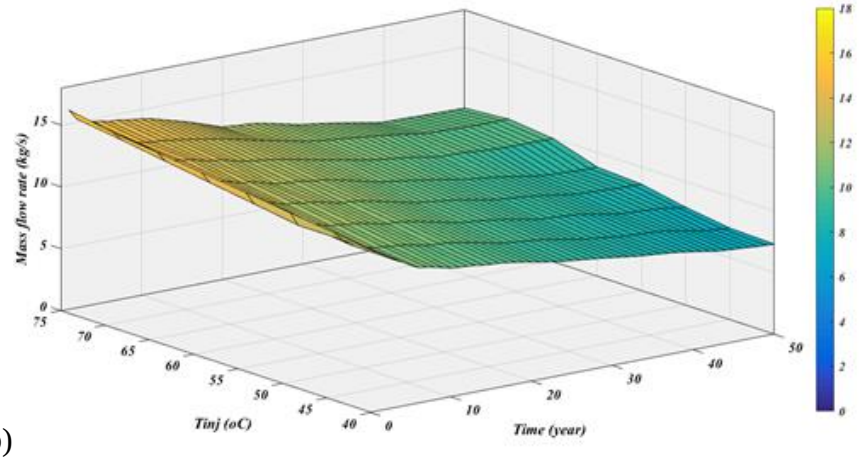

(b)

Figure 4-20. Sensitivity of mass flow rate to the fluid injection temperature; (a) 2D diagram and (b) is a 3D surface plot

Figure 4-21 (a) shows that the produced thermal power with time has the highest value at high injection temperature at the first 5 years. Then, the differences between produced thermal powers become low for designs with different injection fluid temperatures up to 40 years, where the difference can be ignored.

For heat exchange in a system, the temperature difference is the driving factor. However, with the fully coupled of TH and a fluid with temperature and pressure dependent thermodynamics properties, the impact of various injection temperature on the produced thermal power is generally observed at the early stages of heat extraction, see Figure 4-21 (b).

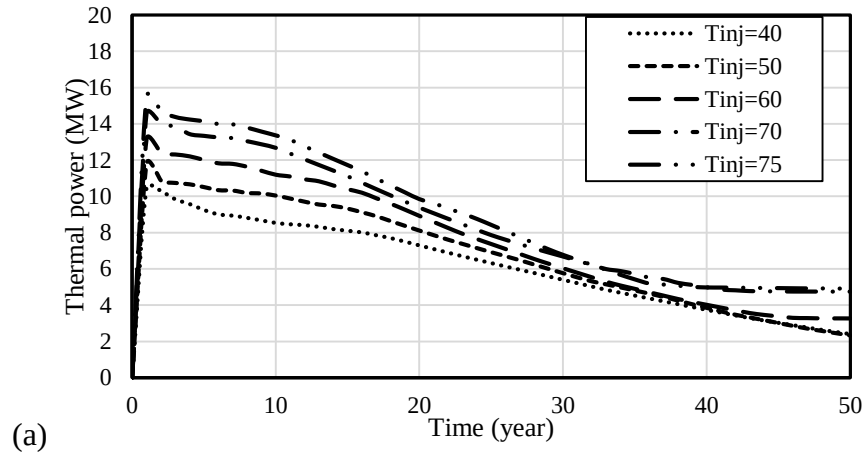

(a)

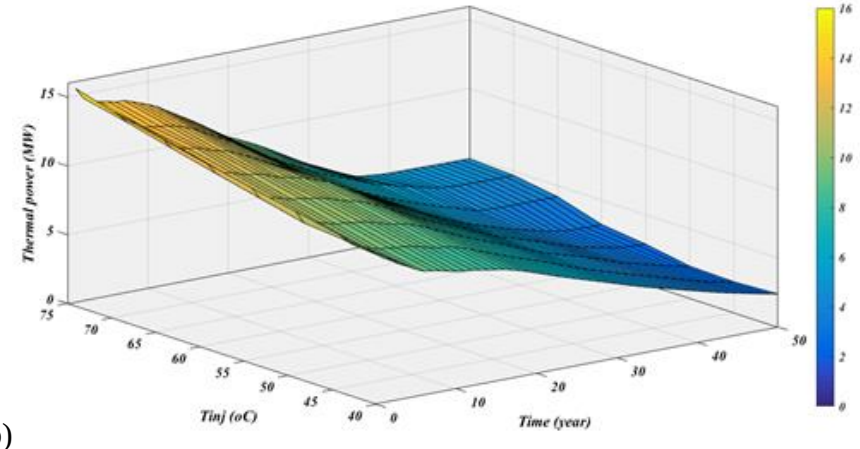

(b)

Figure 4-21. Sensitivity of thermal power to the fluid injection temperature; (a) 2D diagram and (b) is a 3D surface plot.

4.5 Sensitivity Analysis of Design Parameters on Reservoir Performance at the Breakthrough Time of EGS Reservoir

The sensitivity of the reservoir performance to the artificial design parameters are also investigated based on their impacts on the service life of the reservoir (breakthrough time when the thermal drawdown reaches 10 %) and accumulative thermal power at the breakthrough time. This is important to identify key sensitive variables for the fitness function of the Multi-objectives GA optimisation technique in the next chapter.

In order to investigate the impact of each design parameter at the end of the reservoir service life (breakthrough time), all the parameters, breakthrough time and accumulative thermal power

at breakthrough time are normalised a range of 0 to 1. For the design parameters, 0 refers to the least value and 1 is the highest value. For example, for the well spacing, 0 refers to 200 m while 1 refers to 600 m. However, for the sensitivity results 0 refers to the failure of the reservoir when thermal drawdown is 10% or more at 10 years of heat extraction process. While, 1 refers to 50 years for the breakthrough time and 283 MW for the accumulative thermal power, which is the highest value achieved for the sensitivity analysis process.

4.5.1 Effect of Well Spacing (d)

Thermal breakthrough time of the reservoir with short well spaces occurred before 10 years and resulted in the failure of the reservoir. Then, from *d* of 0.2 to the end, Thermal breakthrough time increases with increasing *d*. Nevertheless, the accumulative power at the breakthrough time increases up to 0.9 of *d*; then, it starts to decline with increasing *d* to 1, see Figure 3-14.

The thermal power is therefore highly sensitive to the change in *d* value. This is because, the velocity of the fluid flow and the mass flow rate increase with the shorter distance between the wells. As a result, accelerating the depletion of the reservoir at initial stages of heat extraction process. Therefore, the distance between the wells is to be considered significantly important within the optimisation process.

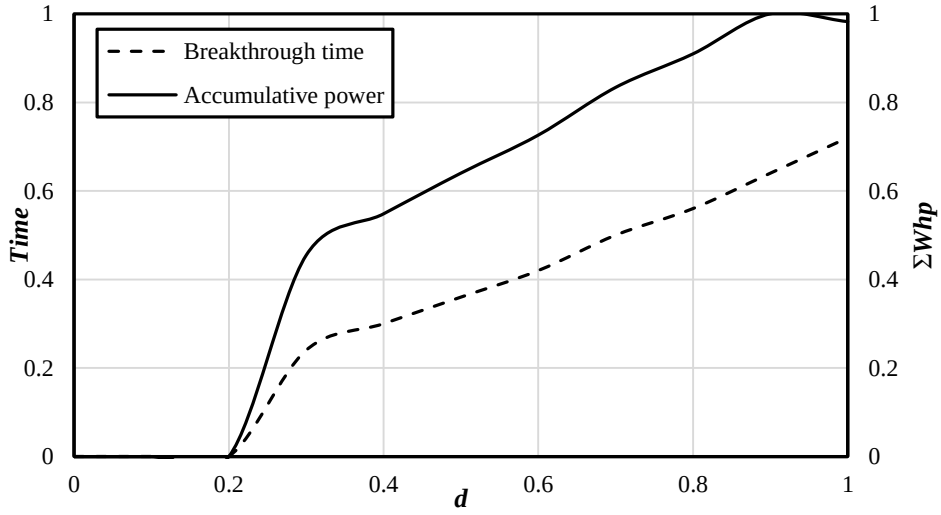

Figure 4-22. Impact of well distance on both thermal drawdown (dash line) and thermal power production (solid line)

4.5.2 Effect of Injection Fluid Pressure (Pinj)

The change of the fluid injection pressure affects the long-term performance of EGS reservoirs through the acceleration of the breakthrough time. At the same time, the accumulative thermal power at the breakthrough time steeply increased at up to 0.3 of the normalised *Pinj*. Then, the behaviour slightly changes with increasing the injection pressure up to 0.8, which at the end it shows a steep decline and failed at 1. This is because the higher injection pressure produces higher mass flow rate, it also increases the flow velocity, and consequently, the breakthrough time significantly declines, see Figure 3-15. Therefore, *Pinj* is strongly recommended to be considered within the optimisation process.

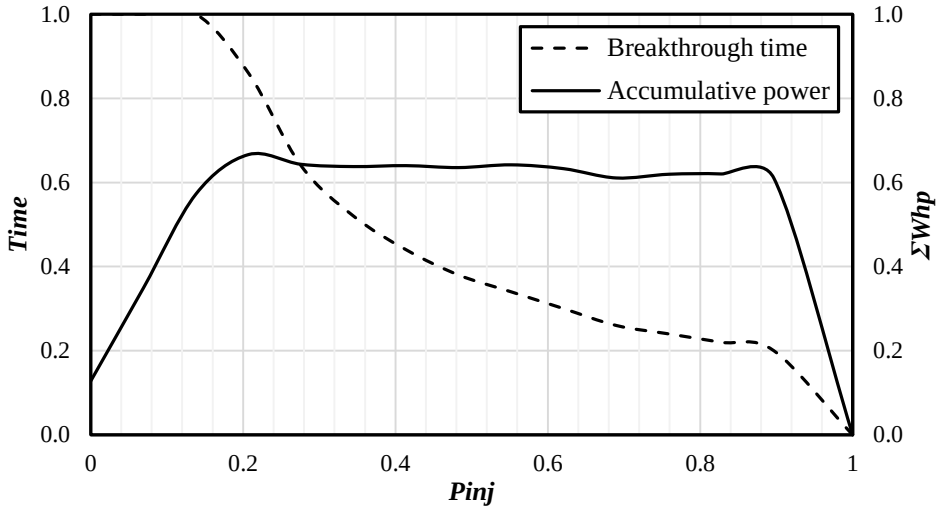

Figure 4-23. Impact of fluid injection pressure on both thermal drawdown (dash line) and thermal power production (solid line)

4.5.3 Effect of Fractured Zone Permeability (k)

With the increase of *k*, the breakthrough time generally declines while the accumulative thermal power increases at up to 0.2 of the normalised permeability of the fractured zone, see Figure 3-16. While the lower permeability increases the breakthrough time, it also reduces the thermal power production because of low values of mass flow rate. On the other hand, higher permeability of the fractured zone results in significant drops of reservoir temperature and breakthrough time at early stages of the heat extraction process. This has been also conducted by others such as Watanabe et al. (2010) and Mudunuru et al. (2016). Furthermore, it can be seen that the behaviour of the fractured zone permeability is similar to the fluid injection pressure due to their direct proportional to the fluid mass flow rate. Thus, this shows that the permeability is, as powerful design parameter as the injection pressure that should be considered within a proposed optimisation model.

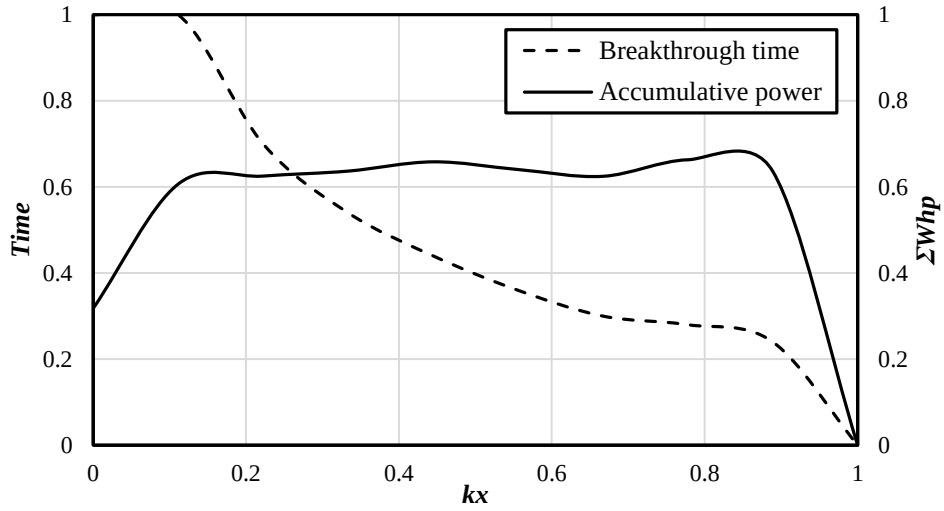

Figure 4-24. Impact of permeability of the fractured zone on both thermal drawdown (dash line) and thermal power production (solid line)

4.5.4 Effect of Maximum Reservoir Depth (Dh)

As can be seen in Figure 3-17, the depth of the reservoir has less impact on the breakthrough time, but it has significant influence on the productivity of the thermal power at the breakthrough time of the reservoir. This is obvious since the subsurface temperature increased with depth by a gradient of 0.03 (^{o}C/m), see Section 3.4.2, resulting in higher productions of thermal power. However, according to Heidinger (2010), the total drilling cost increases exponentially with depth. Thus, the maximum depth of the reservoir is an important design parameter that requires be identifying for a commercial EGS reservoir and thus considering within the optimisation process.

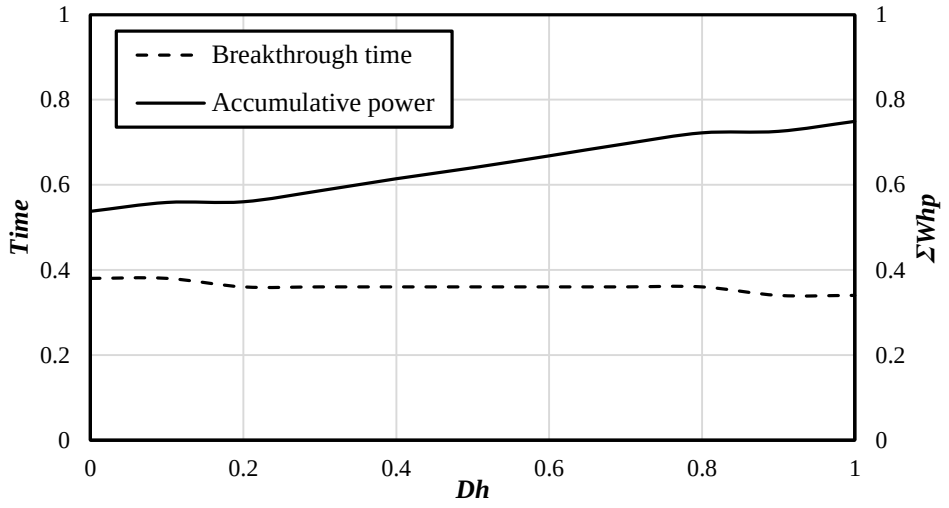

Figure 4-25. Impact of maximum reservoir depth on both thermal drawdown (dash line) and thermal power production (solid line)

4.5.5 Effect of Injection Fluid Temperature (Tinj)

Although the range is very wide, there is only a slight impact on both breakthrough time and the accumulative thermal production power at the breakthrough time, see Figure 3-18. The injection temperature is therefore ignored in the proposed research. This has been also concluded by Mudunuru et al. (2016).

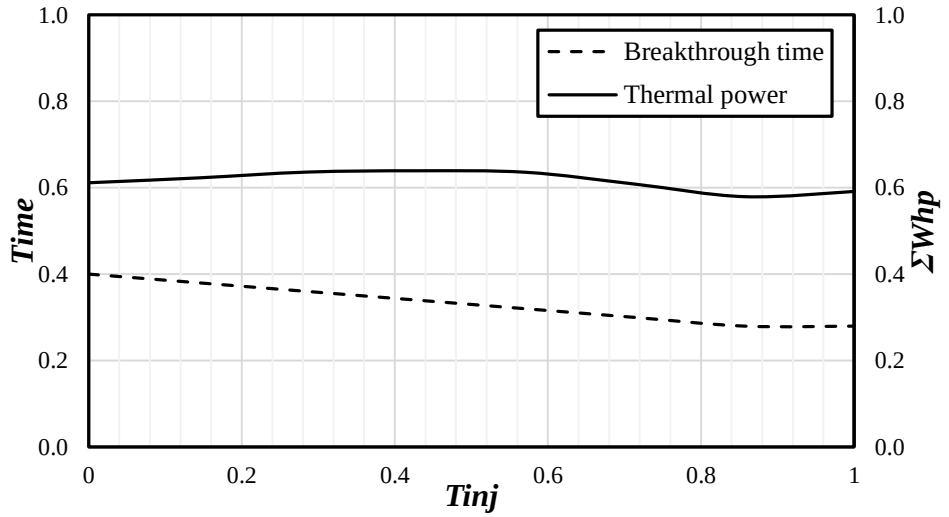

Figure 4-26. Impact of fluid injection temperature on both thermal drawdown (dash line) and thermal power production (solid line)

4.6 Conclusions

This chapter presented the development of the FE model for a doublet EGS reservoir. A sensitivity analysis is conducted for the impacts of the artificial reservoir design parameters to the reservoir long-term performance using two methods; first, define the impacts of design parameters on the reservoir performance over time; second, their impacts on the reservoir performance at the breakthrough time. Results of the parametric study indicated the following:

- Well spaces, injection pressure, permeability of the fractured zone and the maximum depth of the reservoir highly affect the reservoir long-term performance; while, the temperature of the injected fluid has insignificant impact compared to the other four parameters.
- The contributed design parameters do not affect the reservoir long-term performance in the same manner, except the injection pressure and the equivalent permeability, which have the same behaviour of influence.
- In addition, the results show that it is challenge to find favourable values for *d*, *Pinj* and *k*. However, higher values of *Dh* are favourable for the accumulative thermal power at the breakthrough time, yet it needs more cost to drill wells in deep reservoirs.

To sum up, find the optimum design is a challenge for EGS reservoir designers. Thus, multi-variables and multi-objectives GA is a preferred optimisation technique to find out optimum solutions for EGS reservoir designs due to its efficiency in solving complex multi-variables and multi-objectives problems. Therefore, for the optimisation of the long-term performance of doublet well reservoirs, four design parameters including *d*, *Pinj*, *k* and *Dh*, are considered as variables for the GA technique.

CHAPTER FIVE

5 OPTIMISATION OF EGS DOUBLET RESERVOIRS

5.1 Introduction

In this Chapter, the optimisation of the FE model in Chapter Three is conducted. This chapter is a part of published results in Samin et al. (2018).

In this chapter, the long-term performance of EGS is achieved via maximising thermal power *Whp* and minimising both the thermal drawdown *TD* and the total cost C_t using a multi-objective optimisation strategy for a doublet well reservoir.

The three long-term performance objectives presented above are employed for the objectives of the fitness function in the hybrid optimisation system. While, the contributed design parameters i.e. *d*, *Pinj*, *k* and *Dh* are the variables of the optimisation process. The actual *TD*, *Whp* and *Ct* are calculated in the GA code based on the outputs of the FE, by changing the variables selected by genetic operators.

Based on the sensitivity analysis results of Chapter Three, the maximum reservoir depth (*Dh*), distance between the injection and production wells (*d*), fractured zone permeability (*kx*) and fluid injection pressure (*Pinj*) are selected to be the optimisation variables. The constraints for these variables are presented in Table 5-1.

Table 5-1. Constraints of the variables in GA multi-objectives

constraints	Variables			
	Maximum reservoir depth (*Dh*)	Well position (*d*)	Fracture zone permeability (*kx*)	Injection fluid pressure (*Pinj*)
	m	m	m^2	MPa
Lower bound	4000	300	1e-13	1
Upper bound	6000	500	1e-16	20

The following points were considered during selection of these constraints:

- The depth of the reservoir is estimated between 4000-6000 m. This range is assumed as it is more practical for drilling process (Heidinger, 2010).
- The distance between the injection and the production wells in rectangular reservoirs (which is the case in this research) depends on the industry considerations where the production and the injection wells should be at the centre of two adjacent circles, which have the same radius, equal to a half of the reservoir width (Van Wees et al., 2010), see Figure 5-1.

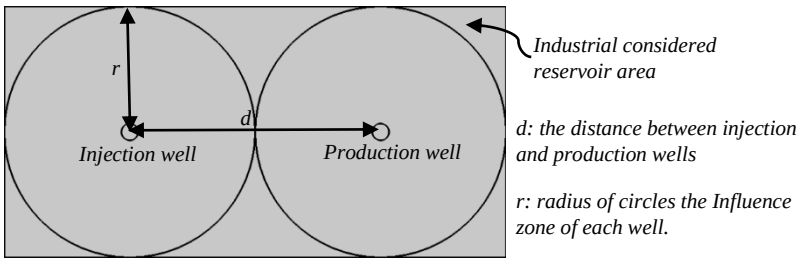

Figure 5-1. Industrial consideration for reservoir area based on the Influence zone of each well, after Van Wees et al. (2010)

Therefore, based on the industrial consideration, the minimum boundaries of the injection and production wells are chosen to be at 150m distance from the reservoir edge.

- The permeability of the fractured zone has values within the range 10-13 m^2 – 10-16 m^2 (Kosack et al., 2010).
- The injection pressure is varied between 1MPa to 20 MPa. The value of 20 MPa was determined after several initial trial and error simulations.

The total cost of EGS reservoir design is considered during the economic analysis and it is calculated using Equation 3.13. In which, creation and operation costs are calculated using Equations 3.9, and 3.11 respectively, see Section 3.2.4. in Chapter Three. In this chapter, the

Spa Urach case study is used and the values for the operation cost parameters are respected to the price in Germany. Thus, *pp* =15.52 (US$/kwh), *pr*=22.35 (US$/GJ) and *r*=1.4% have been used.

5.2 Results and Discussions

An algorithm was developed to integrate a FE analysis with a GA to find optimum values of the bi-objective fitness function. The first objective is to minimise the total reservoir cost and the second objective is to maximise the accumulative thermal power production *Whp* of the reservoir at the breakthrough time. The thermal drawdown of the reservoir is implicitly considered in the later by applying the threshold value of 10%*TD* during the optimisation process. The parameters of the Multi-objectives GA optimisation are summarised in Table 5-2. These values are chosen based on the number of variables, domain sizes and after a number of trial and errors.

Table 5-2. Parameters used for the Multi-objective GA in the present research

Number of Populations	50
Maximum generation number	400
Selection	Tournament size 2
Crossover	0.7
Mutation	Constraint dependent

Two scenarios are considered for the optimisation process. In the first scenario, all the sensitive design parameters (i.e. *Dh, d, k* and *Pinj*) are included during the optimisation of EGS design. The second scenario is carried out in order to determine the optimum solutions in the absence of any changes to the reservoir fracture configuration (i.e. without changing the equivalent permeability of the reservoir). The GA-FE optimisation algorithm was run several times using different randomised initial points to ensure global optimum solutions are achieved. The following sections present the results of the two optimisation scenarios.

The optimum designs achieved from both scenarios can be seen in Figures 5-2 and 5-3. The solutions revealed that in the case of the first scenario, the process regulated the variables in a way that results in lower reservoir total cost through selecting less deep reservoirs and less injection pressure values compared to the second scenario in order to reduce both creation and operation costs. On the other hand, the optimisation process selected permeability values that relatively higher than the constant permeability in the second scenario and relatively shorter distances have been selected compared to the second scenario. The high permeability and short distances are required in the first scenario to produce high mass flow rates as long as the selected injection pressures are very low.

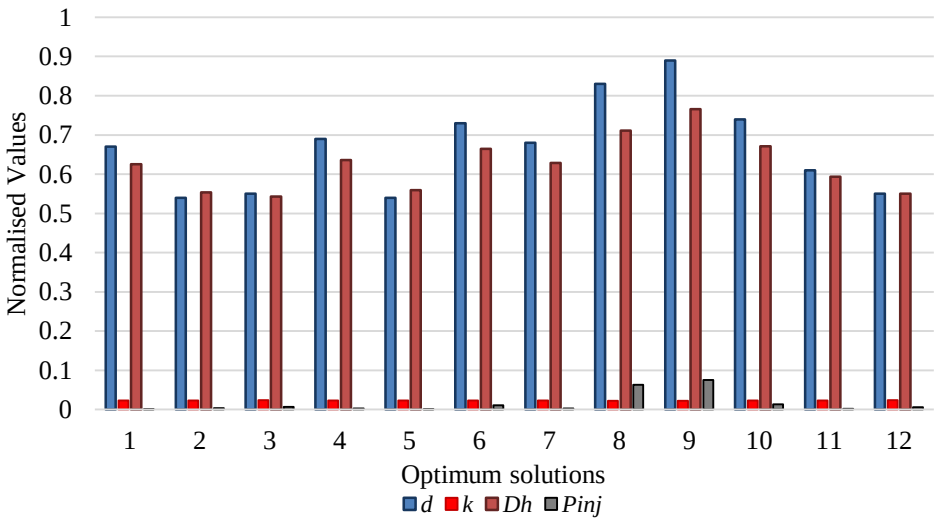

Figure 5-2. Optimum design solutions of the first optimisation scenario

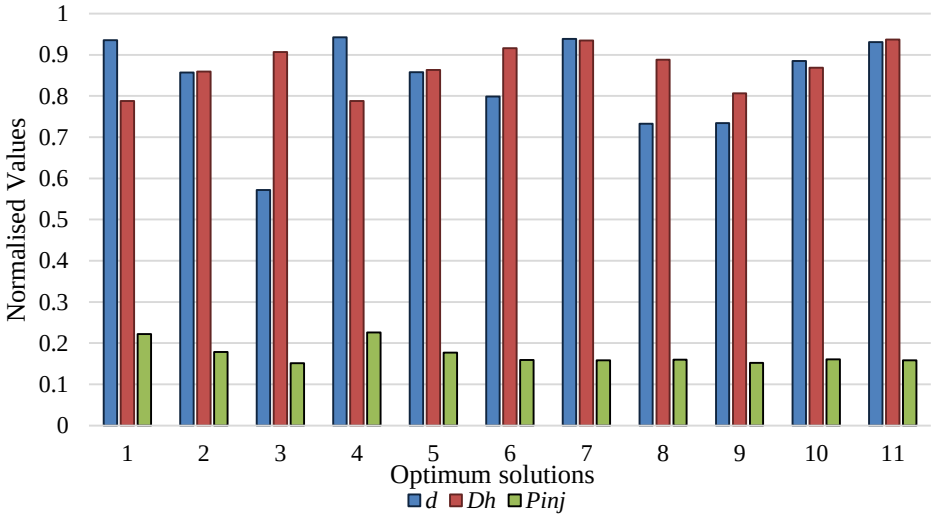

Figure 5-3. Optimum design solutions of the second optimisation scenario

The Pareto fronts of both scenarios are illustrated in Figure 5-4. Figures 5-4 (a, b) have been normalised to the minimum and maximum values of each scenario while Figure 5-4 (c) is normalised with respect to the combined extreme values.

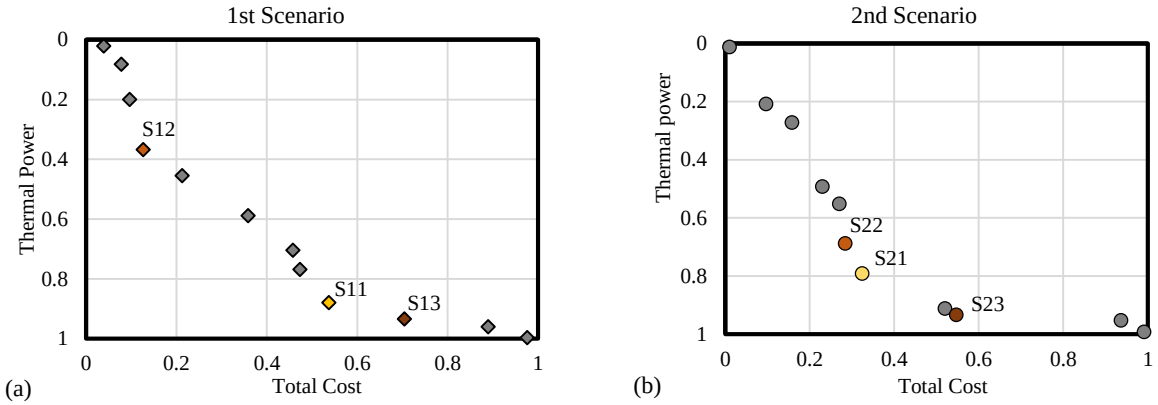

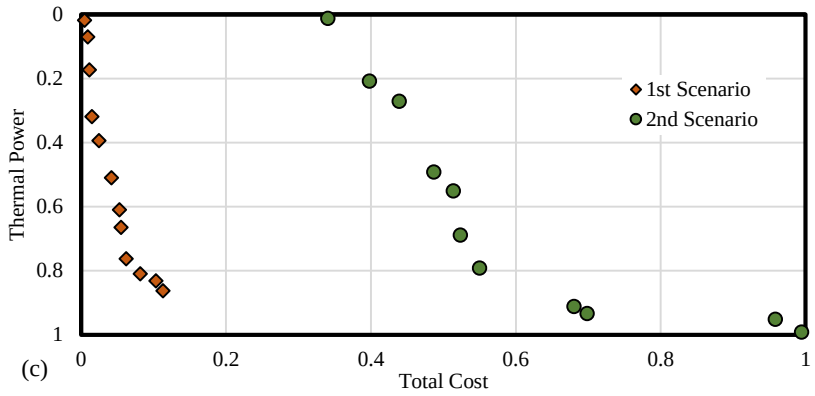

Figure 5-4. Pareto front of the optimum solutions of both scenarios (with and without changing the equivalent permeability of the reservoir), (a) 1st scenario, (b) 2nd scenario and (c) both case scenarios; where S11, S12 and S13 are the selected best designs in the 1st scenario and S21, S22 and S23 are the selected best designs in the 2nd scenario

Figure 5-4 show significant reduction in the value of the first objective (i.e. total cost) particularly in the first scenario. However, for the second objective (i.e. accumulative thermal power) there is no significant difference between the two scenarios, values of the second objective are restricted between 105-154 MW. In the first scenario, high accumulative thermal power designs have a cost between 75 to 88 Million $USA, as can be seen in Figure 5-4 (a). However, in the second scenario, to achieve a productive reservoir with high accumulative thermal power a significantly higher investment is needed (about 110 to 185 Million $USA), see Figure 5-4 (b). Figure 5-4 (c) presents the optimal trade-off curves of both case scenarios considered in the present study. The results show the considerable impact of permeability on the reservoir total cost. It is important to emphasize that this analysis has overlooked the cost of fracturing the reservoir and is only considering the two scenarios together to highlight the influence of permeability. The impact of the permeability on the other variables during the optimisation process is presented in Figure 5-5, where the values of the optimised parameters are normalised to the selected constraints for the GA.

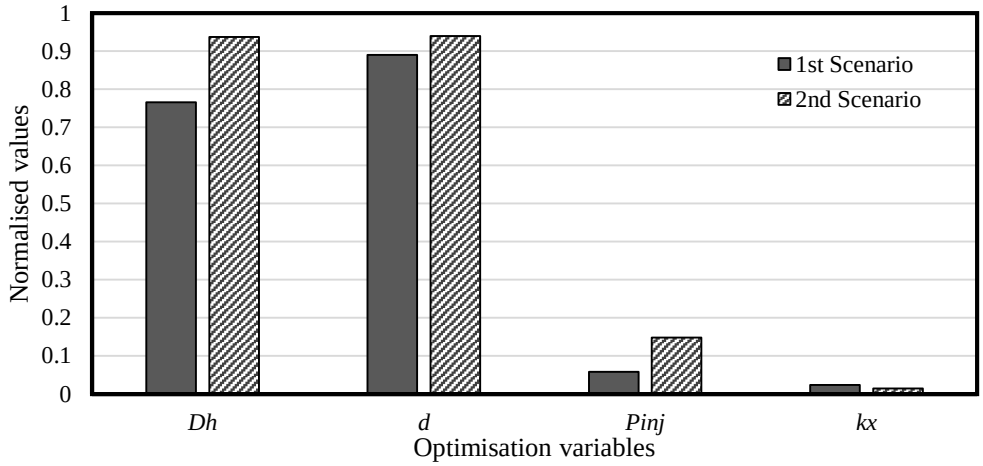

Figure 5-5. Maximum values of the normalised variables for both scenarios (with and without changing the equivalent permeability)

The results show that in the first scenario, when all the sensitive parameters vary within given ranges, the reservoir extended to a moderate depth. This resulted into a lower drilling cost than in the second scenario, where the reservoir depth was much higher and corresponded to more than 0.9 of the normalised depth. This depth was necessary to achieve a higher production temperature, which resulted into a higher drilling cost. In addition, both scenarios intend to select about 0.9 of the normalised distance between the injection and production wells in order to reduce the thermal breakthrough time. Furthermore, the maximum injection pressure in the second scenario is more than twice of that in the first scenario. The high injection pressure in the second scenario is due to the low permeability of the reservoir (about half of the maximum permeability of the first scenario). As a result, the operation cost for the second scenario (without changing the reservoir permeability) is higher than if the change is included.

All the solutions on Pareto front Figure 5-4 can in be considered an optimum designs for both scenarios, considering the circumstances and the design requirements (Hussain, 2015). Should both objectives carry equal weights of importance, the method of the minimum distance to a preferred point, which is 0 in this study, is applied to select the best solution at the Pareto front.

For the first and second scenarios, these solutions are shown as best solutions in Figures 5-4 (a) and 5-4 (b).

For comparison, a selection of solutions is presented in Figure 5-6. In this graph, normalised values of cost and power are both shown for all the cases and are compared with those of the benchmark case study of the Spa Urach geothermal reservoir. The optimisation process considered the minimisation of the cost and maximisation of the thermal power as the objective functions. If enough budget is available for the project, one of the solutions with more focusing on the thermal power is going to be selected rather than the economic cost; for example, solutions S13 and S23 are selected for the proposed two scenarios. On the other hand, if the budget is limited then a solution with the limited cost can be chosen as the best optimum design; hence, S12 and S22 are selected based on engineering judgment. Nevertheless, if the importance of both optimisation objectives (i.e. total cost and thermal power) is the same, then a solution in the corner of the curve satisfying both objectives can be chosen as the best design of reservoirs; then, S11 and S21 are selected to satisfy both optimisation objectives.

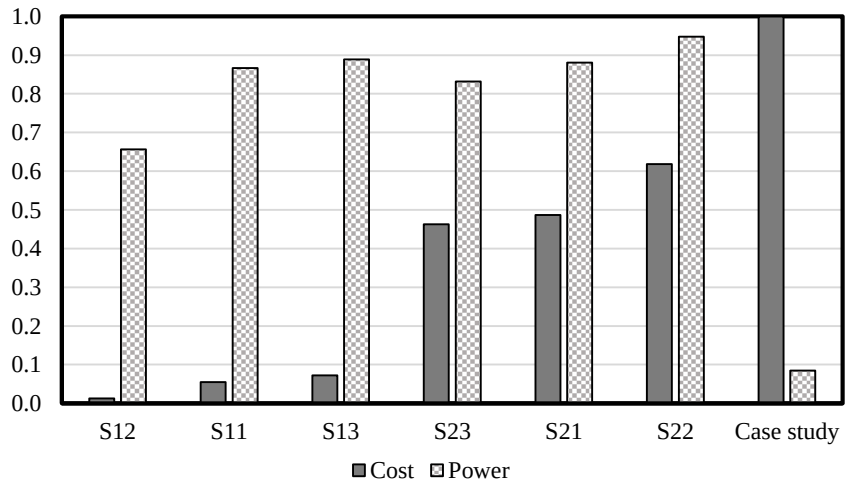

Figure 5-6. Normalised power and cost of the selected best designs (S11, S12 and S13 from 1st scenario on Figure 10(a); S21, S22 and S23 from 2nd scenario on Figure 10(b) and the case study

In addition, the thermal evolution of both best solutions S11 and S21 are compared to the case study in this research. It can be seen in Figure 5-7 that the cold water front in S11 and S21 did not reach the production well. However, the case study has reached the breakthrough time in early stages, which means that the methodology presented in this paper is proven an efficient tool to obtain optimum designs for EGS reservoirs.

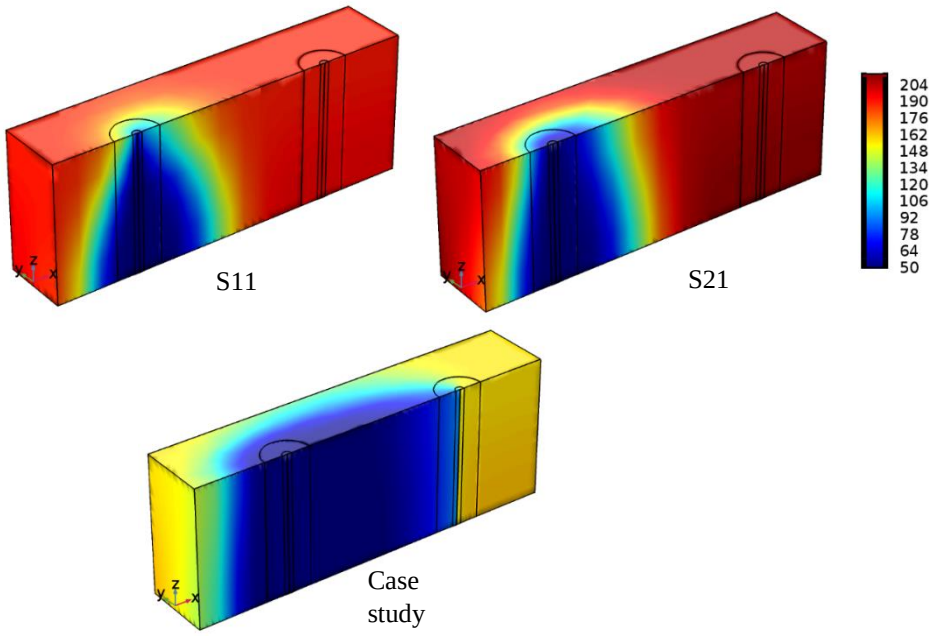

Figure 5-7. Thermal evolution of S11, S21 and the case study models

5.3 Conclusions

In this chapter, an advanced systematic approach to enhance long-term performance of EGS reservoirs is applied for the optimisation of a doublet well EGS reservoir. An integration of FE analysis and GA optimisation technique has been applied to find optimum designs of EGS reservoirs. Two scenarios (with and without changing the equivalent permeability of the reservoir) were considered during the optimisation process to find potential optimum design of EGS reservoirs. The results of the optimisation showed the following:

- This hybrid optimisation approach gives an insightful understanding of EGS long-term performance regarding the reservoir extraction efficiency, commercial feasibility and its service life.
- Results of both optimisation scenarios revealed that the permeability of the reservoir had a significant influence on selecting the other artificial design parameters.
- It was observed that the permeability of the reservoir has a significant influence in the required capital cost for EGS designs. Where, high permeable reservoirs can positively influence in the operation cost through lower injection pressures than reservoirs with lower permeability.
- In addition, the results show that there is a complex interaction between the reservoir design parameters, which can increase challenges for decision-makers that responsible for design and operation of a reservoir with using conventional methods. However, with the use of the presented hybrid optimisation technique, it is possible to consider the design parameters' interconnectivity during the optimisation process in order to find optimum solutions to design EGS reservoirs.

CHAPTER SIX

6 DEVELOPING A NUMERICAL ANALYSIS FOR ENHANCED GEOTHERMAL MULTI-WELLS RESERVOIRS BASED ON FINANCIAL CONSIDERATION (CASE STUDY SOULTZ-SOUS-FORÊTS IN FRANCE)

6.1 Introduction

In this Chapter, the development of the finite element model of a multi-wells reservoir is presented. The subsections present brief descriptions of EGS model geometry, materials properties and initial and boundary conditions used for the FE model. It also presents the impact of number of wells on EGS multi-well reservoirs performance through conducting a sensitivity analysis for the commercial viability of the design to the number of wells.

6.2 Finite Element Development

Soultz-Sous-Forêts in France contains permeable ground structures over a relatively large volume of the reservoir, at the depth of 5 km. This EGS has a three-well system, i.e. two production wells centred by a single injection well (Genter et al., 2010). Thus, due to the available experimental data, it can be used as a case study site for a multi-well reservoir design. Therefore, it was selected as a case study in this research due to its manifest representation of a deep EGS multi-well reservoir.

A finite element (FE) model of the reservoir is built, using COMSOL Multiphysics, to simulate a fully saturated multi-well EGS with an isotropic permeability equivalent to both, the fractured zone and the rock matrix. Other properties of the FE model can be found in Table 6-1 based on Genter et al. (2010).

Table 6-1. Design parameters of FE model (Genter et al., 2010)

Parameters	***Symbols***	**Value**	**Unit**
Space between wells	L	600	m
Reservoir height	h_r	500	m
Rock matrix			
Density	ρ_r	2850	kg/m^3
Permeability	k	1e-14	m^2
Porosity	θ	0.005	
Specific heat capacity	c_{p_r}	1000	J/(kg.K)
Thermal conductivity	λ_r	2.5	W/(m.K)
Injected fluid			
Density	ρ_f	1000	kg/m^3
Specific heat capacity	c_{p_f}	4210	J/(kg.K)
Thermal conductivity	λ_f	0.6	W/(m.K)
Dynamic viscosity	μ	2e-4	Pa.s
Others			
Initial temperature	*Tinit*	473.15	K
Initial pressure	*Pinit*	49	[MPa]
Production well BHP	*Ppro*	48.25	[MPa]
Injection well BHP	*Pinj*	49.91	[MPa]

Different design scenarios of the reservoir were analysed to allow different production well numbers (*Npw*), to be investigated, from which the impact of *Npw* on the production flow rate in the short-term and reservoir's performance in the long-term, was assessed. Initially, the Soultz EGS reservoir was modelled using the current flow rate of 50 kg/s in order to calculate the necessary injection pressure to maintain this value of flow rate. Then, the calculated value

of pressure was imposed on different models of the same reservoir each with different number of production wells (i.e. *Npw*> 2) to investigate the impact of increasing *Npw* on the reservoir performance and to examine the achievement of a commercial mass flow rate by increasing *Npw*. In the next stage, these processes were repeated with a minimum production mass flow rate of 80kg/s.

6.2.1 Numerical Model and Simulation Approach (Thermal Model)

In the proposed study, the COMSOL Multiphysics package is employed to carry out a three-dimensional (3D) numerical simulation. The FE model simulates the EGS multi-well reservoir as a fully saturated porous medium with isotropic permeability (*kx=ky=kz*) equivalent to a combination of fractured zone and rock matrix. To do so, assumptions are applied for the FE model in order to reduce the degree of freedom, see Section 3.2.1. of Chapter Three.

6.2.2 Initial and Boundary Conditions

Initial conditions: the experimental data from the GPK 2 log borehole, see Figure 6-1, show that the temperature of the Soultz at the lower reservoir (T_o) at depth (z) of 5000 m is about 200 ^{o}C, which is the focus of the present study, and the temperature gradient (T_g) is around 0.03 K/m (Genter et al., 2010), see Figure 6-2. Thus, the temperature of the reservoir can be calculated using Equation 6.1:

$$T_\circ = 200\,℃ + T_g(-5000 + z) \quad (6.1)$$

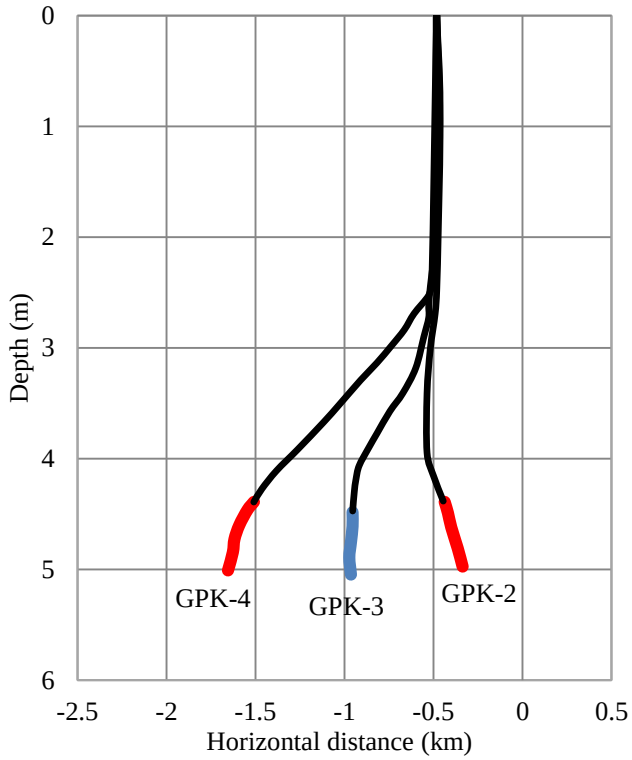

Figure 6-1. The existing boreholes at depth of 5000m at Soultz field (lower reservoir) (after (Genter et al., 2010))

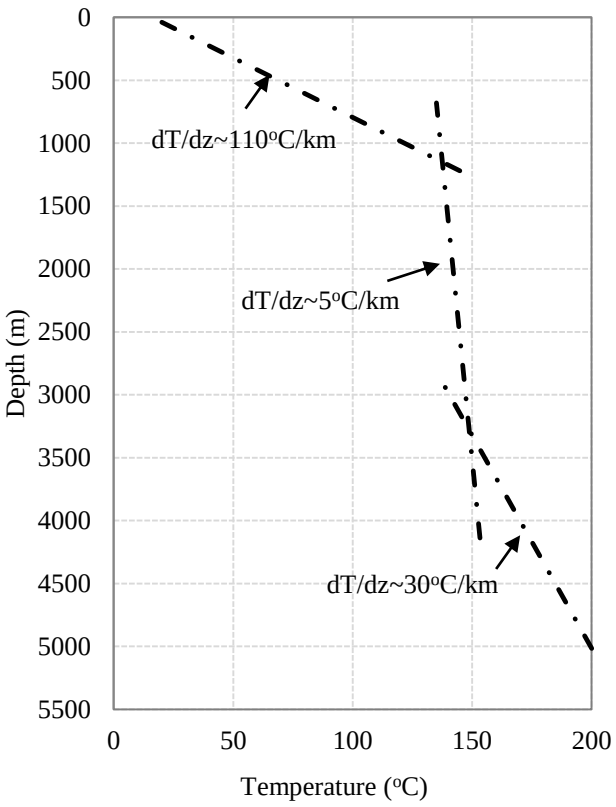

Figure 6-2. Temperature profile at Soultz field (after (Genter et al., 2010))

The initial pressure for the reservoir is assumed to be depth dependent and it is calculated using Equation 6.2:

$$Pinit = \rho \cdot g \cdot z \tag{6.2}$$

Boundary conditions: According to McDermott et al. (2006) an injection fluid temperature of 50 ^{o}C is required to avoid chemical dissolution of the rock matrix by very low injection fluid temperature. The fluid injection pressure (*Pinj*) is assumed constant at 5.3 MPa at the surface to achieve a total mass flow rate of 50 kg/s. The boundary conditions of the wells are calculated using Equations 6.3 and 6.4.

$$Pinj = \rho_f gz + 5.3 \text{ (MPa)} \tag{6.3}$$

$$Ppro = \rho_f gz - 5.3 \text{ (MPa)} \tag{6.4}$$

For the boundary conditions of the reservoir it is assumed that there is no flow and no heat transfer is allowed from the surrounded areas, see Section 2.1; and thus the Neumann boundary condition using Equations 6.5 and 6.6 is applied for the surrounded rock matrix surfaces.

$$\mathbf{n} \,.\, \rho_f \mathbf{u} = 0 \tag{6.5}$$

$$\mathbf{n} \,.\, \mathbf{q} = 0 \tag{6.6}$$

6.2.3 Geometry

The Soultz reservoir in France is strongly representing EGS multi well reservoirs as long as it is enhanced to contain permeable structure (Genter et al., 2010). The present study illustrated a fully coupled three-dimensional 3D deep EGS multi-well reservoir model. According to Genter et al. (2010), at a depth of 5 km the Soultz reservoir is a three well system two production wells GPK-2 and GPK-4 centered by a single injection well GPK-3, see Figure 6-1.

Due to the irregular shapes of stimulated rock blocks, it is desirable to simulate a circular shape for the fractured zone (Kuo et al., 1977). In addition, the fluid flow in the rock matrix is almost radially distributed (Smit 2010). Therefore, the reservoir is assumed to have a cylindrical shape in the present study to explore the optimum design of EGS multi well reservoirs by reducing the impact of the geometry boundary on the configuration of the production wells around a single injection well. The distance between the injection and production wells assumed to be 600 m (Genter et al., 2010). There is a need to set up the models in such a way that the boundary effects do not have high influences on the optimisation results in which it could be considered a second order effect. Thus, the distance from the boundary to the centre of production wells is selected using trial and errors method.

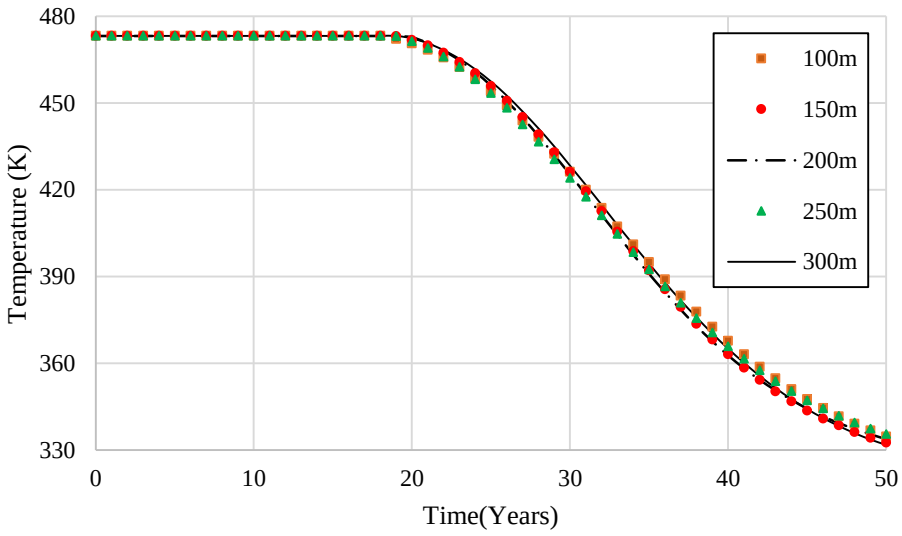

Figure 6-3. Temperature of a point at the mid distance between the injection and production wells after 30 years of heat extraction

The results for sensitivity analysis of the boundary space show that the boundary distance has no sensible impacts on the temperature at the mid distance between the injection and production wells (300 m) at the base of the reservoir, see Figure 6-3. Thus, 100 m has been selected for the boundary distance to the production wells centre for the models due to the unpronounced error

and time-consuming modelling. The geometry of the selected proposed model can be seen in Figure 6-4.

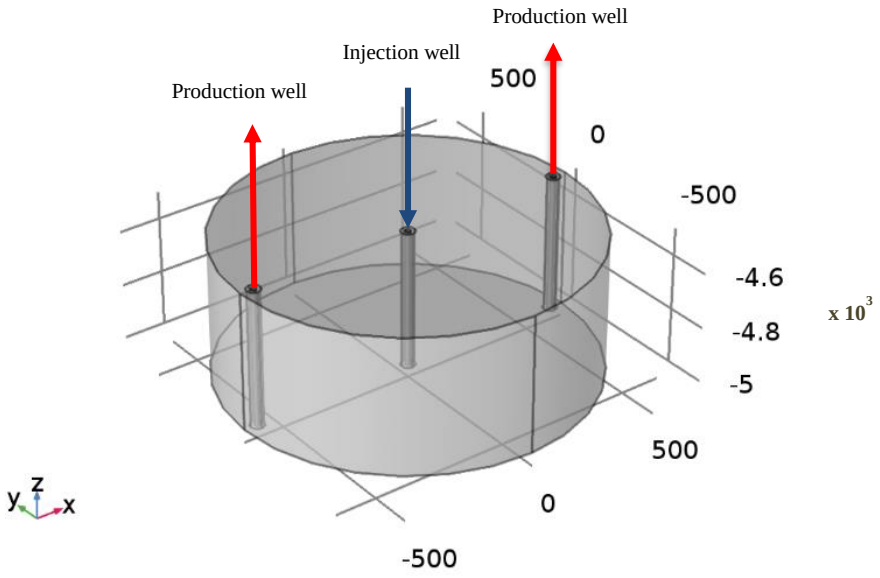

Figure 6-4. The geometry of the proposed FE model

6.2.4 Meshing

The last part of the numerical simulation is the finite element mesh. The reliability of the numerical simulation is based on the accuracy of numerical model and this can be obtained using a well-defined mesh for the model. The biggest challenge in meshing such subsurface structures is the huge difference between the size of the model parts such as the rock matrix and the wells. To control the fluid mass flow and the heat transfer, it is important to predefine the mesh for the surface area of the wells as long as the injection and production pressure and the injection temperature is applied as a surface area of the wells. Thus, the mesh used for the finite element of the present study model consists of predefined very fine mesh applied to the wells and grows outwards to the surrounding area. This is strongly required to control the fluid mass flow rate and heat transfer during the simulation process, see Figure 6-5.

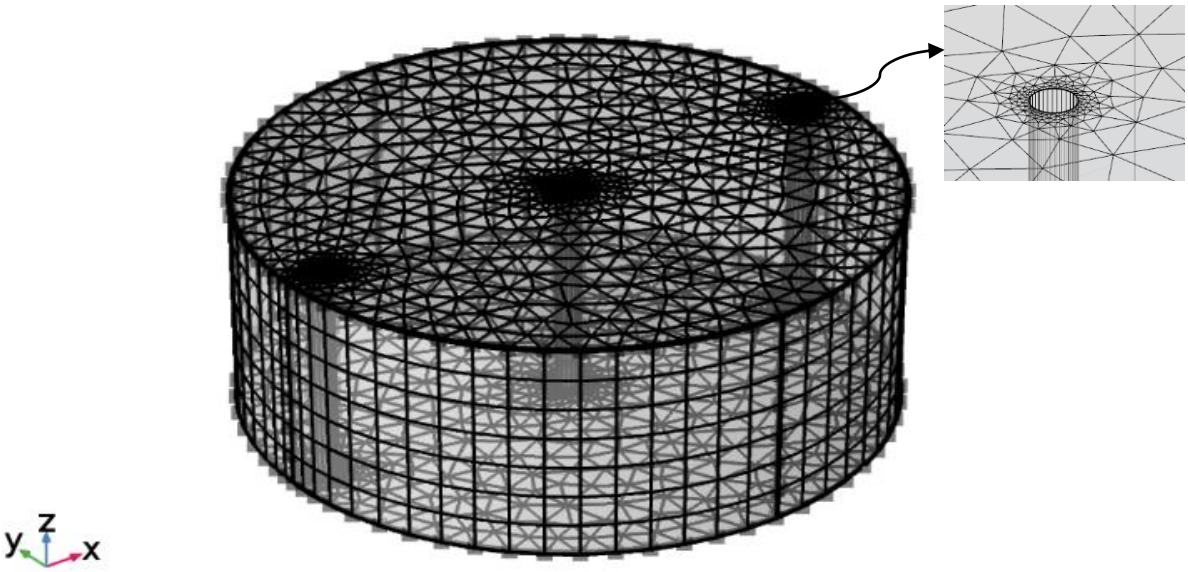

Figure 6-5. Mesh details for the proposed model

Since the hybrid optimisation approach can involve millions of runs of FE models, to maintain the accuracy of the response results while reducing the execution time of the FE model, four different mesh sizes were examined. First (mesh 1), coarse mesh is selected, where the complete mesh consists of 25002 domain elements, 7968 boundary elements, and 896 edge elements with a simulation time of 194 seconds. Second (mesh 2), fine mesh is selected, where the complete mesh consists of 35332 domain elements, 11640 boundary elements, and 1000 edge elements with a simulation time of 324 seconds. Third (mesh 3), finer mesh is selected, where the complete mesh consists of 50310 domain elements, 9504 boundary elements, and 1120 edge elements, with a simulation time of 425 seconds. Fourth (mesh 4), very fine mesh is selected where the complete mesh consists of 97546 domain elements, 17120 boundary elements, and 1344 edge elements with a simulation time of 1089 seconds. These cases have been compared with response to the temperature profile of the reservoir base point in the mid distance between the injection and production wells for 50 years of heat extraction.

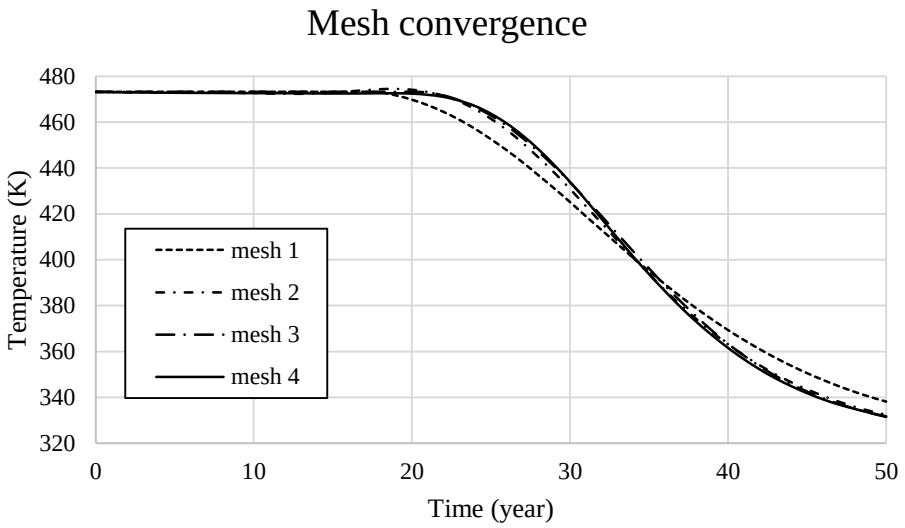

Figure 6-6. Mesh convergence of the proposed FEM

The results presented in Figure 6-6 shows that there is unpronounced change with mesh sizes 2, 3 and 4, which means the mesh converged at that values. However, while the optimisation technique in this research using integration of FE and GA will need to run thousands models to find the best design scenario, it is therefore mesh 2 has been selected for the FE model, as it requires less time than the others do.

6.3 Combining Hydro-Thermal with Economic Models

The procedure of the sensitivity analysis of multi-well reservoir to number of production wells consists of three parts. First, it deals with the numerical analysis of the EGS multi-well reservoir taking into consideration the geological, physical and processes of the heat exploitation process. Second part of the procedure deals with the economic analysis of the required cost for the creation processes in which it depends on the cost of the number of wells at depth of 5000 m. The last part of the analysis deals with the evaluation financial consideration of the long-term performance in terms of the extracted energy and the total cost of the creation on processes. The following subsections present more details of the sensitivity analysis procedure and results.

6.3.1 Economic Model

In order to investigate the optimum design of EGS reservoirs for long-term performance, it was important to take into account the financial consideration. In this Chapter, the drilling cost (C_D) of wells was considered as a key parameter for the evaluation of the economic analysis. Thus, the drilling cost is considered for all the wells within the multi-well reservoir using Equation 3.10 in Section 3.2.4.1. of Chapter Three.

6.3.1.1 Financial Considerations

In order to evaluate the commercial viability of each of the above scenarios, an economic analysis based on the levelised cost of energy was performed. In general, the levelised cost of energy is defined as net current value of unit cost of energy over service-life of a resource. For this study, levelised cost of geothermal energy was defined as the drilling unit costs of thermal power production over the reservoir service life. To evaluate the cost of different reservoir designs, the thermal analysis was integrated with economic considerations. It was important to calculate the minimum cost of MW of accumulative thermal power production in each design scenario using Equation 3.8 in Section 3.2.3.2. of Chapter Three. This step is important to enable the full impact of the proposed approach to be fully assessed. Therefore, to quantify this aspect of the EGS design, a model was defined to calculate the thermal economy using Equation 6.7.

$$TE = \frac{\Sigma C_D}{\sum_{t=0}^{t=J} Thermal\ power} \tag{6.7}$$

where *TE* is the levelised cost of geothermal power and its unit is millions of US dollars per MW; *J* (year) is the time at the threshold thermal drawdown (Bödvarsson and Tsang, 1982).

Importantly, in addition, the economic analysis and the thermal power production were assessed for each design scenario of both non-commercial and commercial EGS designs. Figure 6-7, depicts the overall methodology used to assess design approaches for EGS.

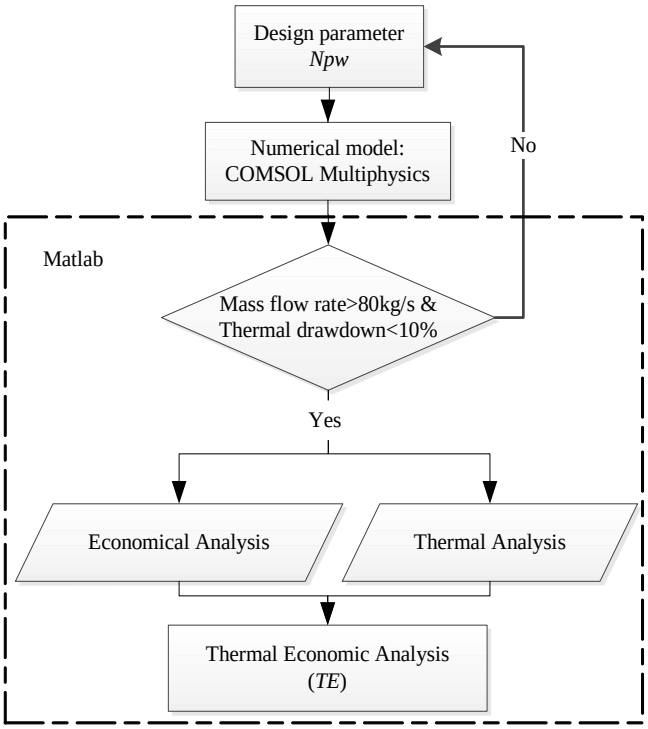

Figure 6-7. Procedure to design commercial EGS reservoirs

6.4 Results and Discussions

A 3D multi-well reservoir was simulated using experimental data from the Soultz-sous-Forêts, France with a total 50 kg/s mass flow rate and 200 °C temperature at the base of the reservoir. When considering different scenarios, the mass flow rate was increased by increasing the number of production wells (*Npw*). Eight scenarios of *Npw*, as illustrated in Figure 6-8, were considered to study the impact of increasing *Npw* on reservoir performance. The fluid injection pressure for each analysis scenario and distance between injection and production wells remain constant for each scenario, to enable focus on key ground related impacts on EGS outputs.

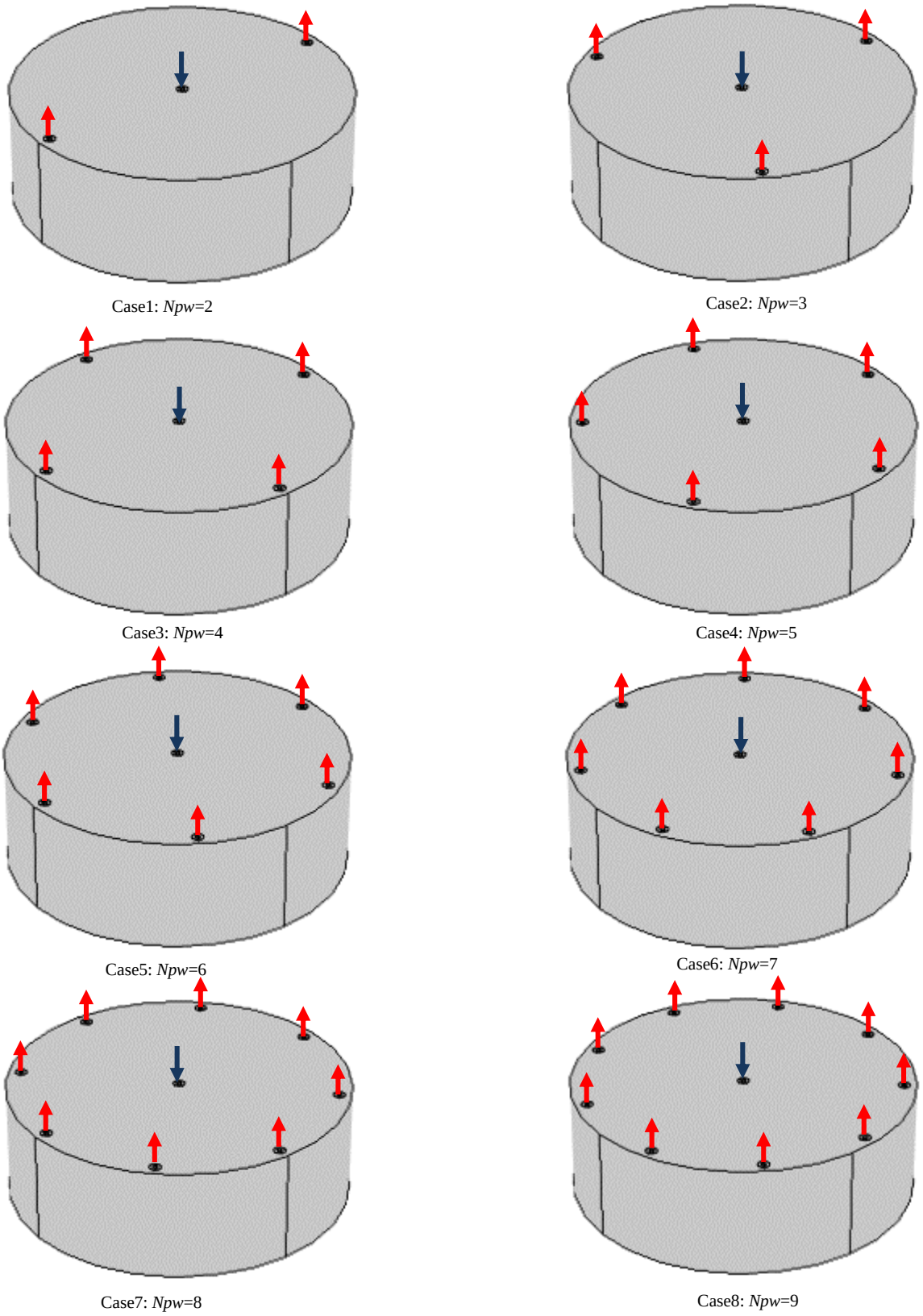

Figure 6-8. Schematic drawings of the eight cases of number of production wells (*Npw*) red and blue arrows representing production and injection wells respectively

6.4.1 Impact of Well Number on Thermal Power and Mass Flow Rate

The impact of *Npw* was investigated in two stages; firstly, the fluid injection pressure was kept constant (to maintain minimum mass flow rate of 50 kg/s during 50 years of heat extraction) to study the performance of the reservoir with increasing *Npw*. Secondly, a minimum mass flow rate of 80 kg/s was assumed for the benchmark model and then the impact of *Npw* in the reservoir long-term performance based on the same fluid injection pressure required to maintain 80kg/s mass flow rate for 2 *Npw* was investigated.

6.4.1.1 Influence of Npw on the Case Study Performance

Npw was increased for the benchmark model to investigate the impact of increasing *Npw* on the thermal power production and the production mass flow rate over 50 years of heat extraction.

The results of the accumulative thermal power at the breakthrough time and the production mass flow rate for different *Npw* are presented in Figure 6-9.

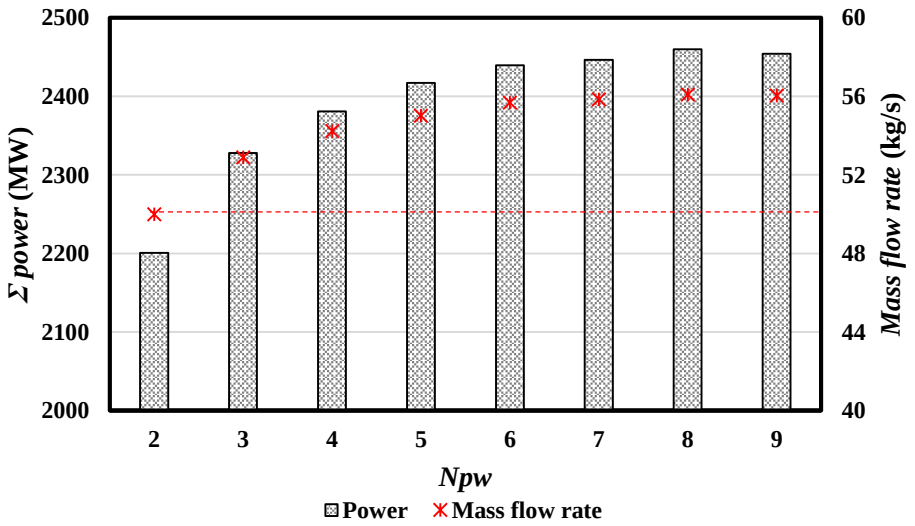

Figure 6-9. Accumulative thermal power and the mass flow rate of different Npw

Results from Figure (6-9) show that, in general, production power and mass flow rate rise with higher number of production wells, for relatively low number of production wells. However, it is evident that this increase becomes less visible with more production wells, demonstrating asymptotic characteristics. Nevertheless, the calculated mass flow rate in all cases did not reach the commercial target of 80kg/s.

6.4.1.2 Influence of Npw on a Commercial Reservoir

To understand the reservoir condition required to satisfy the need of maintaining the minimum 80 kg/s mass flow rate, additional analyses were carried out as per the following. Achieving 80 kg/s of mass flow rate for the benchmark model, requires a constant injection fluid pressure of 8.7MPa. This value was obtained from the results of trial FE analysis. To assess the impact of the Number of production wells, the number of wells were increased while the injection pressure was kept constant at 8.7MPa. The results are presented in Figure 6-10.

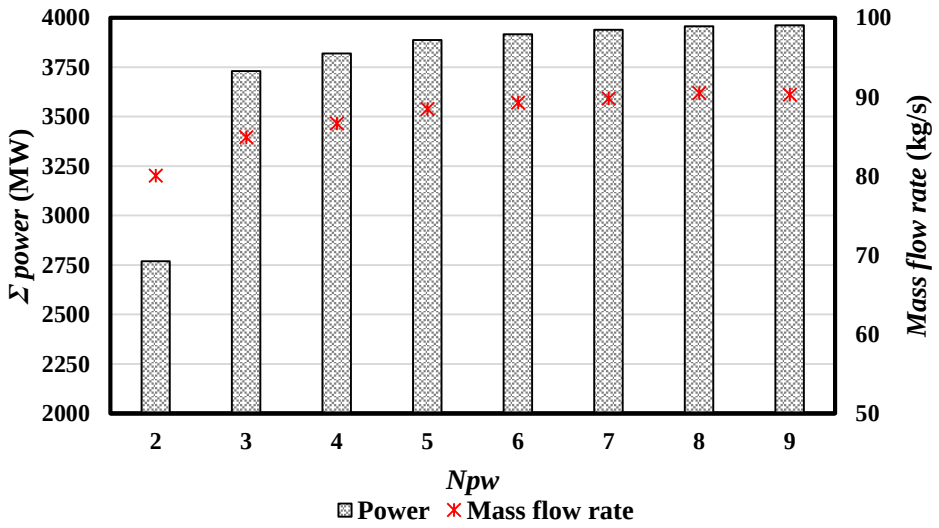

Figure 6-10. Accumulative thermal power and the mass flow rate of different Npw for commercial reservoir designs

From Figure 6-10, it can be seen that the same trend of increase in power production and flow rate occurs as seen with the previous scenarios (see Figure 6-9). However, with the new injection pressure, the increase in power is much more pronounced when moving to three

production wells (above 35%), again as seen in the previous scenario, see Figure 6-9. However, in both scenarios, the gradient of mass flow rate did not change significantly compared with the benchmark model.

The thermal evolution of the reservoir in different *Npw* for the commercial case study (i.e. the second scenario) is presented in Figure 6-11. This figure shows that the thermal evolution behaviour changes for the reservoirs with more than two wells. This can be seen in the graphs where higher values of temperature can be observed in vicinity of all production wells, whereas, in the two production wells the cold front (light blue colour) has already reached the production wells.

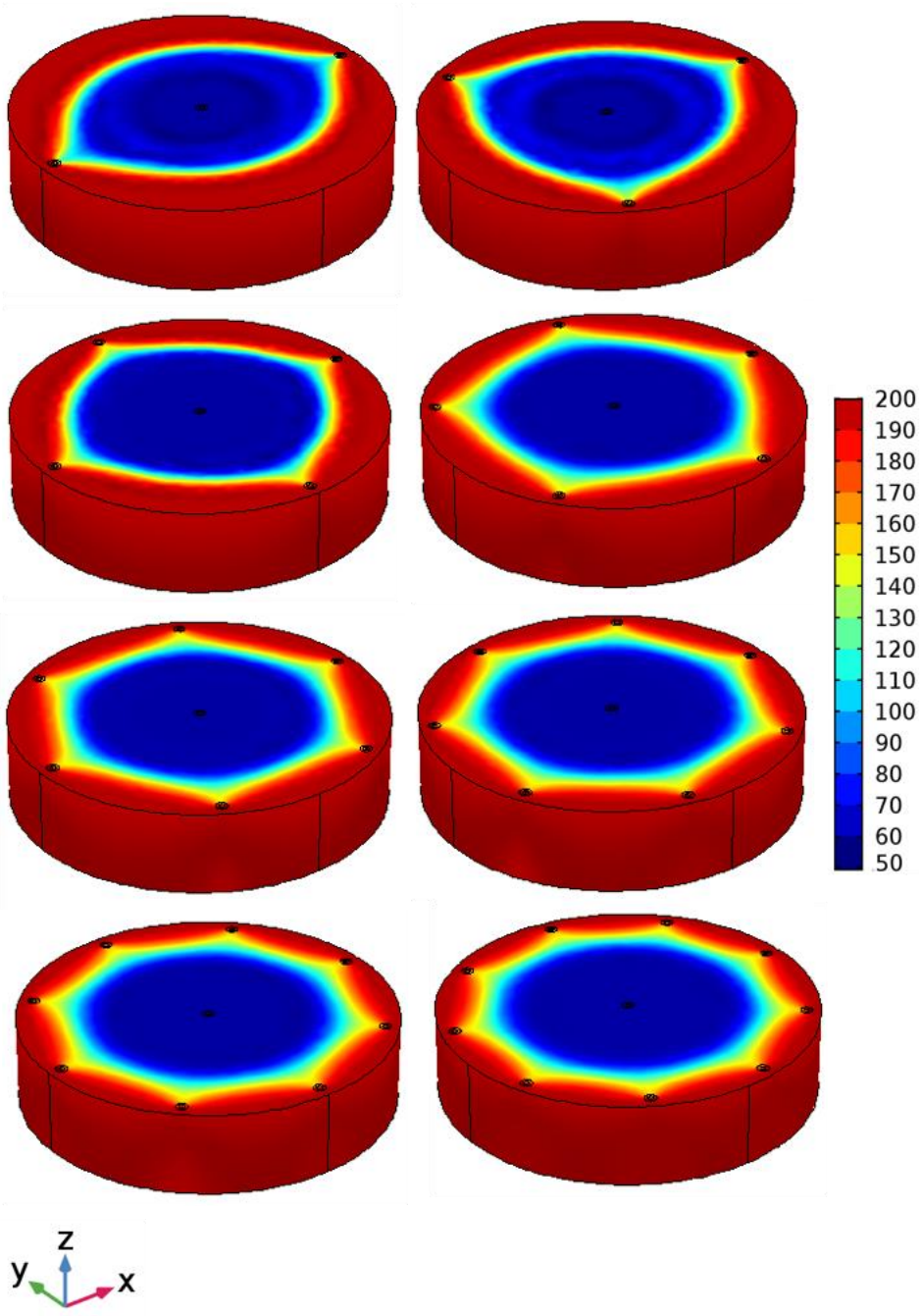

Figure 6-11. Thermal evolution of different Npw (temperature in °C)

6.4.2 Economic Analysis

Obviously, increase in *Npw* results in increase of the drilling cost, but in a linear manner. However, according to the results shown in sections 6.4.1.1. and 6.4.1.2., the thermal power production increases nonlinearly therefore lead to overall nonlinear changes in the levelised cost of power. Thus, for both the non-commercial and commercial conditions, the relationship

between *TE* and *Npw* has different behaviour with *Npw* up to four wells. The overall affect is that the ratio of *TE* has a general linear trend against *Npw* as can be seen in Figure 6-12 (a&b).

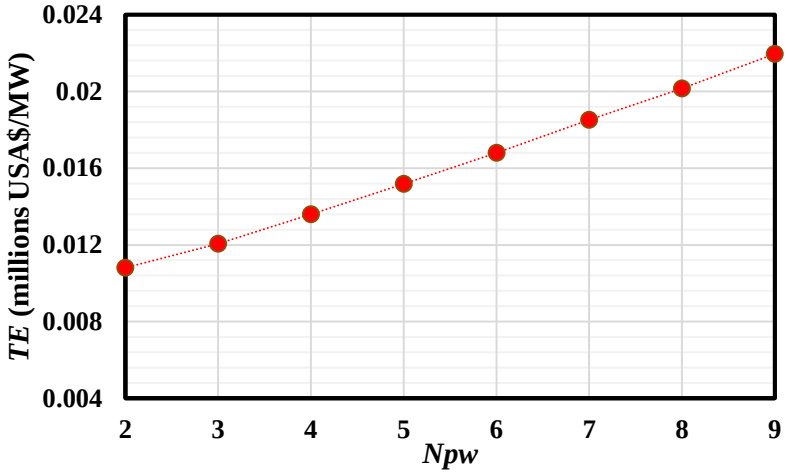

(a)

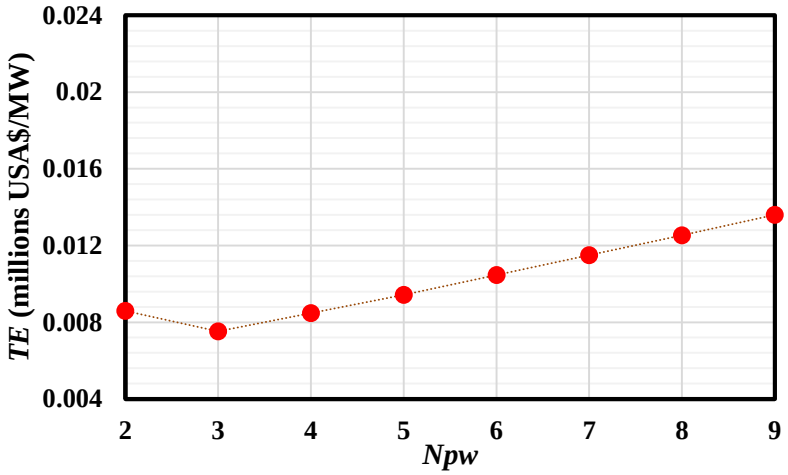

(b)

Figure 6-12. TE of different Npw; (a) non-commercial design when mass flow rate < 80kg/s and (b) commercial case when mass flow rate ≥ 80kg/s

From Figure 6-12, it can be observed that for cases with non-commercial conditions (see Figure 6-12 (a)), increasing the number of wells, increases the production power, but with no positive impacts on the levelised cost of the project. However, this is not the case for commercial geothermal systems (see Figure 6-12 (b)) since the levelised cost has dropped when moving from two to three production wells.

To investigate the influence of increasing *Npw* for both scenarios (i.e. non-commercial and commercial designs), the gradient of mass flow rate, accumulative thermal power and *TE* were calculated and compared against the benchmark values (see Figures 6-13 (a) and 6-13 (b)). For this analysis, improvement was defined as the ratio of changes over the benchmark values (e.g. improvement of *TE* is $(\frac{TE\ new\ design - TE\ benchmark}{TE\ benchmark} \times 100)$. In Figure 6-13, zero in the vertical axes, refers to the benchmark values.

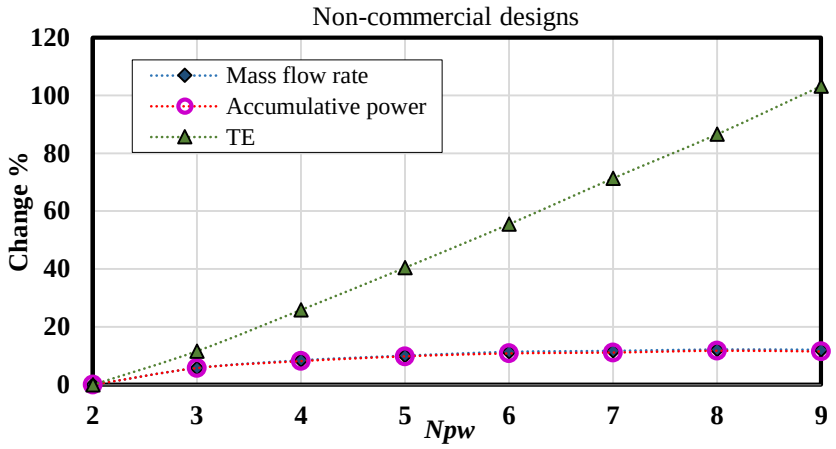

(a)

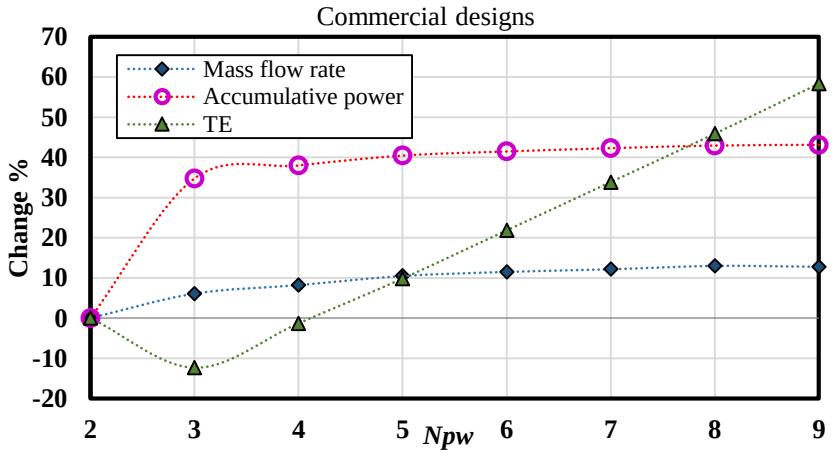

(b)

Figure 6-13. The percentage changes of the main objectives (i.e. mass flow rate, accumulative thermal power and TE) for both scenarios; (a) non-commercial design; (b) commercial design

As shown in Figure 6-13 (a), the change in *TE* for the first scenario (i.e. non-commercial reservoir) increases exponentially with increasing *Npw* compared to the benchmark (i.e. *Npw* is 2), with a minimum change of about 11% at three production wells and a maximum change of over100% at nine production wells, which indicates that the levelised cost increased with increasing *Npw* to more than 2 wells. However, in the second scenario (i.e. commercial reservoir), the change has a different trend and the levelised cost improved at *Npw* for three wells through a decrease in *TE* by about -12%. After this point, there are no improvements in the levelised cost with increasing *Npw* up to nine wells. However, the percentage change in *TE* was still smaller compared to the value that the first stage increased.

The improvement in the accumulative thermal power for non-commercial designs was around 6% at *Npw* of 3, the rate of the improvement was thereafter insignificant for all cases of *Npw*, (see Figure 6-13 (a)). However, for commercial designs, there was a significant improvement for the accumulative thermal power at *Npw* of three of about 34% above the benchmark. Thereafter, the rate of the improvement can be seen to increase slightly up to *Npw* of seven and with insignificant improvement observed thereafter (see Figure 6-13 (b)). Nevertheless, the improvement of accumulative thermal power in commercial reservoir was more effectively improved by the increase *Npw* than for non-commercial reservoirs.

With respect to the percentage improvement of the production mass flow rate, it can be seen clearly in both stages (i.e. non-commercial and commercial reservoir) that these are almost the same with a slight improvement in the commercial case (see Figures 6-13 (a) and 6-13 (b)).

This demonstrated the importance of key design considerations, showing the impact of increasing production wells on the reservoir financial and long-term performance in both commercial and non-commercial geothermal reservoir, using the threshold definition of flows rates of 80 kg/s.

6.5 Conclusions

In this Chapter, numerical simulation and optimisation of long-term performance of multi-well reservoir have been conducted for enhanced geothermal system (EGS) reservoirs. The migration of high-pressure injected fluid in the reservoir and its impact on the temperature of the reservoir is simulated using the COMSOL Multiphysics solver. The primary aim was to model the impact of increasing production wells on the reservoir financial and long-term performance on a non-commercial geothermal reservoir, which produce a mass flow rate less than 80 kg/s. Accumulative thermal power production, production mass flow rate and levelised cost are calculated to compare the results with the benchmark reservoir for two scenarios of commercial feasibility of the reservoir (non-commercial and commercial reservoir). The results of this study indicate the following:

- Increasing the number of production wells in a non-commercial geothermal reservoir, with a constant fluid injection pressure and distance between the injection and production wells, enhances the production mass flow rate.
- However, increasing the number of production wells cannot maintain the commercial mass flow rate target (80 kg/s), which show that increasing the mass flow rate requires additional design parameters that have been recommended by the MIT report.
- On the other hand, in the case of a commercial geothermal reservoir with two production wells, the increase in production wells has the potential to improve the thermal production power by three times, compared to the non-commercial case.
- The results show that there is a strong combination in the positive impact of increasing both injection pressure and the number of production wells, which is the case in the commercial designs.

- In the commercial stage, the levelised cost of the power production has improved by 12% within a reservoir comprising three production wells. However, within the non-commercial case, not all scenarios of increasing the number of production wells could achieve lower cost than the benchmark levelised cost.
- Although EGS reservoirs with high number of production wells theoretically feasible, may not be practically doable. The results presented in this chapter is more a numerical exercise than real cases. This is to show the impact of well numbers on the long-term performance of EGS reservoirs.
- The analyses demonstrated complex interactions between the number of wells, reservoir parameters and their overall effects on the reservoir performance, particularly when combined with financial considerations.

The current study in this chapter was conducted using log borehole data available from Soultz. The analyses were carried out with the assumptions that other contributing factors such as permeability, distance between wells, injection fluid temperature and the geological data do not change. Hence, the conclusion of “three well production as optimum” cannot necessary be extended to other reservoirs. Additional investigations have to be carried out to include these factors and their mutual interactions. However, this work provides useful insights on how optimised designs for multi-well reservoirs can potentially be achieved.

CHAPTER SEVEN

7 A COUPLED DESIGN AND MANAGEMENT FRAMEWORK TO OPTIMISE EGS MULTI-WELLS RESERVOIRS

7.1 Introduction

Chapters Four, Five and Six showed that achieving an optimum design of an EGS reservoir with a commercial viability is a complex challenge for design engineers. In addition, previous studies e.g. (Chen and Jiang, 2015, Chen et al., 2015, Fu and Carrigan, 2014, Vörös et al., 2007, Yang and Yeh, 2009) have also investigated the sensitivity of different design parameters for multi-well reservoirs. However, the literature (see Chapter two) shows that there are no studies so far that have investigated the interdependency of reservoir design parameters and their impacts on the long-term performance of EGS multi-well reservoirs, together with the commercial feasibility of the system within an optimisation technique. Thus, this chapter outlines the exploration of an optimisation procedure taking into consideration the interdependency of the design parameters of EGS multi-well reservoirs and its influence on reservoir performance over long periods in addition to the commercial feasibility of such type of EGS reservoirs.

7.1.1 Economic Model

The total cost of EGS reservoir design is considered during the economic analysis and it is calculated using Equation 3.13. In which, creation cost and operation costs are calculated using Equations 3.10, and 3.12 respectively, see Section 3.2.4. in Chapter Three.

In this chapter, the Soultz geothermal site is used and the values are respected to the price in France. Thus, pp =11.95 (US$/kwh), pr=20.33 (US$/GJ) and r=1.4% have been used.

7.2 Optimisation Model

The proposed methodology in Chapter Three was used for the optimisation procedure of the proposed EGS multi well reservoir used in this research. The optimisation approach was developed based on the optimal number and configuration of production wells, equivalent permeability of the reservoir and the fluid injection pressure.

The optimisation problem was formulated as a fitness function to evaluate different design scenarios as an optimal value based on maximisation of the long-term performance of thermal power production and commercial viability of the system).

7.3 Application

The developed hybrid optimisation technique (FE-GA) was applied to one of the most widely investigated multi-well EGS reservoir in the Soultz France field. This research involved fully coupled TH process and was subjected to: different boundary conditions, constant fluid injection and production pressures, constant fluid injection temperature, and impermeable boundaries with no fluid flow and heat flux allowed.

7.3.1 Formulation of Reservoir Design Models

The reservoir was subjected to different design scenarios; the efficiency of each design scenario in terms of accumulative thermal power production and total cost was investigated and compared. Three schemes are considered in each design scenario, where the design was considered failed when:

- Thermal drawdown after 10 years$\geq$10%.
- Production mass flow rate $<$ 80 kg/s.
- Reservoir Impendence > 0.1 (MPa.s/l).

The optimisation process aims to maximise the accumulative thermal power production (f1) as well as minimise the total cost of the reservoir (f2). The optimisation process is subjected to different constraints for the design variables. To do so, the objective functions are mathematically presented as follows:

$$\max f1 = \sum_{t=0}^{J} N \times q \times (h_p - h_{inj})$$

Where N is the number of wells, q is the mass flow rate (kg/s) and h_p and h_{inj} are the specific enthalpy of the production and injection fluid respectively.

$$\min f2 = N \times \left(1.72 \times 10^{-7} \times {D_h}^2 + 2.3 \times 10^{-3} \times D_h - 0.62\right) + N.q.\sum_{t=0}^{J} \frac{(\Delta P.pp + \rho_l.c_l.\Delta T.pr.\eta)_t}{(1+r)^t}$$

The constraints that bounded the input variables of each design are:

$$0 < Pinj \leq 10\ MPa$$

$$200 < d \leq 600\ m$$

$$0 < k \leq 1e-13\ m^2$$

$$2 < N \leq 10$$

7.4 Results and Discussions

In order to evaluate the interdependency of the contributing parameters and their impacts on the total cost and power production, a multi-optimisation process based on a genetic algorithm was employed. In the developed optimisation approach, the optimum solutions are addressed using multi objectives genetic algorithm (GA) using 400 generations and a population size of 50. The crossover used was 0.7 and mutation was 0.25 to generate the decision variables within the upper and lower limits.

The goal was to build a model that with minimum possible cost produces the maximum power. However, the analysis shows that as the power increases the total cost increases as well. This makes the problem a matter of finding an optimum solution, based on the available resources in different scenarios of real cases. The variables were normalised within the optimisation process between (0-1), where 0 refers to the minimum constraint of the variable and 1 refers to the maximum values. The accumulative thermal power was also normalised such that 0 refers to the minimum produced power of 575 MW and 1 refers to the maximum power of 3712 MW, see Figure 6-1. As can be seen in Figure 7-1, before a decision on the selection of the best optimum design is made, it is desired to evaluate the range of the design parameters that are required for optimum solutions.

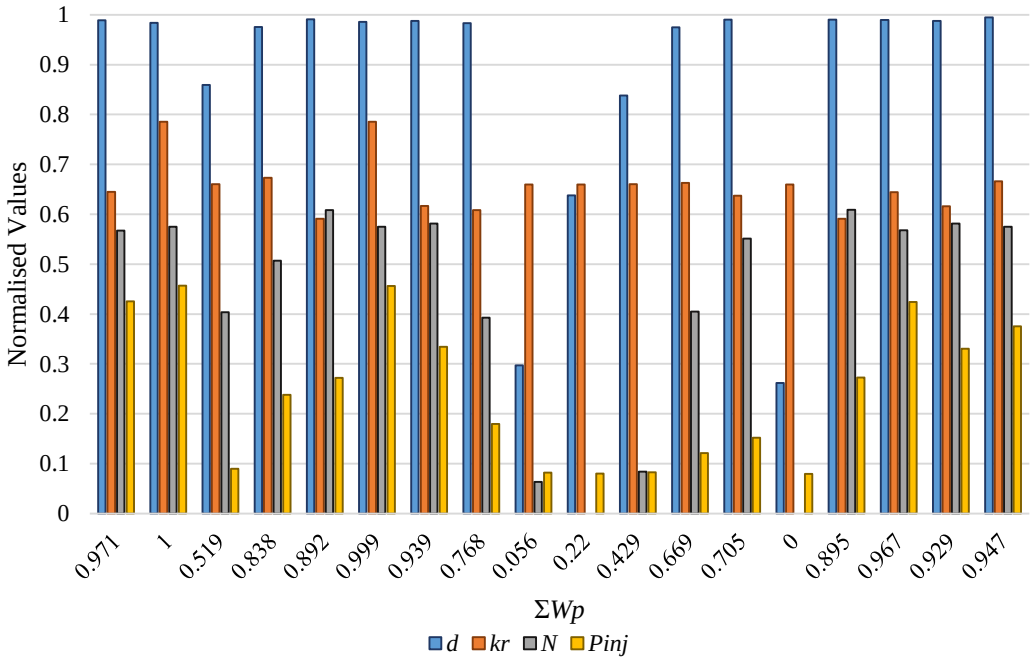

Figure 7-1. Design parameters of the GA optimum designs

Thus resulted in a Pareto front shown in Figure 7-2, which shows that as the variables regulate themselves to decrease the Total cost the *ΣWhp* drops, and vice versa. Each point on the Pareto front refers to one set of values for the variables.

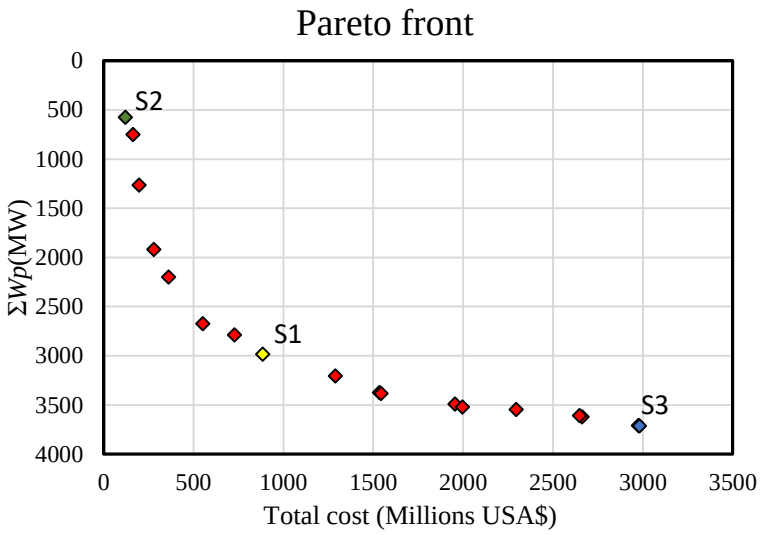

Figure 7-2. Pareto front of the multi-objectives GA results

Hussain (2015), suggested that the most optimum solution in a Pareto front was the closest to the origin. Based on this approach, Point S1 on the Pareto front (Yellow dot in Figure 7-2) is the highest performance to satisfy both objectives (i.e. total cost and accumulative thermal power).

Even though different methods have been suggested to deal with the result of multi-optimisation analysis, and pick the best one. It still can be an open problem, since in many cases the total cost is set beforehand. Because of this, only a part of the Pareto front may be possible to use and thus S2 on the Pareto front (Green dot in Figure 7-2) is the least total cost design. Alternatively, on the other hand, the amount of power, which is needed, is a fixed objective, and the total cost can vary within a range. Thus, S3 (Blue dot in Figure 7-2) is the highest accumulative thermal power. In either case, the above-mentioned methods can be used to evaluate the possible sets of contributing model design parameters.

The design parameters of the three selected best designs (i.e. S1, S2 and S3) can be seen in Table 7-1. The design parameters of the least cost design (S2) reveal that for design with the least cost, the variables regulate to have minimum number of production wells, fluid injection

pressure and distance between the injection and production wells, with a relatively high equivalent permeability. Compared to S2, S3 has a high number of production wells, fluid injection pressure and distance between the injection and production wells, with high equivalent permeability. Nevertheless, the best solution satisfying both objectives (cost and power) has conservative design parameters with respect to the other selected best solutions (i.e. S2 and S3).

Table 7-1. The design parameters of the selected best optimum solutions S1, S2 and S3

Best designs	*d* (m)	*k* (m^2)	*N*	*Pinj* (MPa)
S1	593	6.086e-14	5	1.793
S2	305	6.598e-14	2	0.793
S3	594	7.856e-14	7	4.566

The production mass flow rate, temperature profile and hydraulic impedance for the selected optimum designs S1, S2 and S3 are compared in Figure 7-3, Figure 7-4 and Figure 7-5 respectively. The mass flow rate of the three solutions show that the mass flow rate increased proportional to the increase of the number of production wells. However, the effect of high mass flow rate is evident on the temperature decline of the production fluid (thermal draw down). S3 has a fast temperature decline of the reservoir and only could maintain 1% of the initial reservoir temperature for 11 years of heat extraction process, and S1 design has reached the criterion *TD* after 13 years of heat extraction. While, S2 design has a slower decline in reservoir temperature and maintains the high production temperature above 1% of the initial temperature (200 ^{o}C) for the entire 25 years of extraction rate compared to S1 and S3.

Nevertheless, all the selected extreme optimum solutions (i.e. S1, S2 and S3) have result in a very low value of hydraulic impedance over maintaining high mass flow rate through high permeability and low injection pressure. This evidence the importance of select an appropriate value of reservoir permeability.

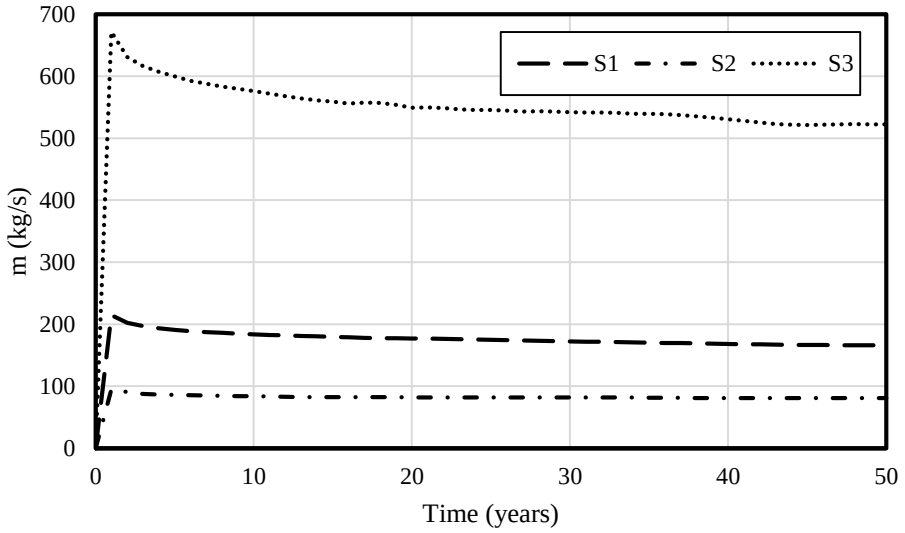

Figure 7-3. Mass flow rate production of S1, S2 and S3

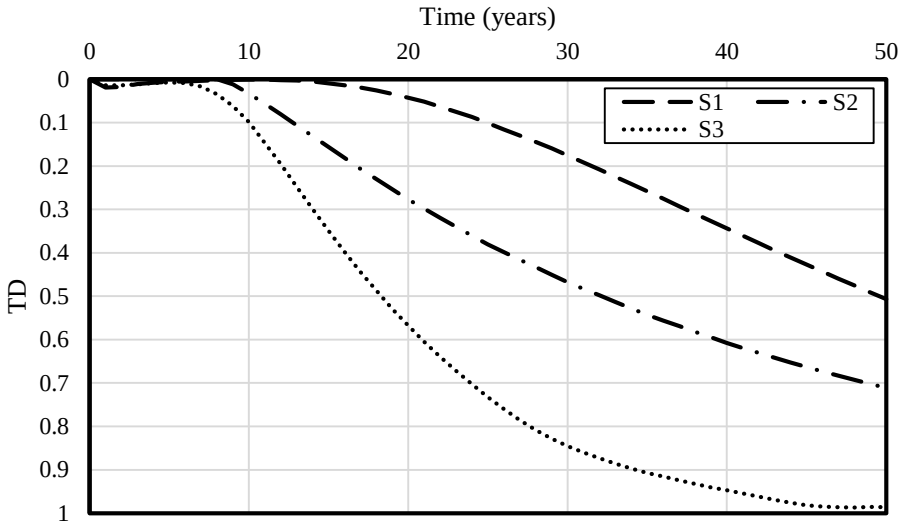

Figure 7-4. Thermal drawdown of S1, S2 and S3

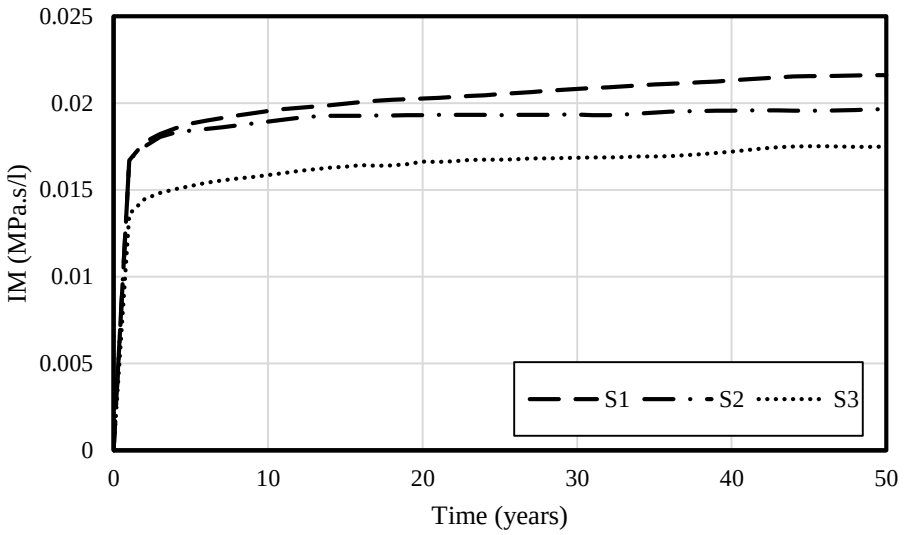

Figure 7-5. Hydraulic impedance of S1, S2 and S3

7.5 Conclusions

In this Chapter, using the numerical simulation conducted in Chapter Six, optimisation of long-term performance of multi-well reservoir have been conducted for enhanced geothermal system (EGS) reservoirs. During the optimisation process, the following points were considered:

- The economic analysis for the total reservoir cost (both creation and exploitation process) was conducted based on the results of the numerical analysis and thermal power production are input as fitness functions in a hybrid optimisation technique conducted with a Multi-objectives genetic algorithm GA based on Livelink COMSOL with MATLAB script.
- Five objectives are considered to be achieved within the optimisation process; three objectives are considered implicitly within the fitness function (reservoir service life (thermal drawdown), mass flow rate of the production wells and the hydraulic impedance of the production wells). While the other two objectives (i.e. power

production and reservoir total cost) are considered as the main multi-objectives within the fitness function.

- The optimisation of the reservoir considered four variables (number of production wells, the distance between injection and production wells, equivalent permeability of the reservoir and injection fluid pressure). These parameters are representing geometry design, material properties and boundary conditions and the optimisation of such multi disciplines within a model induce challenges for researches for the optimisation process. To overcome all of these challenges, a smart code during the numerical modelling and the fitness function was developed.

The results showed that:

- to achieve a long service life, lower cost and low hydraulic impedance, low injection fluid pressure and long distance between injection and production wells are required.
- However, to maintain a commercial mass flow rate (80 kg/s) and an efficient power production, it is significantly important to have a high equivalent permeability of the reservoir and high number of production wells.

CHAPTER EIGHT

8 CONCLUSIONS AND RECOMMENDATIONS FOR FURTHER RESEARCH

Enhanced geothermal system (EGS) reservoirs are artificial deep reservoirs designed to exploit geothermal power in hot dry rocks to generate electricity. Previous research has shown that EGS reservoirs have large potential to be exploited as a cost-effective renewable source of energy providing if their designs are optimised. The key to a cost-effective EGS reservoir design lies in low creation and operation costs, coupled with being able to achieve effective long-term performance (i.e. a commercially feasible design), which has a minimum mass flow rate of 80kg/s and minimum production temperature drop of 10% over long periods of exploitation.

Much research has been conducted to understand the long-term performance of EGS reservoirs. These have been concluded that natural design parameters of EGS reservoirs, such as rock thermal properties, geothermal gradient and porosity, have little impacts on improving the long-term performance of EGS reservoirs. However, artificial (man-made) design parameters, such as well placements, number of wells, injection fluid pressure and reservoir permeability, have significant influence on improving the performance of EGS reservoirs over long periods. Therefore, different optimisation techniques have been applied to investigate optimum designs of EGS reservoirs that meet practical considerations and constraints of a geothermal reservoir i.e. thermal drawdown, thermal power production, reservoir impedance and commercial feasibility of reservoir designs. Most of the previous research published has used parametric studies as optimisation techniques and some have used other techniques such as multivariate adaptive regression, fmincon and genetic algorithm.

However, the results of previous research have showed that artificial design parameters have a complex impact on optimisation objectives. For example, the distance between injection and production wells have various impacts on optimisation objectives, whilst longer distances can improve thermal drawdown, shorter distances can have a negative impact on thermal production energy over long periods. In addition, high values of fluid injection pressure and permeability of reservoirs have major impacts on increasing mass flow rate and subsequently thermal power production, but the same parameters have negative influences on thermal drawdown of reservoirs.

Previous work has mainly focused on investigating the impact of single or multi design parameters in an individual approach on EGS reservoir performance without considering their interdependency during heat extraction process and their impacts on creation and exploitation costs.

Although previous studies provide some basic understanding of EGS reservoir designs, without taking into account the interdependency of key design parameters, solutions of optimum cost-effective designs are not practical. Consequently, this can limit the potential of EGS reservoirs and prevent their use as a reliable and commercially feasible source of energy.

This research therefore proposed to use artificial intelligence combined with computational models to find optimum design of EGS reservoirs. Thus, the research methodology used in the research presented here adopted an advanced systematic approach to enhance long-term performance of EGS reservoirs through integration of finite element (FE) analysis and a genetic algorithm (GA) optimisation technique, to find optimum designs of EGS reservoirs.

This hybrid optimisation approach gives an insightful understanding of EGS long-term performance with regards to thermal power production and financial consideration over its service life.

This chapter presents a summary of key conclusions achieved in this research and recommendations for further research to gain a better understanding of EGS systems.

8.1 Conclusions

The research presented in this thesis conducted an optimisation technique to improve long-term performance of EGS reservoirs. The key contribution of the research is associated the development of numerical models integrated with an artificial intelligence application such as genetic algorithm GA. To do so, the optimisation procedure overall required:

- An understanding of the influences of artificial design parameters of EGS reservoirs on design efficiency over long periods, to define optimisation variables and their constraints on the optimisation process.
- An economical model to analyse the commercial feasibility of EGS reservoir design for both during and post design stages.
- An appropriate code to link FE model and economic model with GA for a robust optimisation procedure to be developed, to allow the study of the interdependency of design parameters during thermal and economy analysis.

The study achieved the conclusions presented in the following subsections.

8.1.1 Impact of Artificial Design Parameters

In Chapter Four, numerical simulation and parametric study of design parameters of the long-term performance of a doublet well EGS reservoir have been conducted through:

1. The migration of injected fluid with high pressure in the reservoir and its impact on production temperature was simulated using COMSOL Multiphysics solver.
2. The verification of the numerical model showed a good agreement with numerical solutions in the literature.

3. Sensitivity analysis was conducted to evaluate the response of long-term performance of EGS reservoirs to different artificial design parameters using two methods:
    - First method consisted of parametric studies to analysis the impacts of these design parameters on reservoir production temperatures, mass flow rates and thermal power production over a given time.
    - Second method was used to determine the impacts of the same design parameters on accumulative thermal power production of the reservoir design at thermal breakthrough times i.e. end of reservoir service life.

The results of the sensitivity analysis showed that:

- It is highly important to consider the accumulative thermal power production to the end of the reservoir service life, which is the thermal breakthrough time, rather than to the end of a given time. This assumption was applied to avoid overestimations of thermal power production of a reservoir design as long as reservoirs are going to be depleted at the thermal breakthrough time.
- The results also showed that well spaces directly affect the determination of the heat coverage volume of the reservoir i.e. the actual volume of EGS reservoirs that is subject to heat exploitation. Consequently, well spacing affects the amount of the exploited heat from the rock and thus the thermal breakthrough time of reservoirs. Short distances result in high mass flow rate and consequently produce high thermal power production at early stages of heat extraction processes. However, increasing distance between injection and production wells produce low mass flow rate but effective thermal power over longer periods.
- On the other hand, based on the accumulative thermal power at thermal breakthrough time, the results presented in this thesis showed that there is a peak value of distance

between injection and production wells that produces the maximum thermal power production; in this research, this was found to be 0.85 of the given values during the parametric study.

- The first method of sensitivity analysis showed that longer distances could provide high thermal power production. However, based on the second method, the results revealed that the highest values of the distance between injection and production wells are not the peak value that produces maximum accumulative thermal power.
- The results further showed that fluid injection pressure and reservoir permeability have the same trend with respect to the impact on reservoir production temperature, thermal power and mass flow rate. Both parameters are directly proportional to the production mass flow rate i.e. high values of injection pressure and reservoir permeability produce high mass flow rates. As a result, these directly affect the rate of heat extraction from EGS reservoirs.
- On the other hand, increases in injection pressure or reservoir permeability, results in accelerating temperature drop of production wells. Nevertheless, the results based on accumulative thermal power at breakthrough time, revealed that a range of value ratios of both parameters could produce high accumulative thermal power. For example, for the injection pressure, range of 0.20 to 0.88 of injection pressure values produce high accumulative power with a maximum value at 0.21 of injection pressure. While, for the reservoir permeability, range of 0.13 to 0.87 of the given values produce high accumulative thermal power with a maximum production at 0.87 of permeability given values.
- In addition, the depth of EGS reservoirs directly affects the rate of heat extraction because deeper reservoirs have higher temperatures with respect to geothermal gradient.

On the other hand, deeper reservoirs require higher capital costs for the creation process. Therefore, there is a strong need to find out the peak value of reservoir depth that provides a cost-effective design.

- Fluid injection temperature was showed to be inversely proportional to the primary rate of heat extraction. However, based on accumulative thermal power, fluid injection temperature had insignificant impact on reservoir thermal production power compared to the other contributed design parameters.
- Furthermore, maximum mass flow rate could be produced was 30 kg/s, and this value was achieved during the parametric study of injection pressure and reservoir permeability. It can be observed that different designs of doublet well EGS reservoirs still could not maintain commercial mass flow rate (80 kg/s).

The results of the sensitivity analysis using the first method showed good agreements with the previous studies of the impact of the artificial design parameters on the reservoir performance over a given time. However, using the second sensitivity method i.e. based on accumulative thermal power at breakthrough time, the results showed disagreements with previous studies. This was because thermal power is a function of temperature and mass flow rate; therefore, reservoirs can still produce thermal power theoretically with high mass flow rates having low temperature. Thus, there is an overestimation of thermal power production when considering the power production after the breakthrough time.

8.1.2 Optimisation of Doublet Well Reservoir

Chapter Five proposed an advanced systematic approach to enhance long-term performance of EGS reservoirs. In Chapter Five, an integration of FE analysis and multi-objective and multi-

variable GA optimisation technique was applied to find optimum designs of a doublet well reservoir.

During the optimisation process, two scenarios were considered:

- The first scenario considered distance between wells, injection pressure, reservoir permeability and maximum depth of reservoir design as variables.
- While the second scenario considered the same variables except reservoir permeability, which was kept constant.

Results of both optimisation scenarios revealed that:

1. The permeability of the reservoir had a significant influence on selecting the other artificial design parameters. For example, in the case of keeping reservoir permeability constant, the optimisation process selected higher injection pressures, deeper reservoir depths and longer well spaces compared to the case of considering permeability as a variable.
2. The selection of the parameters during the optimisation process were made based on the optimisation objectives. Consequently, high mass flow rate and consequently thermal power production could be maintained through the permeability of the reservoir rather than the injection fluid pressure. Thus, low injection pressure had been selected to achieve low exploitation costs.
3. This hybrid optimisation approach gives an insightful understanding of EGS long-term performance regarding thermal production power of EGS reservoir designs, financial consideration and reservoir service life.

4. In addition, the results show that there is a complex interaction between the reservoir design parameters, which can increase challenges for decision-makers responsible for design and operation of an EGS reservoir.

8.1.3 Impact of Number of Production Wells

In Chapter Six, numerical simulation and parametric study was used to find optimum number of wells in a multi-well reservoir. The primary aim in Chapter Six was to model the impact of increasing production wells on the reservoir financial and long-term performance in a non-commercial geothermal reservoir. Accumulative thermal power production, production mass flow rate and levelised cost were calculated to compare the results with the benchmark reservoir for two scenarios of financial consideration of the reservoir (non-commercial and commercial reservoir).

The results of this study indicated the following:

- Increasing number of production wells in a non-commercial geothermal reservoir with a constant fluid injection pressure and distance between the injection and production wells enhances the production mass flow rate. However, more wells could not maintain the commercial mass flow rate target (80 kg/s).
- On the other hand, in the case of a commercial geothermal reservoir with two production wells, the increase in production wells has the potential to improve the thermal production power by three times, compared to the non-commercial case.
- During the commercial stage, the levelised cost of the power production improved within a reservoir comprising three production wells. However, for the non-commercial case, none of the designs i.e. with more production wells, could achieve lower levelised cost than the two production wells.

The study in Chapter Six was conducted using log borehole data available from Soultz. The analyses were carried out with the assumptions that other contributing factors such as permeability, distance between wells, injection fluid temperature and the geological data did not change. Hence, the conclusion of "three well production as optimum" cannot necessary be extended to other reservoirs.

8.1.4 Optimisation of Multi-Well Reservoirs

In Chapter Seven, optimisation of long-term performance of a multi-well reservoir was conducted. During the optimisation process, the following points are considered:

1) The economic analysis for the total reservoir cost (both creation and exploitation process) was conducted based on the results of the numerical analysis and thermal power production. A hybrid optimisation technique conducted with a Multi-objectives genetic algorithm GA based on LiveLink COMSOL with MATLAB script
2) Five objectives were achieved within the optimisation process covering many objectives of long-term performance of EGS reservoirs. Three of them were considered implicitly within the fitness function (reservoir service life (thermal drawdown), mass flow rate of the production wells and the hydraulic impedance of the reservoir). While the thermal power production and reservoir total costs were considered as the main multi-objectives within the fitness function.
3) The optimisation of the reservoir considered four variables including number of production wells, the distance between injection and production wells, reservoir permeability and injection fluid pressure.

The results showed that to achieve a long service life, lower cost and low hydraulic impedance, low injection fluid pressure and long distance between injection and production wells are

required. However, to maintain a commercial mass flow rate (80 kg/s) and an efficient power production, it is important to have a high equivalent permeability of the reservoir and high number of production wells.

8.2 Recommendations for Further Research

The proposed methodology, in this thesis, can be used to:

- Transform the way EGS reservoirs are currently exploited leading to a cost effective power source.
- It has the flexibility and potential to be adapted during and post design of EGS reservoirs.
- In addition, if further information becomes available, such as the availability of more experimental data for reservoir exploitation over long periods, the code has the ability to include more objectives such as chemical impacts of different injection fluids to improve reservoir long-term performance.
- Moreover, it can be applying to optimise other disciplines such as oil and gas reservoirs, due to its applicability to include the interconnection of design parameters in a single optimisation technique.

Due to the limited time for the research, the following points are recommended for further research:

1) Research needs to be extended to consider a site including many wells and reservoirs. This is important to calculate the impact of the distance between reservoirs on the site long-term performance.
2) It is highly recommended to consider the required maintenance cost for the reservoir after the breakthrough time and how this affects the reservoir long-term performance.

3) Modelling and optimisation of EGS reservoirs with fractures are important to monitor reservoir long-term performance with different fracture shapes and other design properties.
4) Risk assessment of seismic is important to be added to optimisation process as long as it was one of the serious issues that resulted in EGS reservoir failure and consequently project shut down.

REFERENCES

ABD-ELHAMID, H. F. & JAVADI, A. A. 2011. A cost-effective method to control seawater intrusion in coastal aquifers. *Water resources management,* 25**,** 2755-2780.

ALIYU, M. D. & CHEN, H.-P. 2017a. Optimum control parameters and long-term productivity of geothermal reservoirs using coupled thermo-hydraulic process modelling. *Renewable Energy,* 112**,** 151-165.

ALIYU, M. D. & CHEN, H.-P. 2017b. Sensitivity analysis of deep geothermal reservoir: Effect of reservoir parameters on production temperature. *Energy,* 129**,** 101-113.

ALIYU, M. D. & CHEN, H.-P. 2018. Enhanced geothermal system modelling with multiple pore media: thermo-hydraulic coupled processes. *Energy*.

ARTUS, V., DURLOFSKY, L. J., ONWUNALU, J. & AZIZ, K. 2006. Optimization of nonconventional wells under uncertainty using statistical proxies. *Computational Geosciences,* 10**,** 389-404.

ASAI, P., PANJA, P., MCLENNAN, J. & MOORE, J. 2018. Performance evaluation of enhanced geothermal system (EGS): Surrogate models, sensitivity study and ranking key parameters. *Renewable Energy,* 122**,** 184-195.

AUGUSTINE, C., YOUNG, K. R. & ANDERSON, A. 2010. Updated US geothermal supply curve.

BANKS, D. 2012. *An introduction to thermogeology: ground source heating and cooling*, John Wiley & Sons.

BARBIER, E. 2002. Geothermal energy technology and current status: an overview. *Renewable and Sustainable Energy Reviews,* 6**,** 3-65.

BARIA, R., JUNG, R., TISHNER, T., NICHOLLS, J., MICHELET, S., SANJUAN, B., SOMA, N., ASANUMA, H., DYER, B. & GARNISH, J. Creation of an HDR reservoir at 5000 m depth at the European HDR project. Thirty-First Workshop on Geothermal Reservoir Engineering, Stanford University, 2006. 8 pages.

BEDRE, M. G. & ANDERSON, B. J. 2012. Sensitivity analysis of low-temperature geothermal reservoirs: effect of reservoir parameters on the direct use of geothermal energy: Geothermal Resources Council Transactions. *Geothermal Resources Council Transactions,* 36**,** 1255-1261.

BENIM, A. C., CICEK, A. & EKER, A. M. 2018. A Computational Investigation of the Thermohydraulics of an EGS Project. *Journal of Thermal Science,* 27**,** 405-412.

BERTANI, R. 2012. Geothermal power generation in the world 2005–2010 update report. *Geothermics,* 41**,** 1-29.

BIAGI, J., AGARWAL, R. & ZHANG, Z. 2015. Simulation and optimization of enhanced geothermal systems using CO 2 as a working fluid. *Energy,* 86**,** 627-637.

BIRKHOLZER, J., RUTQVIST, J., SONNENTHAL, E. & BARR, D. 2008. DECOVALEX—Task D: Long-term permeability changes due to THC and THM processes. Technical Report 2008: 43, Swedish Nuclear Power Inspectorate, Stockholm.

BÖDVARSSON, G. S. & TSANG, C. F. 1982. Injection and thermal breakthrough in fractured geothermal reservoirs. *Journal of Geophysical Research: Solid Earth,* 87**,** 1031-1048.

BORJA, R. I. & AYDIN, A. 2004. Computational modeling of deformation bands in granular media. I. Geological and mathematical framework. *Computer Methods in Applied Mechanics and Engineering,* 193**,** 2667-2698.

BORSETTO, M. 1980. *Coupled seepage, heat transfer and stress analysis with application to geothermal problems*.

BOSCHETTI, F., DENTITH, M. C. & LIST, R. D. 1996. Inversion of seismic refraction data using genetic algorithms. *Geophysics,* 61**,** 1715-1727.

BÖTTCHER, N., WATANABE, N. & KOLDITZ, O. 2015. HIGRADE Tutorial Computational Energy Systems I: Basics of Geothermal Processes.

BOWER, K. & ZYVOLOSKI, G. 1997. A numerical model for thermo-hydro-mechanical coupling in fractured rock. *International Journal of Rock Mechanics and Mining Sciences,* 34**,** 1201-1211.

BP 2015. British Petroleum ,2015, online accessed 27th October 2016 http://www.bp.com/en/global/corporate/energy-economics/statistical-review-of-world-energy/renewable-energy/geothermal-power.html

BREEDE, K., DZEBISASHVILI, K., LIU, X. & FALCONE, G. 2013. A systematic review of enhanced (or engineered) geothermal systems: past, present and future. *Geothermal Energy,* 1**,** 1-27.

BROWN, D., DUTEAUX, R., KRUGER, P., SWENSON, D. & YAMAGUCHI, T. 1999. Fluid circulation and heat extraction from engineered geothermal reservoirs. *Geothermics,* 28**,** 553-572.

BROWN, D. W. 1991. Recent progress in HDR reservoir engineering. Los Alamos National Lab., NM (USA).

BRUEL, D. 1995. Heat extraction modelling from forced fluid flow through stimulated fractured rock masses: application to the Rosemanowes Hot Dry Rock reservoir. *Geothermics,* 24**,** 361-374.

BUJAKOWSKI, W., BARBACKI, A., MIECZNIK, M., PAJĄK, L., SKRZYPCZAK, R. & SOWIŻDŻAŁ, A. 2015. Modelling geothermal and operating parameters of EGS installations in the lower triassic sedimentary formations of the central Poland area. *Renewable Energy,* 80**,** 441-453.

CAVICCHIO, D. J. 1970. Adaptive search using simulated evolution.

CHAMPEL, B. 2006. Discrepancies in brine density databases at geothermal conditions. *Geothermics,* 35**,** 600-606.

CHEN, J. & JIANG, F. 2015. Designing multi-well layout for enhanced geothermal system to better exploit hot dry rock geothermal energy. *Renewable Energy,* 74**,** 37-48.

CHEN, M., TOMPSON, A. F., MELLORS, R. J. & ABDALLA, O. 2015. An efficient optimization of well placement and control for a geothermal prospect under geological uncertainty. *Applied Energy,* 137**,** 352-363.

CHENG, A. D., GHASSEMI, A. & DETOURNAY, E. 2001. Integral equation solution of heat extraction from a fracture in hot dry rock. *International Journal for Numerical and Analytical Methods in Geomechanics,* 25**,** 1327-1338.

CHENG, W.-L., WANG, C.-L., NIAN, Y.-L., HAN, B.-B. & LIU, J. 2016. Analysis of influencing factors of heat extraction from enhanced geothermal systems considering water losses. *Energy,* 115**,** 274-288.

COMSOL-MULTIPHYSICS 2016. INTRODUCTION TO COMSOL Multiphysics: Version 5.2a. Stockholm, Sweden: COMSOL AB.

DAANEN, R. P., CHITTAMBAKKAM, A., HASELWIMMER, C., PRAKASH, A., MAGER, M. & HOLDMANN, G. 2012. Use of COMSOL Multiphysics to Develop a Shallow Preliminary Conceptual Model for Geothermal Exploration at Pilgrim Hot Springs, Alaska. *Geothermal Resource Council Transactions,* 36**,** 631-635.

DAVIS, L. 1987. Genetic algorithms and simulated annealing.

DE BOER, R. 2006. *Trends in continuum mechanics of porous media*, Springer Science & Business Media.

DE MARSILY, G. 1986. Quantitative hydrogeology: groundwater hydrology for engineers. *Academic, San Diego, CA*.

DECC 2013. Deep Geothermal Review Study. Rev 5.0 ed.: Department of Energy and Climate Change.

DICKSON, M. H. & FANELLI, M. 2001. What is geothermal energy. *International Institute for Geothermal Research, Pisa, Italy*.

DIPIPPO, R. 2012. *Geothermal power plants: principles, applications, case studies and environmental impact*, Butterworth-Heinemann.

DOUGHTY, C., DOBSON, P., WALL, A., MCLING, T. & WEISS, C. 2018. GeoVision Exploration Task Force Report.

DUCHANE, D. & BROWN, D. 2000. Hot dry rock geothermal energy development in the USA. *Los Alamos National Laboratory, Los Alamos, NM*.

DUCHANE, D. V. 1993. Geothermal energy production from hot dry rock: Operational testing at the Fenton Hill, New Mexico HDR test facility. Los Alamos National Lab., NM (United States).

DUFFIELD, W. A. & SASS, J. H. 2003. *Geothermal energy: Clean power from the earth's heat*, US Geological Survey.

EKNELIGODA, T. C. & MIN, K.-B. 2014. Determination of optimum parameters of doublet system in a horizontally fractured geothermal reservoir. *Renewable Energy,* 65**,** 152-160.

EVANS, K. Enhanced/engineered geothermal system: an introduction with overviews of deep systems built and circulated to date. China geothermal development forum. Beijing, 2010. 395-418.

FAUST, C. R. & MERCER, J. W. An analysis of finite-difference and finite-element techniques for geothermal reservoir simulation. SPE Symposium on Numerical Simulation of Reservoir Performance, 1976. Society of Petroleum Engineers.

FRANCISCO, P. R. V. 2013. Simulation and Multi-Objective Optimization of Road Traffic Accidents.

FREI, C., WHITNEY, R., SCHIFFER, H.-W., ROSE, K., RIESER, D. A., AL-QAHTANI, A., THOMAS, P., TURTON, H., DENSING, M. & PANOS, E. 2013. World energy scenarios: Composing energy futures to 2050. Conseil Francais de l'energie.

FRIDLEIFSSON, I. B., BERTANI, R., HUENGES, E., LUND, J. W., RAGNARSSON, A. & RYBACH, L. The possible role and contribution of geothermal energy to the mitigation of climate change. IPCC scoping meeting on renewable energy sources, proceedings, Luebeck, Germany, 2008. Citeseer, 59-80.

FU, P. & CARRIGAN, C. R. Exploring EGS Well Layouts that Mitigate Thermal Drawdown-Induced Flow Channeling. PROCEEDINGS, Thirty-Ninth Workshop on Geothermal Reservoir Engineering, Stanford University, Stanford, California, February 24-26, 2014, SGP-TR-202, 2014.

FYTIKAS, M., ANDRITSOS, N., DALABAKIS, P. & KOLIOS, N. Greek geothermal update 2000-2004. Proceedings World Geothermal Congress, 2005.

GEA 2013. Geothermal Energy Association (GEA). Geothermal.

GENTER, A., EVANS, K., CUENOT, N., FRITSCH, D. & SANJUAN, B. 2010. Contribution of the exploration of deep crystalline fractured reservoir of Soultz to the knowledge of enhanced geothermal systems (EGS). *Comptes Rendus Geoscience,* 342**,** 502-516.

GIARDINI, D. 2009. Geothermal quake risks must be faced. *Nature,* 462**,** 848-849.

GRANT, M. 2013. *Geothermal reservoir engineering*, Elsevier.

GRINGARTEN, A. & SAUTY, J. The effect of reinjection on the temperature of a geothermal reservoir used for urban heating. Proc. Second UN Symposium on the Development and Use of Geothermal Resources, San Francisco, 1975. 1370-1374.

GRIPPI, J. 2018. Reviewing the relationship between thermal reservoir parameters and geothermal energy output. *PAM Review: Energy Science & Technology,* 5**,** 2-21.

HAYASHI, K., WILLIS-RICHARDS, J., HOPKIRK, R. J. & NIIBORI, Y. 1999. Numerical models of HDR geothermal reservoirs—a review of current thinking and progress. *Geothermics,* 28**,** 507-518.

HE, J., SÆTROM, J. & DURLOFSKY, L. J. 2011. Enhanced linearized reduced-order models for subsurface flow simulation. *Journal of Computational Physics,* 230**,** 8313-8341.

HEIDINGER, P. 2010. Integral modeling and financial impact of the geothermal situation and power plant at Soultz-sous-Forêts. *Comptes Rendus Geoscience,* 342**,** 626-635.

HELD, S., GENTER, A., KOHL, T., KÖLBEL, T., SAUSSE, J. & SCHOENBALL, M. 2014. Economic evaluation of geothermal reservoir performance through modeling the complexity of the operating EGS in Soultz-sous-Forêts. *Geothermics,* 51**,** 270-280.

HICKS, T., PINE, R., WILLIS-RICHARDS, J., XU, S., JUPE, A. & RODRIGUES, N. A hydro-thermo-mechanical numerical model for HDR geothermal reservoir evaluation. International journal of rock mechanics and mining sciences & geomechanics abstracts, 1996. Elsevier, 499-511.

HOLLAND, J. H. 1975. Adaptation in natural and artificial systems Ann Arbor. *The University of Michigan Press,* 1**,** 975.

HORNE, R. N. & TESTER, J. W. 2014. Geothermal energy an emerging option for heat and power. *Bridge the Linking Engineering and Society, Emerging Issues in Earth Resources Engineering,* 44**,** 7-15.

HUENGES, E., KOHL, T., KOLDITZ, O., BREMER, J., SCHECK-WENDEROTH, M. & VIENKEN, T. 2013. Geothermal energy systems: research perspective for domestic energy provision. *Environmental Earth Sciences,* 70**,** 3927-3933.

HUSSAIN, M. S. 2015. Numerical simulation and effective management of saltwater intrusion in coastal aquifers.

IEA 2012. International Energy Agency (2012) Electricity information. www.iea.org.

IZADI, G. & ELSWORTH, D. 2015. The influence of thermal-hydraulic-mechanical-and chemical effects on the evolution of permeability, seismicity and heat production in geothermal reservoirs. *Geothermics,* 53**,** 385-395.

JAVADI, A., ABD-ELHAMID, H. & FARMANI, R. 2012a. A simulation-optimization model to control seawater intrusion in coastal aquifers using abstraction/recharge wells. *International Journal for Numerical and Analytical Methods in Geomechanics,* 36**,** 1757-1779.

JAVADI, A. A., FARAMARZI, A. & FARMANI, R. 2012b. Design and optimization of microstructure of auxetic materials. *Engineering Computations,* 29**,** 260-276.

JELACIC, A., FORTUNA, R., LASALA, R., NATHWANI, J., NIX, G., VISSER, C., GREEN, B., RENNER, J., BLANKENSHIP, D. & KENNEDY, M. 2008. An Evaluation of Enhanced Geothermal Systems Technology. *Geothermal Technologies Program, US Department of Energy*.

JIANG, F., CHEN, J., HUANG, W. & LUO, L. 2014. A three-dimensional transient model for EGS subsurface thermo-hydraulic process. *Energy,* 72**,** 300-310.

JING, L. 2003. A review of techniques, advances and outstanding issues in numerical modelling for rock mechanics and rock engineering. *International Journal of Rock Mechanics and Mining Sciences,* 40**,** 283-353.

JING, Z., WILLIS-RICHARDS, J., WATANABE, K. & HASHIDA, T. 2000. A three-dimensional stochastic rock mechanics model of engineered geothermal systems in fractured crystalline rock. *Journal of Geophysical Research: Solid Earth,* 105**,** 23663-23679.

JUNG, R. EGS—Goodbye or Back to the Future. ISRM International Conference for Effective and Sustainable Hydraulic Fracturing, 2013. International Society for Rock Mechanics.

KALBACHER, T., WANG, W., WATANABE, N., PARK, C.-H., TANIGUCHI, T. & KOLDITZ, O. 2008. Parallelization concepts and applications for THM coupled finite element problems. *Journal of Environmental Science for Sustainable Society,* 2**,** 35-46.

KALININA, E. A., HADGU, T., KLISE, K. A. & LOWRY, T. S. 2014. Thermal Performance of Directional Wells for EGS Heat Extraction. Sandia National Lab.(SNL-NM), Albuquerque, NM (United States).

KARRECH, A. 2013. Non-equilibrium thermodynamics for fully coupled thermal hydraulic mechanical chemical processes. *Journal of the Mechanics and Physics of Solids,* 61**,** 819-837.

KOHL, T. 1992. *Modellsimulation gekoppelter Vorgänge beim Wärmeentzug aus heissem Tiefengestein.* ETH Zurich.

KOLDITZ, O. 1995. Modelling flow and heat transfer in fractured rocks: Dimensional effect of matrix heat diffusion. *Geothermics,* 24**,** 421-437.

KOLDITZ, O. & CLAUSER, C. 1998. Numerical simulation of flow and heat transfer in fractured crystalline rocks: application to the hot dry rock site in Rosemanowes (UK). *Geothermics,* 27**,** 1-23.

KOLDITZ, O. & DE JONGE, J. 2004. Non-isothermal two-phase flow in low-permeable porous media. *Computational Mechanics,* 33**,** 345-364.

KOLDITZ, O. & SHAO, H. 2009. Developer Benchmark Book on THMC Components of Numerical Codes GeoSys/Rockflow V. 4.9. *Helmholtz Centre for Environmental Research (UFZ), Leipzig*.

KONG, Y., PANG, Z., SHAO, H., HU, S. & KOLDITZ, O. 2014. Recent studies on hydrothermal systems in China: a review. *Geothermal Energy,* 2**,** 19.

KONG, Y., PANG, Z., SHAO, H. & KOLDITZ, O. 2017. Optimization of well-doublet placement in geothermal reservoirs using numerical simulation and economic analysis. *Environmental Earth Sciences,* 3**,** 1-7.

KOSACK, C., VOGT, C., RATH, V. & MARQUART, G. Stochastic estimates of the permeability field of the Soultz-sous-Forêts geothermal reservoir-comparison of bayesian inversion, MC geostatistics, and EnKF assimilation. EGU General Assembly Conference Abstracts, 2010. 4383.

KRUGER, P. & ROBINSON, B. Heat extracted from the long term flow test in the Fenton Hill HDR reservoir. NINETEENTH WORKSHOP GEOTHERMAL RESERVOIR ENGINEERING, 1994.

KUO, M.-C. T., KRUGER, P. & BRIGHAM, W. SHAPE-FACTOR CORRELATIONS FOR TRANSIENT HEAT-CONDUCTION FROM IRREGULAR-SHAPED ROCK FRAGMENTS TO SURROUNDING FLUID. MECHANICAL ENGINEERING, 1977. ASME-AMER SOC MECHANICAL ENG 345 E 47TH ST, NEW YORK, NY 10017, 106-106.

LAM, S., HUNSBEDT, A., KRUGER, P. & PRUESS, K. 1988. Analysis of the Stanford geothermal reservoir model experiments using the LBL reservoir simulator. *Geothermics,* 17**,** 595-605.

LAUGHLIN, A., EDDY, A., LANEY, R. & ALDRICH, M. 1983. Geology of the Fenton Hill, New Mexico, hot dry rock site. *Journal of Volcanology and Geothermal Research,* 15**,** 21-41.

LEE, S. H. & GHASSEMI, A. Themo-Poroelastic Analysis of Injection-Induced Rock Deformation and Damage Evolution. Proceedings of the Thirty-Fifth Workshop on Geothermal Reservoir Engineering, Stanford University, Stanford, California, 2010. 1-3.

LEWIS, R. W. & SCHREFLER, B. A. 1998. *The finite element method in the static and dynamic deformation and consolidation of porous media*, Wiley Chichester.

LI, K. 2015. Update on Comparison of Geothermal with Solar and Wind Power Generation Systems. *Update,* 19**,** 25.

LI, K., BIAN, H., LIU, C., ZHANG, D. & YANG, Y. 2015. Comparison of geothermal with solar and wind power generation systems. *Renewable and Sustainable Energy Reviews,* 42**,** 1464-1474.

LI, T., SHIOZAWA, S. & MCCLURE, M. W. 2016. Thermal breakthrough calculations to optimize design of a multiple-stage Enhanced Geothermal System. *Geothermics,* 64**,** 455-465.

LI, Z.-W., FENG, X.-T., ZHANG, Y.-J. & XU, T.-F. 2018. Effect of hydrological spatial variability on the heat production performance of a naturally fractured geothermal reservoir. *Environmental Earth Sciences,* 77**,** 496.

LONG, J., REMER, J., WILSON, C. & WITHERSPOON, P. 1982. Porous media equivalents for networks of discontinuous fractures. *Water Resources Research,* 18**,** 645-658.

LU, S.-M. 2018. A global review of enhanced geothermal system (EGS). *Renewable and Sustainable Energy Reviews,* 81**,** 2902-2921.

LUKAWSKI, M. Z., ANDERSON, B. J., AUGUSTINE, C., CAPUANO, L. E., BECKERS, K. F., LIVESAY, B. & TESTER, J. W. 2014. Cost analysis of oil, gas, and geothermal well drilling. *Journal of Petroleum Science and Engineering,* 118**,** 1-14.

LUND, J. W. 2007. Characterisitcs, Development and Utilization of Geothermal Resources.

MACDONALD, P., STEDMAN, A. & SYMONS, G. The UK geothermal hot dry rock R&D programme. Seventeenth Workshop on Geothermal Reservoir Engineering, 1992.

MAIER, F., OBERDORFER, P., KOCABAS, I., GHERGUT, I. & SAUTER, M. Using Temperature Signals to Estimate Geometry Parameters in Fractured Geothermal Reservoirs. Proceedings of the 2012 Comsol Conference Milan, 2012.

MCCLURE, M. W. & HORNE, R. N. 2014. An investigation of stimulation mechanisms in Enhanced Geothermal Systems. *International Journal of Rock Mechanics and Mining Sciences,* 72**,** 242-260.

MCDERMOTT, C. & KOLDITZ, O. 2006. Geomechanical model for fracture deformation under hydraulic, mechanical and thermal loads. *Hydrogeology Journal,* 14**,** 485-498.

MCDERMOTT, C. I., RANDRIAMANJATOSOA, A. R., TENZER, H. & KOLDITZ, O. 2006. Simulation of heat extraction from crystalline rocks: The influence of coupled processes on differential reservoir cooling. *Geothermics,* 35**,** 321-344.

MOAVENI, S. 1999. Finite element analysis: theory and application with ANSYS. *Mankato: Minnesota State University***,** 527.

MOCK, J. E., TESTER, J. W. & WRIGHT, P. M. 1997. Geothermal energy from the earth: its potential impact as an environmentally sustainable resource. *Annual review of Energy and the Environment,* 22**,** 305-356.

MOTTAGHY, D., PECHNIG, R. & VOGT, C. 2011. The geothermal project Den Haag: 3D numerical models for temperature prediction and reservoir simulation. *Geothermics,* 40**,** 199-210.

MUDUNURU, M., KELKAR, S., KARRA, S., HARP, D., GUTHRIE, G. & VISWANATHAN, H. 2016. Reduced-Order Models to Predict Thermal Output for Enhanced Geothermal Systems.

MURPHY, H., BROWN, D., JUNG, R., MATSUNAGA, I. & PARKER, R. 1999. Hydraulics and well testing of engineered geothermal reservoirs. *Geothermics,* 28**,** 491-506.

NEUVILLE, A., TOUSSAINT, R. & SCHMITTBUHL, J. 2010. Fracture roughness and thermal exchange: A case study at Soultz-sous-Forêts. *Comptes Rendus Geoscience,* 342**,** 616-625.

NOORISHAD, J., TSANG, C. & WITHERSPOON, P. 1984. Coupled thermal-hydraulic-mechanical phenomena in saturated fractured porous rocks: Numerical approach. *Journal of Geophysical Research: Solid Earth (1978–2012),* 89**,** 10365-10373.

O'SULLIVAN, M. J., PRUESS, K. & LIPPMANN, M. J. 2001. State of the art of geothermal reservoir simulation. *Geothermics,* 30**,** 395-429.

OLASOLO, P., JUÁREZ, M., MORALES, M. & LIARTE, I. 2016a. Enhanced geothermal systems (EGS): A review. *Renewable and Sustainable Energy Reviews,* 56**,** 133-144.

OLASOLO, P., JUÁREZ, M., OLASOLO, J., MORALES, M. & VALDANI, D. 2016b. Economic analysis of Enhanced Geothermal Systems (EGS). A review of software packages for estimating and simulating costs. *Applied Thermal Engineering,* 104**,** 647-658.

OMER, A. M. 2008. Ground-source heat pumps systems and applications. *Renewable and sustainable energy reviews,* 12**,** 344-371.

PAN, C., ROMERO, C. E., LEVY, E. K., WANG, X., RUBIO-MAYA, C. & PAN, L. 2018. Fully coupled wellbore-reservoir simulation of supercritical CO2 injection from fossil fuel power plant for heat mining from geothermal reservoirs. *Journal of CO2 Utilization,* 27**,** 480-492.

PANDEY, S. & VISHAL, V. 2017. Sensitivity analysis of coupled processes and parameters on the performance of enhanced geothermal systems. *Scientific reports,* 7**,** 17057.

PANG, Z., HU, S., WANG, S., XU, P., WANG, G. & YANG, F. 2015. Geothermal systems and resources. *Geothermic and its applications. Science Press, Beijing*.

PASHKEVICH, R. I. & TASKIN, V. V. Numerical simulation of exploitation of supercritical enhanced geothermal system. Proceedings of thirty-fourth workshop on geothermal reservoir engineering. Stanford (California): Stanford University, 2009.

POLLACK, H. N., HURTER, S. J. & JOHNSON, J. R. 1993. Heat flow from the Earth's interior: analysis of the global data set. *Reviews of Geophysics,* 31**,** 267-280.

POLSKY, Y., CAPUANO, L., FINGER, J., HUH, M., KNUDSEN, S., MANSURE, A., RAYMOND, D. & SWANSON, R. 2008. Enhanced geothermal systems (EGS) well construction technology evaluation report. *Sandia National Laboratories, Sandia Report, SAND2008-7866***,** 1-108.

PRUESS, K. 1990. Modeling of geothermal reservoirs: fundamental processes, computer simulation and field applications. *Geothermics,* 19**,** 3-15.

PRUESS, K. 2006. Enhanced geothermal systems (EGS) using CO 2 as working fluid—a novel approach for generating renewable energy with simultaneous sequestration of carbon. *Geothermics,* 35**,** 351-367.

REDDY, J. N. 2006. *An introduction to the finite element method*, McGraw-hill New York.

RENNER, J. 2006. The Future of Geothermal Energy. Idaho National Laboratory (INL).

RICHARDS, H., PARKER, R., GREEN, A., JONES, R., NICHOLLS, J., NICOL, D., RANDALL, M., RICHARDS, S., STEWART, R. & WILLIS-RICHARDS, J. 1994. The performance and characteristics of the experimental hot dry rock geothermal reservoir at Rosemanowes, Cornwall (1985–1988). *Geothermics,* 23**,** 73-109.

ROBINSON, B. A. & TESTER, J. W. 1984. Dispersed fluid flow in fractured reservoirs: An analysis of tracer-determined residence time distributions. *Journal of Geophysical Research: Solid Earth,* 89**,** 10374-10384.

ROMANO-PEREZ, C. & DIAZ-VIERA, M. A Comparison of Discrete Fracture Models for Single Phase Flow in Porous Media by COMSOL Multiphysics® Software. COMSOL Conference, 2015 Boston.

RONEY, J. M. 2014. *Geothermal Power Approaches 12,000 Megawatts Worldwide* [Online]. http://www.earth-policy.org/data_highlights/2014/highlights48 Earth Policy Institute. [Accessed 17th of September 2015].

RUTQVIST, J., BARR, D., BIRKHOLZER, J., CHIJIMATSU, M., KOLDITZ, O., LIU, Q., ODA, Y., WANG, W. & ZHANG, C. 2008. Results from an international simulation study on coupled thermal, hydrological, and mechanical processes near geological nuclear waste repositories. *Nuclear Technology,* 163**,** 101-109.

RYBACH, L. The future of geothermal energy and its challenges. Proceedings World Geothermal Congress, 2010a.

RYBACH, L. Legal and regulatory environment favourable for geothermal development investors. Proceedings World Geothermal Congress 2010, 2010b.

SAEID, S., AL-KHOURY, R. & BARENDS, F. 2013. An efficient computational model for deep low-enthalpy geothermal systems. *Computers & geosciences,* 51**,** 400-409.

SAMIN, M. Y., FARAMARZI, A., JEFFERSON, I. & HARIRECHE, O. 2018. A Hybrid Optimisation Approach to Improve Long-Term Performance of Enhanced Geothermal System (EGS) Reservoirs. *Renewable Energy*.

SANYAL, S. K. On minimizing the levelized cost of electric power from Enhanced Geothermal Systems. Proceedings World Geothermal Congress 2010, 2010.

SANYAL, S. K. & BUTLER, S. J. 2005. An analysis of power generation prospects from enhanced geothermal systems. *Geothermal Resources Council Transactions,* 29.

SANYAL, S. K., BUTLER, S. J., SWENSON, D. & HARDEMAN, B. 2000. Review of the state-of-the-art of numerical simulation of enhanced geothermal systems. *TRANSACTIONS-GEOTHERMAL RESOURCES COUNCIL***,** 181-186.

SANYAL, S. K., GRANADOS, E. E., BUTLER, S. J. & HORNE, R. N. An alternative and modular approach to enhanced geothermal systems. World Geothermal Congress, 2005.

SCHROEDER, D. V. 1999. An introduction to thermal physics. AAPT.

SEOL, Y. & LEE, K.-K. 2007. Application of TOUGHREACT to performance evaluations of geothermal heat pump systems. *Geosciences Journal,* 11**,** 83-91.

SHOKRI, A., HEO, E. & KIM, J. 2014. Effects of government policies on deploying geothermal electricity in 35 OECD and BRICS countries. *Geosystem Engineering,* 17**,** 11-16.

SHOOK, G. M., NALLA, G., MINES, G. L. & BLOOMFIELD, K. K. 2004. Parametric Sensivity Study of Operating and Design Variables in Wellbore Heat Exchangers. Idaho National Laboratory (INL).

SMIT, R., SALIMI, H. & WOLF, K. Optimization of Geothermal-Well-Doublet Placement. 76th EAGE Conference and Exhibition 2014, 2014.

SONG, X., SHI, Y., LI, G., YANG, R., WANG, G., ZHENG, R., LI, J. & LYU, Z. 2018. Numerical simulation of heat extraction performance in enhanced geothermal system with multilateral wells. *Applied Energy,* 218**,** 325-337.

STEPHANSSON, O., HUDSON, J. & JING, L. 2004. *Coupled thermo-hydro-mechanical-chemical processes in Geo-Systems*, Elsevier.

SUN, F., YAO, Y., LI, G. & LI, X. 2018. Performance of geothermal energy extraction in a horizontal well by using CO 2 as the working fluid. *Energy Conversion and Management,* 171**,** 1529-1539.

TARON, J. & ELSWORTH, D. 2009. Thermal–hydrologic–mechanical–chemical processes in the evolution of engineered geothermal reservoirs. *International Journal of Rock Mechanics and Mining Sciences,* 46**,** 855-864.

TENMA, N., YAMAGUCHI, T. & ZYVOLOSKI, G. 2008. The Hijiori hot dry rock test site, Japan: evaluation and optimization of heat extraction from a two-layered reservoir. *Geothermics,* 37**,** 19-52.

TENZER, H. 2001. Development of hot dry rock technology. *Bulletin geo-heat center,* 32**,** 14-22.

TENZER, H., PARK, C.-H., KOLDITZ, O. & MCDERMOTT, C. I. 2010. Application of the geomechanical facies approach and comparison of exploration and evaluation methods used at Soultz-sous-Forêts (France) and Spa Urach (Germany) geothermal sites. *Environmental Earth Sciences,* 61**,** 853-880.

TESTER, J. 1990. Economic Prediction for Heat Mining. *A Review and Analysis of Hot Dry Rock (HDR) Geothermal Energy Technology*.

TESTER, J., HERZOG, H., CHEN, Z., POTTER, R. & FRANK, M. 1994. Prospects for universal geothermal energy from heat mining. *Science & Global Security,* 5**,** 99-121.

TESTER, J. W., ANDERSON, B., BATCHELOR, A., BLACKWELL, D., DIPIPPO, R., DRAKE, E., GARNISH, J., LIVESAY, B., MOORE, M. C. & NICHOLS, K. 2006. The future of geothermal energy: Impact of enhanced geothermal systems (EGS) on the United States in the 21st century. *Massachusetts Institute of Technology,* 209.

TSANG, C. F. 1991. Coupled hydromechanical-thermochemical processes in rock fractures. *Reviews of geophysics,* 29**,** 537-551.

VAN WEES, J., KRAMERS, L., KRONIMUS, R., PLUYMAEKERS, M., MIJNLIEFF, H. & VIS, G. 2010. ThermoGIS TM V1. 0 Part II: Methodology.

VARZINA, A. 2015. *Heat Transfer Upscaling in Geothermal Reservoirs.* The University of Bergen.

VÖRÖS, R., WEIDLER, R., DE GRAAF, L. & WYBORN, D. THERMAL MODELLING OF LONG TERM CIRCULATION OF MULTI-WELL DEVELOPMENT AT THE COOPER BASIN HOT FRACTURED ROCK (HFR) PROJECT AND CURRENT PROPOSED SCALE-UP PROGRAM. Proceedings of the Thirty-Second Workshop on Geothermal Reservoir Engineering, Stanford, CA, USA, 2007. 22-24.

WALSH, R., MCDERMOTT, C. & KOLDITZ, O. 2008. Numerical modeling of stress-permeability coupling in rough fractures. *Hydrogeology Journal,* 16**,** 613.

WANG, G., LI, K., WEN, D., LIN, W., LIN, L., LIU, Z., ZHANG, W., MA, F. & WANG, W. Assessment of geothermal resources in China. Proceedings, Thirty–Eighth Workshop on Geothermal Reservoir Engineering, Stanford University, Stanford, California, Febuary, 2013. 11-13.

WANG, W. & KOLDITZ, O. 2007. Object-oriented finite element analysis of thermo-hydro-mechanical (THM) problems in porous media. *International journal for numerical methods in engineering,* 69**,** 162-201.

WATANABE, N. 2011. Finite element method for coupled thermo-hydro-mechanical processes in discretely fractured and non-fractured porous media.

WATANABE, N., SCHNICKE, T., WANG, W., WIESER, T. & KOLDITZ, O. 2009. Analysis of parallelization efficiency of coupled thermo-hydro-mechanical simulation. *Journal of Environmental Science for Sustainable Society,* 3**,** 50-58.

WATANABE, N., WANG, W., MCDERMOTT, C. I., TANIGUCHI, T. & KOLDITZ, O. 2010. Uncertainty analysis of thermo-hydro-mechanical coupled processes in heterogeneous porous media. *Computational Mechanics,* 45**,** 263-280.

WILLIS-RICHARDS, J. & WALLROTH, T. 1995. Approaches to the modelling of HDR reservoirs: a review. *Geothermics,* 24**,** 307-332.

YANG, S.-Y. & YEH, H.-D. 2009. Modeling heat extraction from hot dry rock in a multi-well system. *Applied Thermal Engineering,* 29**,** 1676-1681.

ZENG, Y.-C., SU, Z. & WU, N.-Y. 2013. Numerical simulation of heat production potential from hot dry rock by water circulating through two horizontal wells at Desert Peak geothermal field. *Energy,* 56**,** 92-107.

ZIMMERMANN, G., MOECK, I. & BLÖCHER, G. 2010. Cyclic waterfrac stimulation to develop an enhanced geothermal system (EGS)—conceptual design and experimental results. *Geothermics,* 39**,** 59-69.

APPENDICES

Appendix A: The Use of COMSOL Multiphysics Solver

Appendix B: Programing Code

Appendix C: The OGS (OpenGeoSys) Software

APPENDIX A

THE USE OF COMSOL MULTIPHYSICS SOLVER

A-1 An Introduction to COMSOL Multiphysics

COMSOL Multiphysics code was used in the finite element analysis as this is an appropriate solver, which has tools to overcome non-linear initial and boundary conditions problems resulted from a fully coupled Thermal-hydraulic process during the simulation of heat extraction process.

A-2 General Steps of Model Development in COMSOL Multiphysics

The creation of a model in COMSOL Multiphysics require the following main steps (COMSOL-Multiphysics, 2016):

Definitions; In order to efficiently create and handle the FE model, parameters, initial condition functions, and properties of surfaces of interest are defined. In addition, certain domains, boundaries and points are defined and named to specify probe areas to get outputs. In this manner building and probing the output throughout the model is more efficient particularly when the FE integrated with the GA. It is worth mentioning that the step function is defined during building of the FE model in order to guarantee the initial conditions of the reservoir for both the pressure and temperature.

Geometry; the geometry tool is used to build the FE model with different space dimensions such as 0D, 1D, 1D axisymmetric, 2D, 2D axisymmetric, or 3D. The reservoirs in both models doublet and multi-wells designs were modelled in 3D solid domain. While the wells are modelled in 2D (more details can be found later in chapters 4 and 6). In this research, the size, shape and positions of the reservoirs and their parts were parametrised (explained in this chapter) using the parameter tool in COMSOL.

Material definition; through adding a blank material in COMSOL, list of properties is accessible and allow the user to define appropriate values for each material used during the FE analysis. In this research, in order to guarantee the fully coupled of the Thermal-Hydraulic process, the properties of the water are assumed pressure and temperature dependent, see Figure A-1. More details about the rock matrix properties can be found in Chapters Four and Six.

Material Contents

Property	Name	Value	Unit	Property group
Dynamic viscosity	mu	eta(T[1/K])[...	Pa·s	Basic
Ratio of specific heats	gamma	1.0	1	Basic
Heat capacity at constant pressure	Cp	Cp(T[1/K])[...	J/(kg·K)	Basic
Density	rho	rho(T[1/K])...	kg/m³	Basic
Thermal conductivity	k	k(T[1/K])[W...	W/(m·K)	Basic
Electrical conductivity	sigma	5.5e-6[S/m]	S/m	Basic
Speed of sound	c	cs(T[1/K])[...	m/s	Basic

Figure A-1. Material properties of the water during the numerical analysis

Physics; the set of the constitutive models in the FE model in COMSOL Multiphysics requires defining the physics involved in the numerical analysis. In this research, the coupled thermal-hydraulic physics are involved. Thus the heat transfers in porous media and the subsurface flow (Darcy's Law) modulus are selected as the governing equations (see section 2.5.1 in Chapter Two) to replicate the real behaviour of the reservoir during heat extraction process.

Initial and boundary conditions; In COMSOL the initial and boundary conditions can be easily defined by adding appropriate features to the physics of the problem in form of sub-nodes. In this research, the initial and boundary conditions for the temperature and pressure are defined for the models, more details can be found in Chapters Four and Six.

Meshing; In COMSOL, there are two approaches available to create the mesh, which are physics controlled mesh and user controlled mesh. In this research, the user control approach

is preferred because it is less time consuming, more details about the meshing of the developed FE models can be found in Chapters Four and Six.

A-3 Challenges During Methodology Development

The guarantee of the integration of FE and GA requires the parametrise of all variables within the numerical simulation approach. The challenges of the research consider the variability of the geometry, boundary and initial conditions, material properties and output results. Therefore, there was a strong need to find mathematical relations to allow the run of new designs within the GA.

To overcome this issue, the following relations have been set during the modelling of both doublet and multi-wells models for each variable in the optimisation process:

A-3-1 Parametrise Model Geometry

For the doublet well reservoir, the reservoir is taken as a symmetry model therefore, half of the reservoir is modelled, and more details can be seen in Chapter Four. The distance between injection and production well is taken as a variable (*d*). In addition, the maximum depth of the reservoir is taken as the variable (*Dh*). Accordingly, the geometry of the reservoir is taken in terms of *d* and *Dh*, see Figure A-2.

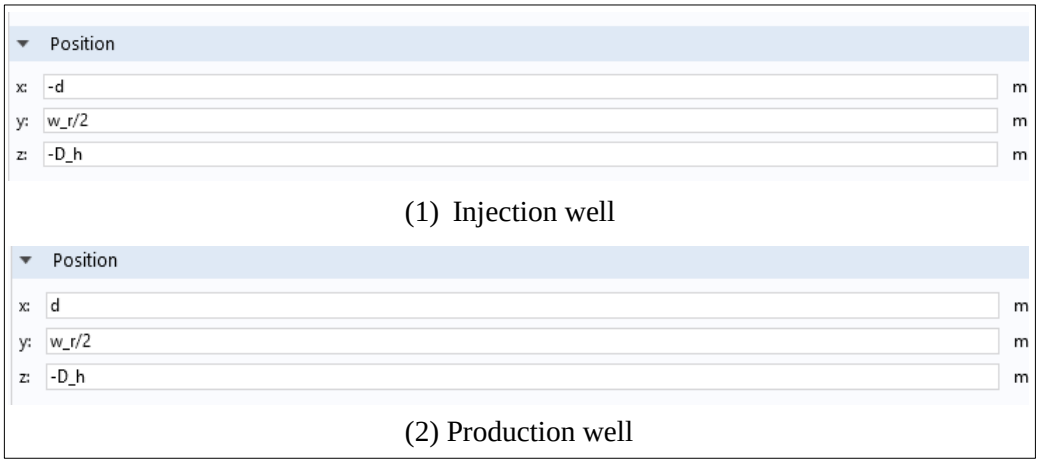

Figure A-2. Wells position within building the geometry of the doublet well reservoir design

In the case of the Multi-well reservoir model, the geometry requires more parametrising in order to guarantee the wells configuration and numbers to be taken as variables within the optimisation process. Accordingly, the number of production wells has been set in terms of *N*, see Figure A-3.

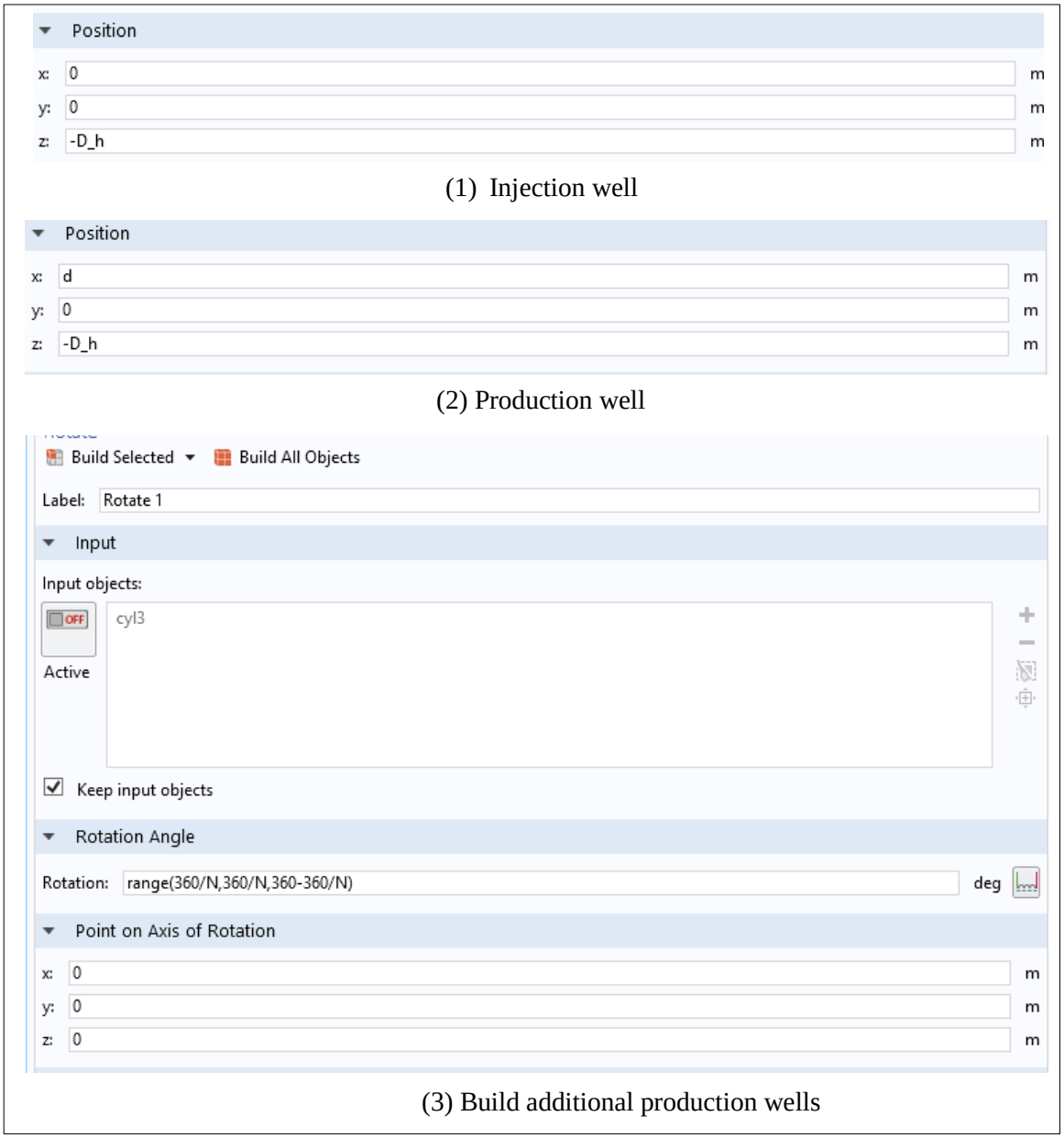

Figure A-3. Wells position within building the geometry of the multi-well reservoir design

A-3-2 Parametrise Initial and Boundary Conditions

For the doublet and multi-wells reservoir designs, the initial and boundary conditions are treated the same, because both models are considered fully coupled of thermal and hydraulic processes (see Section 3.1.2.). The initial condition for both models (doublet and multi-wells) is divided into two parts including initial thermal and hydraulic conditions, more details can be found in Chapters 4 and 6. Hence, the parametrise of injection temperature, injection pressure and initial

thermal and pressure of the reservoir is in terms of *Tinj*, *Pinj*, *Tinit* and temperature gradient *Tg*, as can be seen in Figure A-4 Maximum depth of z is at *Dh* which is a variable within the optimisation process.

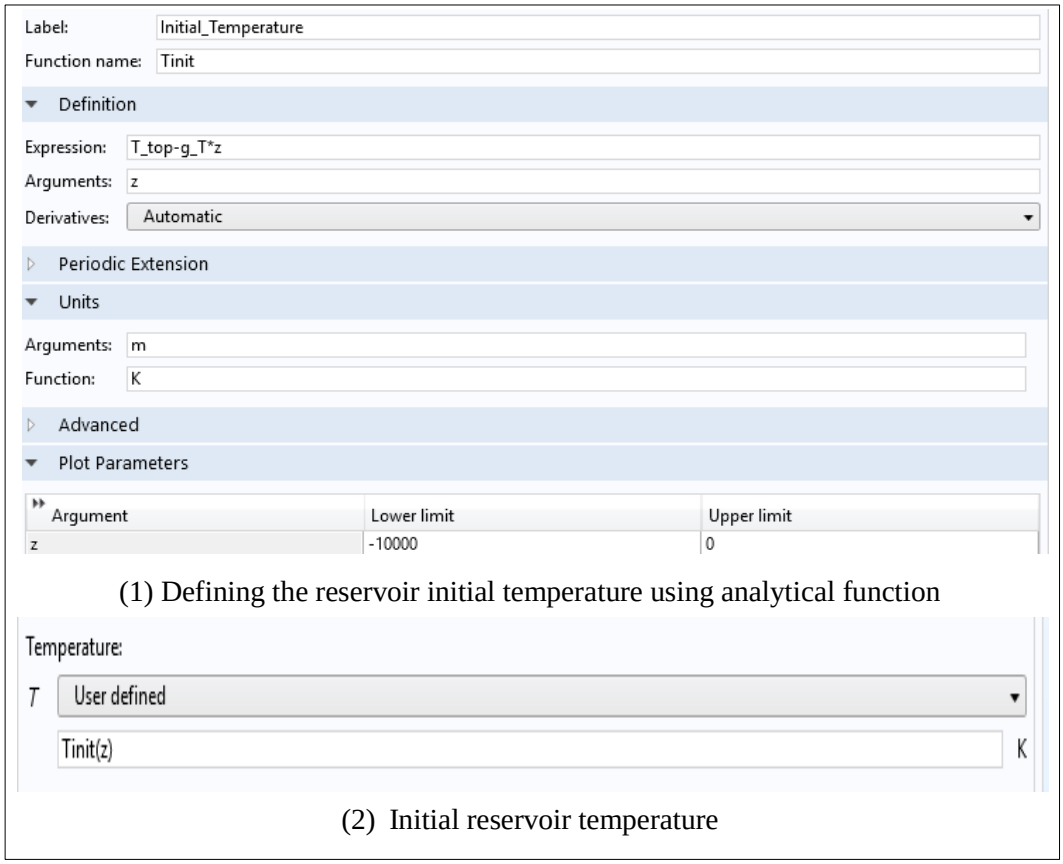

(1) Defining the reservoir initial temperature using analytical function

(2) Initial reservoir temperature

Figure A-4. Parametrise the initial temperature of both reservoir designs

In the case of the initial hydraulic conditions, the flow within the reservoir is considered as laminar and in a hydrostatic condition, hence Darcy's law is employed. The initial reservoir pressure is changing during GA in terms of *Dh* (i.e. maximum z is at *Dh*), see Figure A-5.

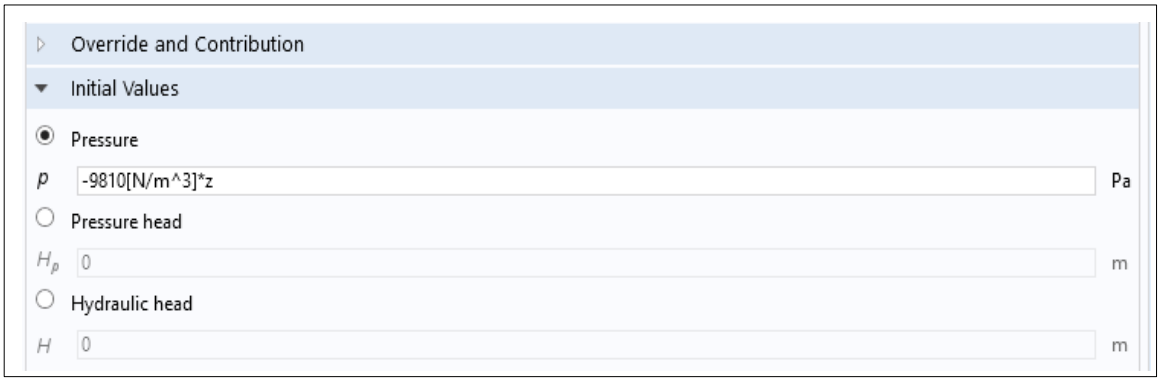

Figure A-5. Parametrise the initial temperature of both reservoir designs

For the boundary conditions, the following parametrise actions were required in order to consider the impact of the change in the variables within GA:

Pressure of injection well: injection pressure of the fluid is an artificial design parameter and it has been selected to be a design variables during GA, see Chapter Four. Thus, it is parametrised in terms of *Pinj*. To do so, it was desired to build a step function to guarantee the initial condition of the injection well, as it can be seen in Figure A-6.

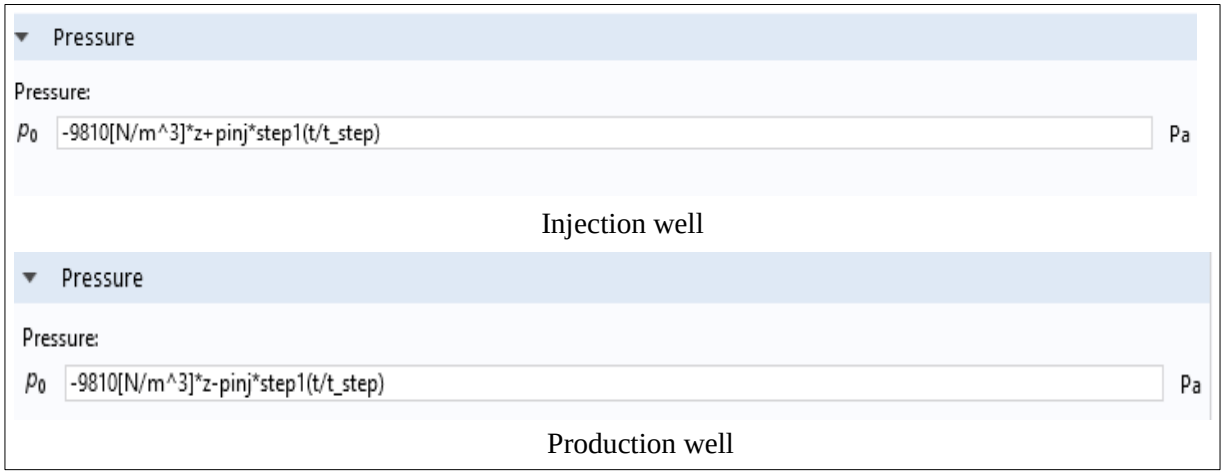

Figure A-6. Parametrise the boundary condition of injection and production pressures

Temperature of Injection well: injection temperature of the fluid is an artificial design parameter and it was required to be tested to find out the sensitivity of the reservoir long-term performance

of EGS to this factor, see Chapter Four. Thus, it has been parametrised in terms of *Tinj*, see Figure A-7.

Figure A-7. Parametrise the boundary condition of injection temperature

A-3-3 Parametrise Model Material

The reservoir is considered as single porosity with a continuum rock matrix and equivalent permeability is applied to present both rock matrix and fracture; more details can be seen in Chapter 4 and 6. The equivalent permeability is taken as a variable (*k*). Accordingly, the material of the reservoir is taken in terms of *kx, ky* and *kz* for the doublet well reservoir and *kr* for the multi-well reservoir, see Figure A-8.

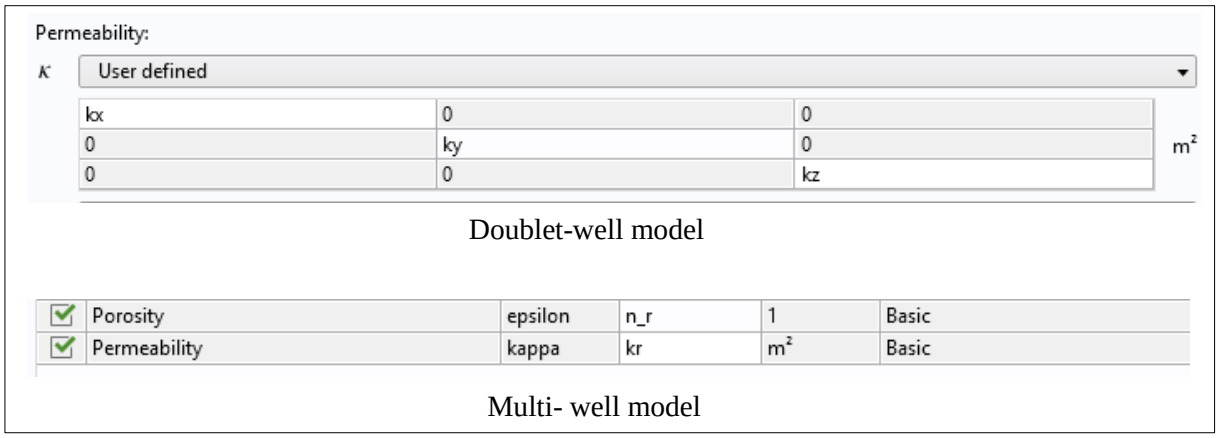

Figure A-8. Parametrise the material of both doublet and multi-well models

A-3-4 Parametrise Outputs

In order to analysis output data of FE model within the optimisation process, parameterising the output was desired particularly when the output position is changing with both variables *d* and *Dh*. For both models doublet and multi-well reservoirs, the downhole of production wells are considered to be the critical point that requires to be taken for the analysis. To do so, the output values are defined from points at the base in terms of *d* and *Dh*, for all the required outputs including production temperature, mass flow rate, density, specific heat, dynamic viscosity and enthalpy, see Figure A-9.

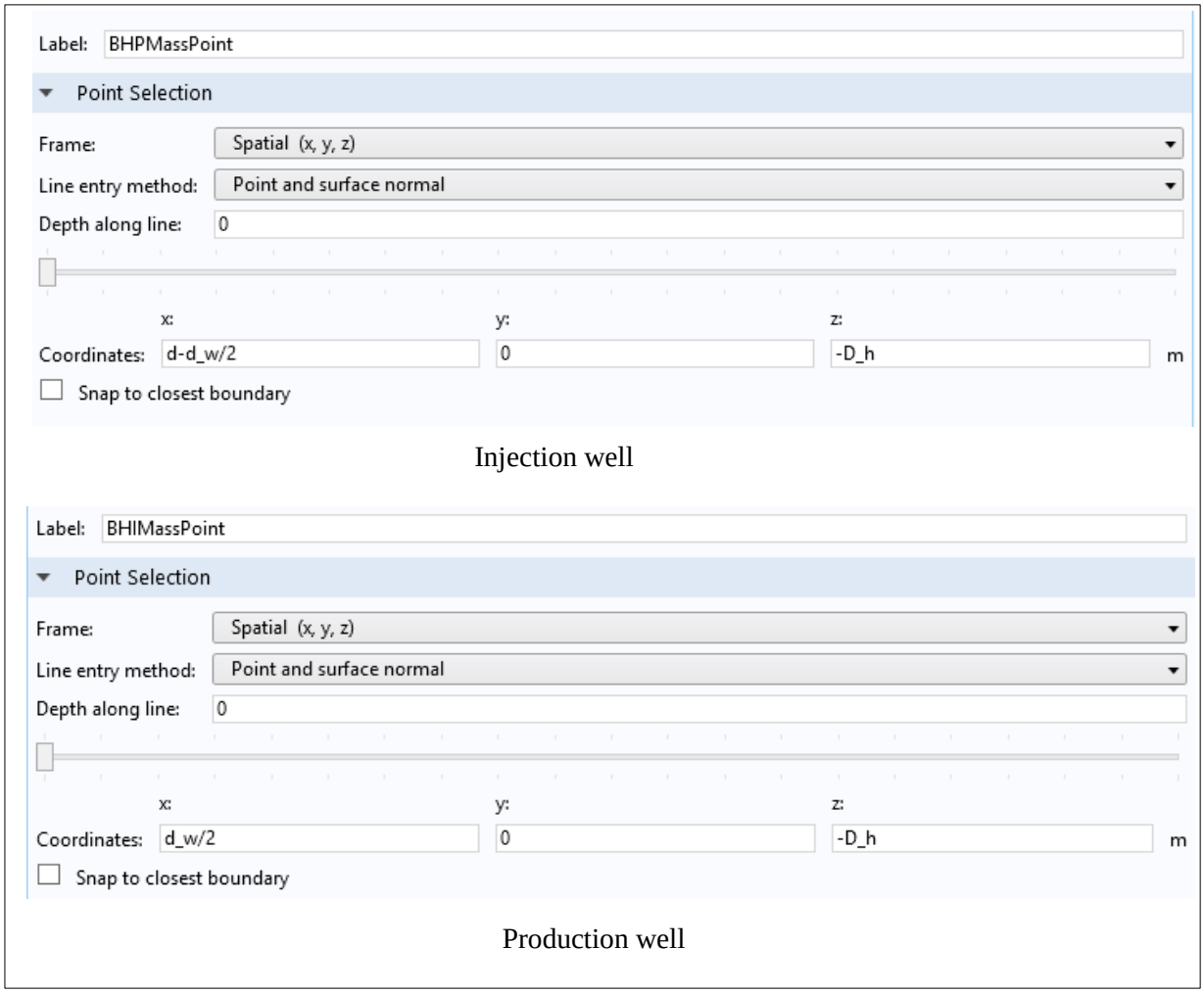

Figure A-9. Wells position within building the geometry of the doublet well reservoir design

Study; since the research aims to optimise the long-term performance of EGS reservoirs, the transient analysis is applied for the FE analysis. Thus, the time dependent study was selected. In order to guarantee the initial conditions of the FE model, the function Step within the component definition was used and used as the following.

Results; COMSOL provides outputs at predefined points, edges, surfaces and domains. These results can be presented in form of graphics or table of values. The produced results of the FE model in COMSOL is accessible from either COMSOL itself or the linked MATLAB script. This feature is important as long as the hybrid optimisation technique requires using the outputs of the FE model as inputs within GA in each iteration.

Linking with MATLAB; the advantage of using COMSOL as the FE model and Matlab for GA is the coupling capability of these two software through the COMSOL MATLAB LiveLink tool. Using this advantage allows to process the optimisation fluently.

APPENDIX B

PROGRAMING CODE

In order to use the hybrid optimisation technique, the following codes have been developed during the research:

B-1 Link FE with MATLAB Script

```
function y= ModelMulti(myd,mykr,myN,myPinj)


%%%
global TP
global PEntha
global qp
global InjEntha
global qin
global T0
global DenW
global CPw


format long e
%%%


import com.comsol.model.*;
import com.comsol.model.util.*;


model = mphload('BSnoSelection');


model.param.set('d',[num2str(myd), '[m]']);
model.param.set('kr',[num2str(mykr), '[m^2]']);
```

```
model.param.set('N',num2str(myN));
model.param.set('Pinj',[num2str(myPinj), '[MPa]']);


model.sol('sol1').run;


% y = mphinterp(model,'v','coord',[0;1]);
% TP= model.result.table('tbl2').getTableData(false);
% PEntha= model.result.table('tbl3').getTableData(false);
% qp= model.result.table('tbl1').getTableData(false);
% InjEntha= model.result.table('tbl6').getTableData(false);
% qin= model.result.table('tbl4').getTableData(false);
% Tinjec= model.result.table('tbl5').getTableData(false);
%
y1 = mphinterp(model,'dl.pr2.Mflow','coord',[myd-0.5;0;-4500]);
y2 = mphinterp(model,'T','coord',[myd-0.5;0;-4500]);
y3 = mphinterp(model,'ht.H','coord',[myd-0.5;0;-4500]);
y4 = mphinterp(model,'dl.pr1.Mflow','coord',[0.5;0;-4500]);
y5 = mphinterp(model,'T','coord',[0.5;0;-4500]);
y6 = mphinterp(model,'ht.H','coord',[0.5;0;-4500]);
y7 = mphinterp(model,'dl.rho','coord',[myd-0.5;0;-4500]);
y8 = mphinterp(model,'ht.Cp','coord',[myd-0.5;0;-4500]);
qp= y1;
TP= y2;
PEntha =y3;
qin= y4;
Tinjec= y5;
InjEntha = y6;
T0=TP(1);
Tin=Tinjec(50);
```

```
DenW=y7;

CPw=y8;


end
```

B-2 Fitness Function:

```
function [y]= FitMultNorm(A)

% global Pd


global TP

global PEntha

global qp

global InjEntha

global qin

global T0

global DenW

global CPw

% A(1)=1;A(2)=0;A(3)=1;A(4)=1;

tic

TD=ones(51,1);power=ones(51,1);Cost=ones(51,1);IM=ones(51,1);M=ones(51,1);

format long e

minx(1)=200;maxx(1)=600;

minx(2)=0;maxx(2)=1e-13;

minx(3)=2;maxx(3)=10;

minx(4)=0;maxx(4)=30;


x(1)=A(1)*(maxx(1)-minx(1))+minx(1);

x(2)=A(2)*(maxx(2)-minx(2))+minx(2);
```

```
x(3)=A(3)*(maxx(3)-minx(3))+minx(3);

x(4)=A(4)*(maxx(4)-minx(4))+minx(4);


d=round(x(1));

% d=int(600);

kr=x(2);

% kr=1e-14;

N=round(x(3));

% N=int(4);

Pinj=x(4);

% Pinj=8;

ModelMulti(d,kr,N,Pinj)


pp=11.95 ; pr=20.33 ; r=0.014;effe=0.45;

DR=1.72e-7*5000^2+2.3e-3*5000-0.62;

% Pd=0+(DR-1.9971)*(0.1-0)/(5.3971-1.9971) This is for normalised

Pd=(N+1)*DR;

for i=1:51

TD(i)=(T0-TP(i))/(T0-323.15);

power(i)=(PEntha(i).*qp(i)+InjEntha(i).*qin(i))/1E6;

Cost(i)=1e-3*qp(i)*(((Pinj*pp/3.6)+DenW(i).*CPw(i)*1e-9*(T0-

TP(i))*pr*effe)/(1+r)^(i))*3.154e7;

M(i)=qp(i);

IM(i)=(2*Pinj)/(M(i)/N);

end

pwh=0; CP=0; W=0;

% if(qp(50)<80)

%     pwh=-1;Tcost=1;

%    else
```

```
if (TD(11)>=0.1 || M(11)<80 || IM(11)>0.2)
    pwh=0;
    Tcost=10000;
% %     Pd=100;
% if(M(11)<=80);
%     pwh=0;
%     Tcost=10000;
% %     Pd=100;
% if(IM(11)>0.2);
%     pwh=0;
%     Tcost=10000;
% %     Pd=100;
else
for i=1:51
if (TD(i)<0.1 || M(i)>=80 || IM(i)<=0.2)

   pwh= pwh+power(i);
   CP=CP+Cost(i);
else
    break

end

end



% end
```

```
W=CP/1e6;
Tcost=W+Pd;                    %Operation and creation
% Tcost=Pd;    %just drilling cost
%
% y(1)=Tcost;
% y(2)=-pwh;   % % MultiObjectives % %
%


end
MR=M(11);
IMR=IM(11);
TDR=TD(11);
% y=-pwh/Tcost               %this just for one objective
% TcostMax=10000;
% pwhMax=7000;
% ParAlfa=1.2;
% y=(-pwh/pwhMax)+ ParAlfa*(Tcost/TcostMax)    %this  for normalised one
objective
y(1)=-pwh;     %%%%%%%%%%%%%%%%
y(2)=Tcost;


%%%%%%%%%%%%%%%%MultiObjectives
cputime=toc
dtime=datestr(now, 'HH:MM:SS')
fileID = fopen('C:\Users\mys172\my sim\Full1Objhome.txt','a');
formatSpec = 'cputime is %5.1f and MR is %5.2f and IMR is %5.3f and TDR is
%5.3f Pd is %6.2f and W is %6.2f and Tcost is %6.2f and pwh is %5.1f where
d m is %4.1f & kr m^2 is %22.18f & N is %3.1f &  Pinj MPa is %4.2f  f\r\n';
fprintf(fileID,formatSpec,cputime,MR,IMR,TDR,Pd,W,Tcost,pwh,d,kr,N,Pinj)
```

```
fclose(fileID);
% %
% formatSpec = 'cputime is %5.1f and Tcost is %6.2f and pwh is %5.1f where
d m is %4.1f & kr m^2 is %22.18f & N is %3.1f &  Pinj MPa is %4.2f  f\r\n';
% fprintf(fileID,formatSpec,cputime,Tcost,pwh,d,kr,N,Pinj)
% fclose(fileID);
% %
fileID2 = fopen('C:\Users\mys172\my sim\datahome.txt','a');


formatSpec2 = ' %5.2f  %5.3f  %5.3f  %6.2f  %6.2f  %6.2f  %5.1f   %4.1f
%22.18f  %3.1f  %4.2f \r\n';
fprintf(fileID2,formatSpec2,MR,IMR,TDR,Pd,W,Tcost,pwh,d,kr,N,Pinj)
fclose(fileID2);
%
% formatSpec2 = '%6.2f  %5.1f   %4.1f   %22.18f  %3.1f  %4.2f \r\n';
% fprintf(fileID2,formatSpec2,Tcost,pwh,d,kr,N,Pinj)
% fclose(fileID2);
%



end
```

B-3 Use GA Optimisation Tool:

```
% MainProgramm Call GA

clc

clear all

fileID = fopen('C:\Users\mys172\my sim\Full1Objhome.txt','w');

fclose(fileID);

fileID2 = fopen('C:\Users\mys172\my sim\datahome.txt','w');

fclose(fileID2);

optimtool('ga')
```

APPENDIX C

THE OGS (OPENGEOSYS) SOFTWARE

C-1 Introduction

In this study, the research is going to be carried out using an open source project OpenGeoSys (OGS) software (http://www.opengeosys.org/resources/downloads). The OGS software is used to develop numerical models of THM coupled process based on FE method in HDR geothermal reservoir and other application areas such as water resources management, waste depositions, hydrology and CO2 sequestration.

C-2 Case Study

The geological data in this research corresponds to the Spa Urach geothermal field in Germany at depth from 3850 m to 4150 m as shown in Figure C-1. The fractured porous reservoir locates within -4150m < z < -3850m in vertical direction and 0 < x < 400m in horizontal direction from the injection well. This site is applicable as a case study as long as its geothermal gradient is about 30 ^{o}C/km at depth more than 1600 m, and this is likely as the average geothermal of the earth (Watanabe et al., 2009). The model is applied to an equivalent porous medium in three dimensions based on FEM.

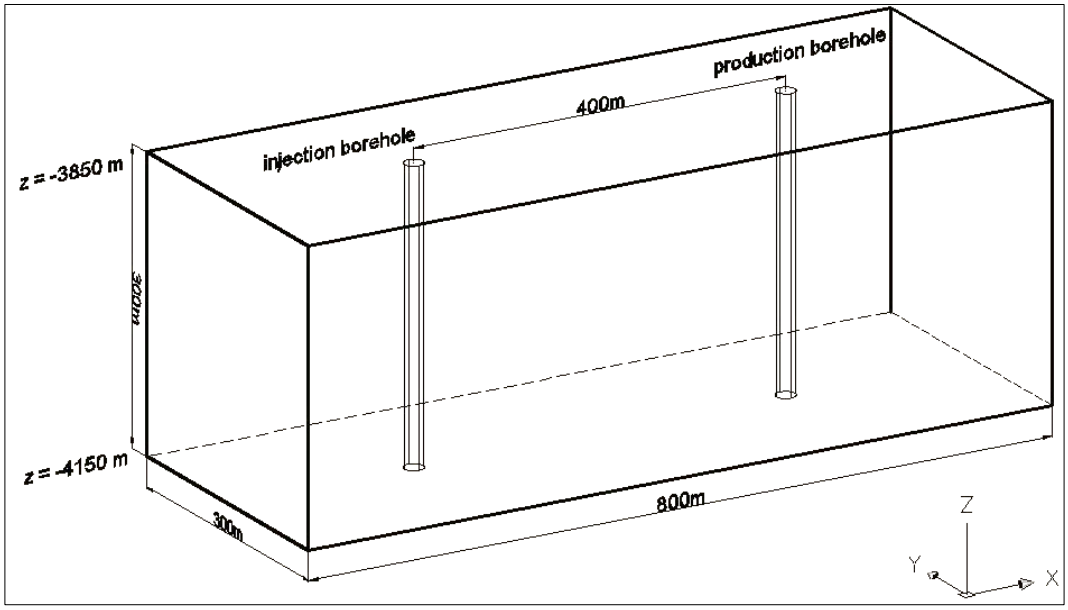

Figure C-1. The reservoir model (adopted from Watanabe et al. (2009))

C-2-1 Input Data

The input data that have been used for the simulation of the HDR geothermal model are:

- The reservoir geometry (wells depth, distance between wells, the reservoir dimensions, etc.).
- Input geometric data (elements, nodes, coordinates, etc.).
- The time discretization (TIM).
- The Initial conditions (the pressure and temperature gradients of the domain at time zero).
- The boundary conditions (the pressure of the liquid flow within the injection and production wells, the injected liquid temperature).
- The material medium properties of the domain (MMp) including porosity, permeability tensor.
- The material fluid properties (MFP) including (the fluid type, the density, the viscosity, the specific heat capacity and the specific heat conductivity).

- The material solid properties (MSP) including (the Young's modulus, the Poisson ratio, the thermal expansion, the heat capacity and the heat conductivity).

The material properties input of the site are presented in Table C-1:

Table C-1. The material properties of the Spa Urach geothermal field (Watanabe et al., 2009a)

Parameter	value	units
Porosity (θ_m)	0.50%	
Permeability (k)	kx= 1.53e-15; ky=kz=0.57e-15	m^2
Specific storage (S_s)	1.00e-10	Pa^{-1}
Solid density (ρ_m)	2850	kg/m^3
Solid specific heat capacity (c_m)	3	J/(kg.K)
Solid heat conductivity (λ_m)	60	W/(m.K)
Young's modulus (E)	0.25	GPa
Poisson ratio (v)	1.00e-05	
Solid thermal expansion coefficient (B_T)	1000	K^{-1}
Fluid density (ρ_w)	0.0002	kg/m^3
Fluid dynamic viscosity (μ)	1000	Pa.sec
Fluid specific heat capacity (c_w)	4210	J/(kg.K)
Fluid heat conductivity (λ_w)	0.6	W/(m.K)

C-2-2 Output Data

The output data is the pressure and the temperature of the domain in terms of values and profiles. In this stage, the main output is specified to be the distance of the maximum temperature profile from the injection well to investigate the thermal evolution of the reservoir as a function of time.

C-3 Sensitivity Analysis

The analysis of the sensitivity of the thermal evolution of the geothermal reservoir to the main parameters is important in order to determine the influence of the most effective input parameters for characterisation of proposed model.

The critical parameters affecting the reservoir performance are the permeability of the matrix, the temperature and the pressure of the injected fluid and the size of the reservoir. Hence, the sensitivity of the thermal evolution of the geothermal reservoir will be tested to the above factors.

C-3-1 Sensitivity to the Time Factor (TIM):

The temperature profile of the geothermal reservoir was calculated for different periods of time (from 1 to 25years) every 5years. With time the reservoir temperature decreased near the injection well as can be seen in Figure C-2, the maximum value of the reservoir temperature (433K°) between 5 to 25 years is gradually moving away by about 28m every 5 years from the injection well. However, for the first year there is a quick moving of (433K°) about 36m away from the injection well, and 38m for the next four years. This is a significant point that should

be considered during the research to avoid this sharp reduction in the temperature profile at the early stages.

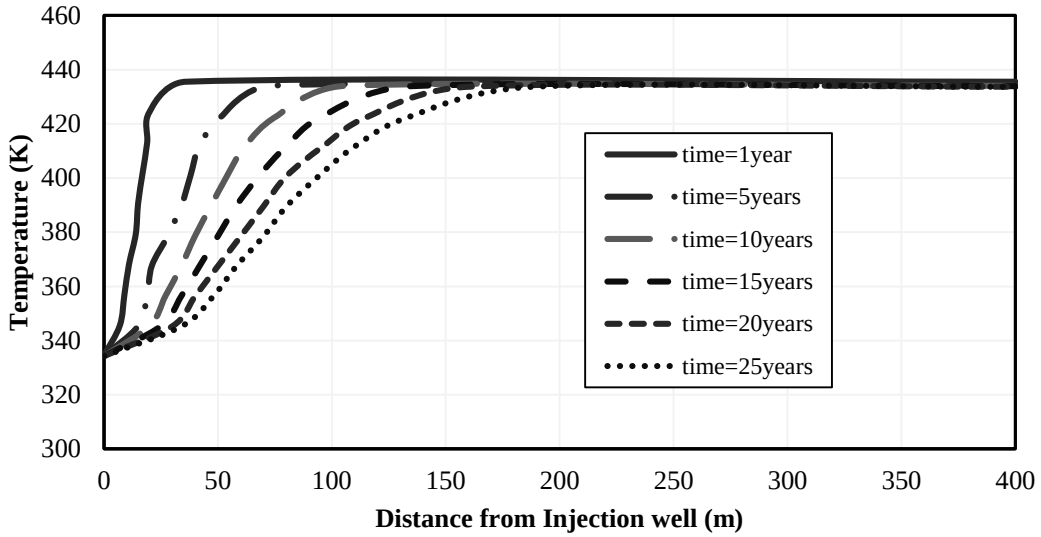

Figure C-2. Comparison of temperature profiles for different times of the reservoir life

C-3-2 Sensitivity to Permeability Tensor:

The permeability of the matrix (crystalline rock) is ranged as (1.0 e-13 to 1.0 e-18) m^2 /sec (Brace, 1984). However, in the case of assuming high permeability the matrix, higher than or equal to (0.99e-14 m^2 /sec), the performance of the reservoir is decreased and as can be seen in the Figure C-3.

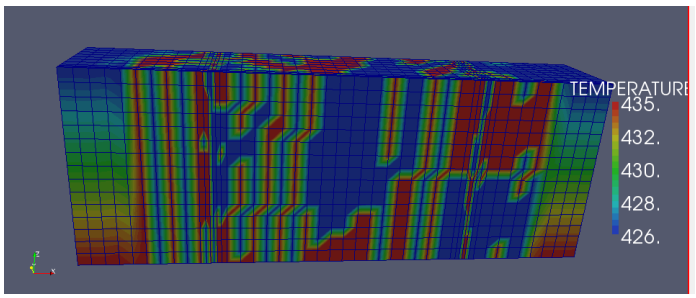

Figure C-3. Thermal evolution of the reservoir to high permeability tensor (k=0.53e-14 m^2/sec)

The high permeability tensor is not applicable in this case study, even if the selected value was within the range in crystalline rock, this might occur when the initial and boundary conditions were not appropriate for higher permeability. Therefore, to assess the sensitivity of the reservoir

to the permeability tensor, small increments (about 2.0 e-15 m^2/sec) is applied to the permeability parameter.

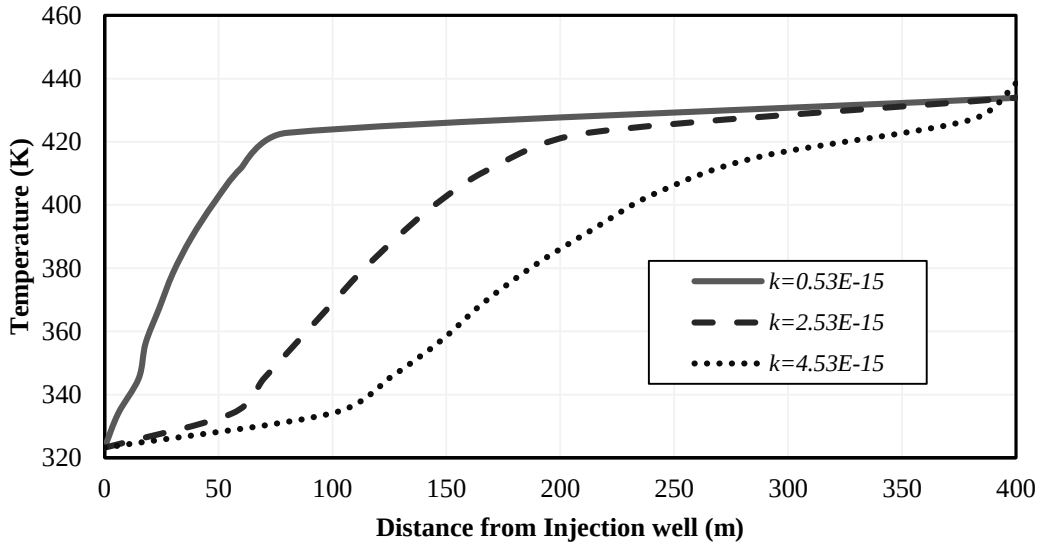

Figure C-4. Comparison of temperature profiles for different permeability values at constant *Pinj* and time of 25 years

With the insignificant increase in the permeability tensor, the maximum temperature significantly moves away from the injection well as can be seen in Figure C-4. This reasonably happened because of the higher fluid flow as long as the fluid flux depends on the permeability of the matrix. Consequently, cause significant drawdown in the temperature of the reservoir.

As can be seen in Table C-2, the extracted temperature can be higher with increasing the permeability of the matrix. However, with time the decrease in the extracted temperature is higher about (29 K) when the permeability is insignificantly high (4.53e-15 m^2) and it is lower or about (1 K) when the permeability is less.

Table C-2. The Max extracted temperature (Kelvin) for different permeability values in different times

Time (Years)	**Permeability**		
	***k*=0.53e-15 m^2/sec**	***k*=2.53e-15 m^2/sec**	***k*=4.53e-15 m^2/sec**
10years	434.01	434.01	469.09
15years	433.88	433.90	445.26
20years	433.77	433.79	441.70
25years	433.66	433.79	440.09

The increase in the permeability parameter can affect the performance of the reservoir and this can clearly be seen through the thermal evolution of the reservoir for the used k_{max} and k_{min} in Figures C-5 and C-6.

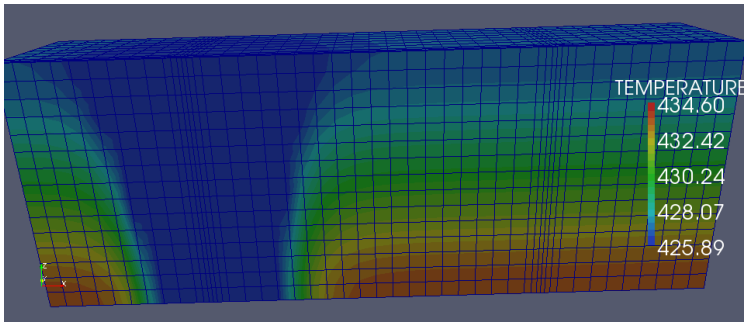

Figure C-5. Thermal evolution of the reservoir at k=0.53e-15 m^2/sec

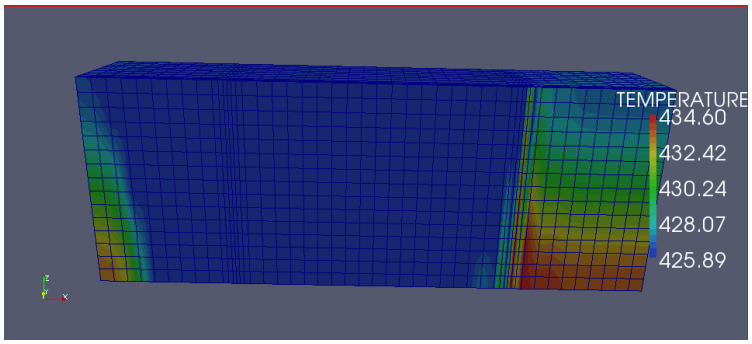

Figure C-6. Thermal evolution of the reservoir at k=4.53e-15 m^2/sec

This concludes that the permeability is a powerful design parameter that should be considered within a proposed optimisation model as it can have significant influence in the thermal

evolution of the reservoir and consequently affects the long-term performance of the HDR geothermal reservoir.

C-3-3 Sensitivity to the Injected Fluid Pressure (Pinj):

With the increase in the pressure of the injected fluid the temperature reduction of the reservoir around the injection well is more. This is due to the fact that the fluid flux is depending on the pressure beside the permeability factor. Therefore, high pressure causes increasing in the discharge flux. Also, the injected pressure would create new fractures during the circulation process, hence increasing the permeability of the reservoir (Ghassemi et al., 2008). Consequently, the distance of temperature profile from the injection well is increased, see Figure C-7.

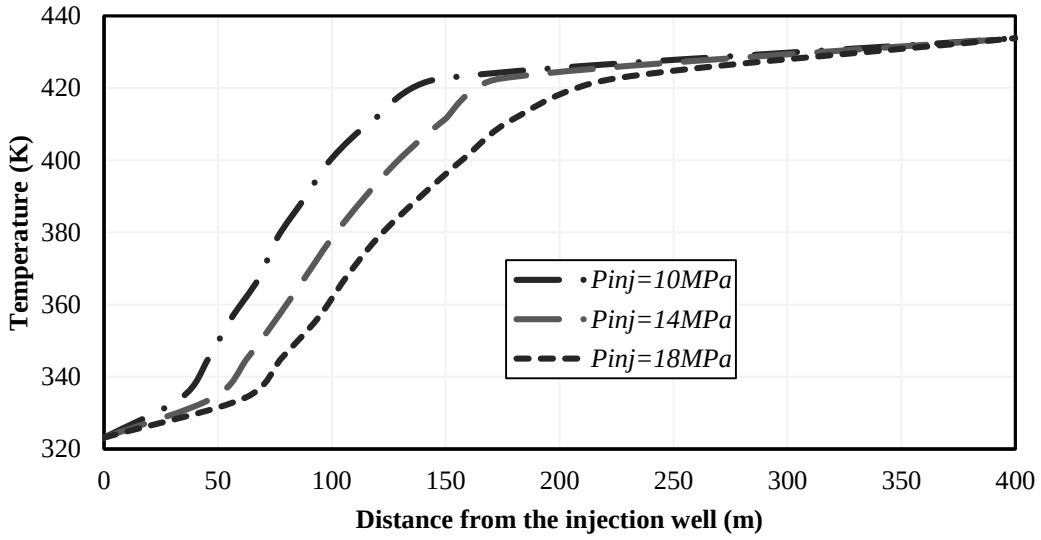

Figure C-7. Comparison of temperature profiles for different Injection fluid pressure (*Pinj*)

Although the extracted temperature is almost the same value with various injected pressure as can be seen in Table C-3, but the performance of the reservoir is affected in terms of thermal evolution of the reservoir (see Figures C-8 and C-9)

Table C-3. Max extracted temperatures (Kelvin) for different injected pressure at different times

Time (years)	**Injection pressure**				
	***Pinj*=10MPa**	***Pinj*=12MPa**	***Pinj*=14MPa**	***Pinj*=16MPa**	***Pinj*=18MPa**
Time=10years	434.01	434.01	434.01	434.01	434.01
Time=15years	433.88	433.88	433.88	433.89	433.89
Time=20years	433.76	433.76	433.79	433.81	433.85
Time=25years	433.66	433.67	433.69	433.77	433.95

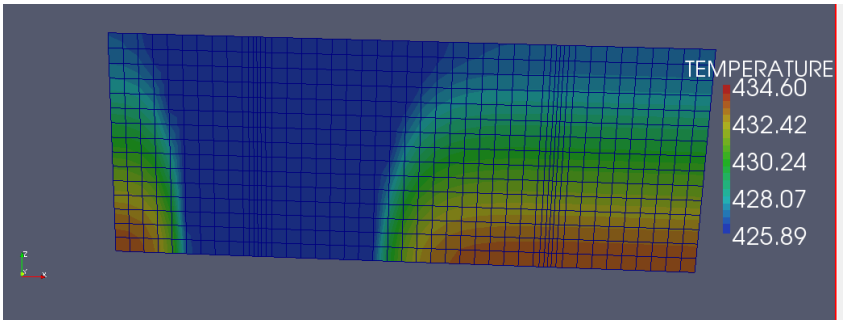

Figure C-8. Thermal evolution of the reservoir at *Pinj* =10MPa after 25 years

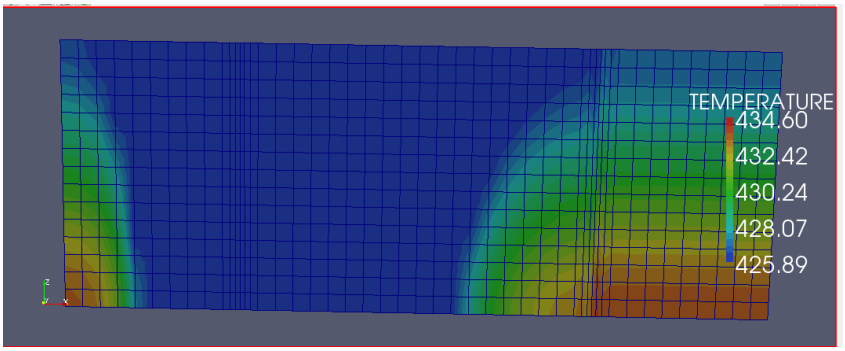

Figure C-9. Thermal evolution of the reservoir at *Pinj* =18MPa after 25 years

C-3-4 Sensitivity to Injection Temperature Tinj

According to Tester et al., (2006), the temperature of the injected fluid has significant influence in the reservoir performance. As it is reported, small values of *Tinj* yields cut off for the fluid flow due to the calcite in the fractures because of chemical deposition.

The sensitivity of the thermal evolution of the reservoir to the *Tinj* is examined for 25 years.

As can be seen in Figure C-10, the temperature profiles a long 150 m from the injection well is very sensitive to the different ranges of *Tinj*, particularly for *Tinj*=10 ^{o}C It is clear that the operation process is very sensitive to *Tinj* and needs to be considered during simulation of proposed models.

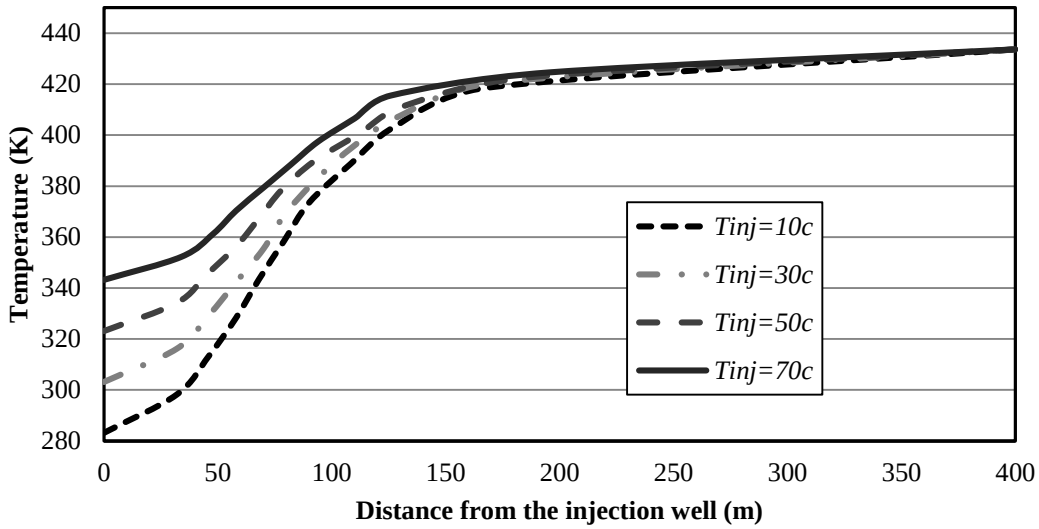

Figure C-10. Comparison of temperature profiles for different Injection temperature *Tinj* at 25 Years

C-3-5 Sensitivity to the Porosity (θmatrix)

The model is being simulated for different porosity of the matrix for the ranges of (0.005%, 0.5%, and 1%) which are naturally occurring. As can be seen in Table C-4, the max extracted temperature is almost the same value at different values of porosity of the matrix.

Table C-4. The Max extracted temperature (Kelvin) for different porosity matrix at different times

Time (years)	**Porosity**		
	θ=0.05e-003 (0.005%)	**θ=4.05e-003 (0.405%)**	**θ=1.05e-003 (1%)**
10years	434.011822	434.01448	434.03668
15years	433.880379	433.882931	433.910289
20years	433.757113	433.76007	433.770143
25years	433.655401	433.658706	433.663556

However, to assess the impact of the porosity in the long term performance the ParaView// Visualisation is used to show the thermal evolution of the reservoir after 25 years for different porosity values. Hence, Figures (C-11, C-12 and C-13) show that the porosity has no significant impacts on the thermal evolution of the reservoir. This is expected to be as long as the permeability is considered constant for the different scenarios.

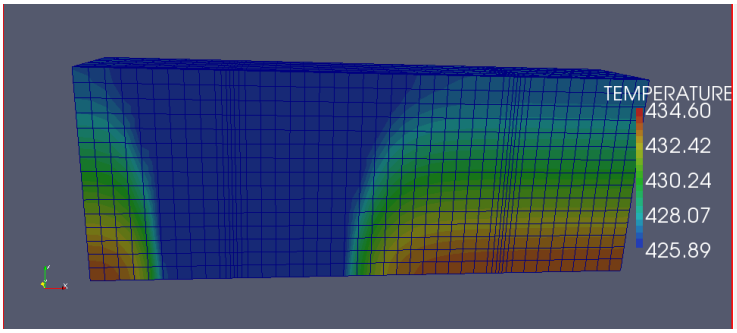

Figure C-11. Thermal evolution of the reservoir at θ=0.005% after 25 years

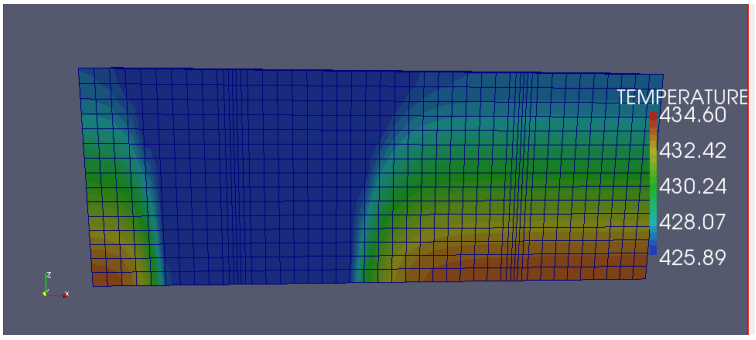

Figure C-12. Thermal evolution of the reservoir at θ=0.5% after 25 years

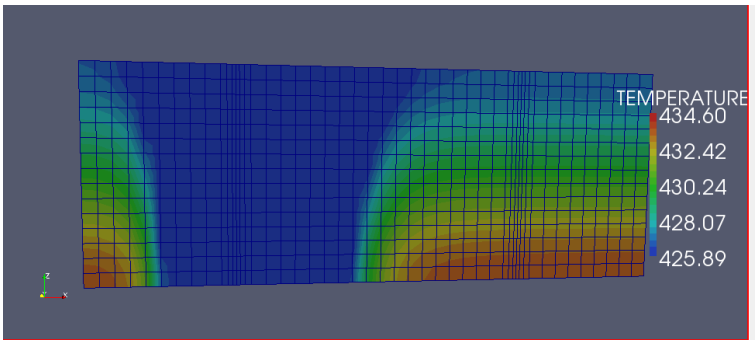

Figure C-13. Thermal evolution of the reservoir at θ =1% after 25 years

C-3-6 Sensitivity to the Specific Heat Conductivity of the Injected Fluid:

Although the thermal conductivity of the fluid is a significant parameter within the governing equation of heat transport, but, and as can be seen in Figure C-14, it does not affect the thermal evolution of the reservoir because it is dependent to the porosity which is very small value for crystalline rocks.

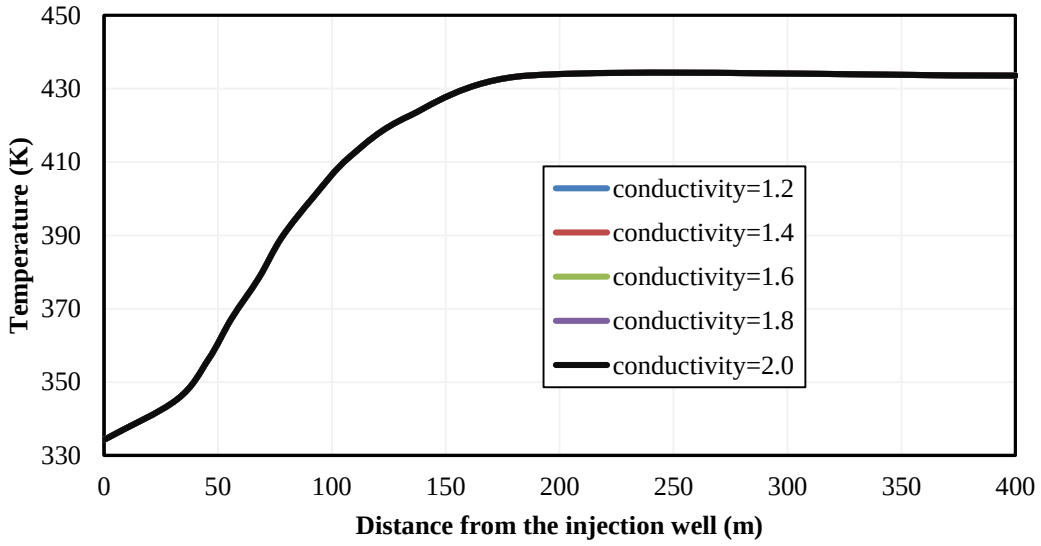

Figure C-14. Comparison of temperature profiles for different specific thermal conductivity of the injected fluid

C-3-7 Sensitivity to the Distance (d) between the Injection and Production Wells

To check the sensitivity to the distance between the injection and production wells, two additional scenarios have been modelled. The additional models were simulated as *d*=360 m & *d*=440 m which are about ±10 percentage of the distance between the injection and production wells. As can be seen in Figure C-15, the results show that with increasing the distance between the wells by 10%, the temperature profile reduced by 2.7% from the injection well. However, with 10% decrease of the distance between them the temperature profile from the injection well increased by 7%.

The results show the significant importance of the selection appropriate location for the injection and production wells within the reservoir. According to Yang and Yeh (2009), the increase in the distance between the wells can improve the long-term performance in an idealised case (no fluid loss or change in the fracture is allowed).

Although the longer distance between the wells can increase the reservoir life span, the stimulation capital cost for such cases is high. Hence, for the decision making it is important to account the overall cost of the project to achieve the sustainability target.

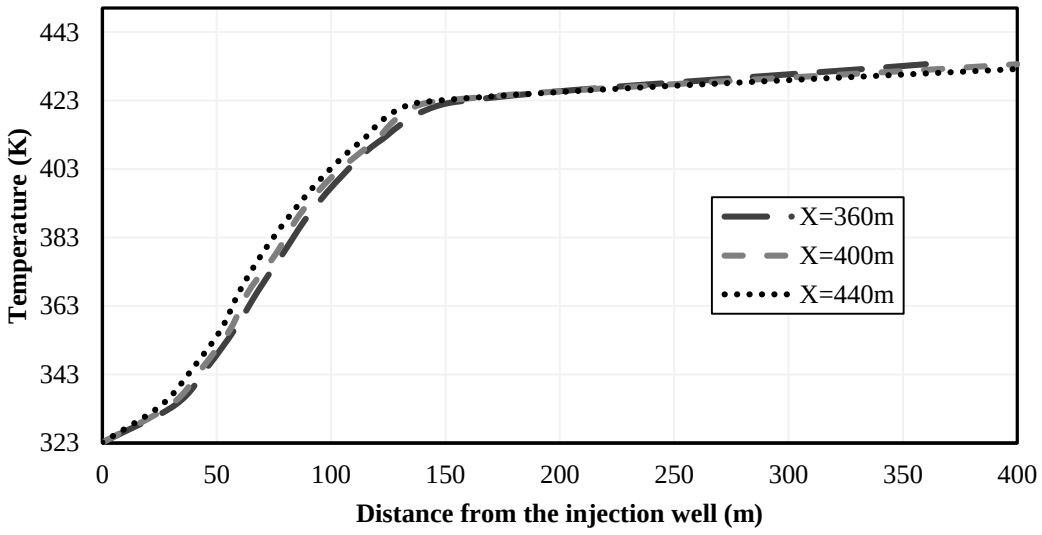

Figure C-15. Comparison of temperature profiles for different distances between the wells

C-4 Summary and Conclusion

The understanding of the influence of injection pressure in the reservoir permeability would result in suggesting the most appropriate locations for the wells within the reservoir. Hence, using the OGS software and an algorithm code different scenario can be examined to find the most appropriate location for the injection and production wells within the reservoir.

In addition, the flow path distance has high effects on the long-term performance. For an economic use of the HDR geothermal energy, the large heat transfer area must sufficiently be achieved for the geothermal exploitation. Therefore, there is a strong need to investigate new designs that achieve the best area of heat transfer.

C-6 References

BRACE, W. 1984. Permeability of crystalline rocks: New in situ measurements. Journal of Geophysical Research: Solid Earth (1978–2012), 89, 4327-4330.

GHASSEMI, A., NYGREN, A. & CHENG, A. 2008. Effects of heat extraction on fracture aperture: A poro–thermoelastic analysis. Geothermics, 37, 525-539.

TESTER, J. W., ANDERSON, B., BATCHELOR, A., BLACKWELL, D., DIPIPPO, R., DRAKE, E., GARNISH, J., LIVESAY, B., MOORE, M. C. & NICHOLS, K. 2006. The future of geothermal energy: Impact of enhanced geothermal systems (EGS) on the United States in the 21st century. Massachusetts Institute of Technology, 209.

WATANABE, N., KUNZ, H. & KOLDITZ, O. 2009. 3D Geothermal Reservoir Modelling Case Study: Urach Spa Step by Step Tutorial.

YANG, S.-Y. & YEH, H.-D. 2009. Modeling heat extraction from hot dry rock in a multi-well system. Applied Thermal Engineering, 29, 1676-1681.